

**STUDY OF DIFFUSIBLE HYDROGEN IN STEEL  
WELDS USING INDIGENOUSLY DEVELOPED  
HOT-EXTRACTION TECHNIQUES**

*By*

**GIRISH KUMAR PADHY**

**Enrolment No.: CHEM 02200704016**

**Indira Gandhi Centre for Atomic Research, Kalpakkam**

*A thesis submitted to the  
Board of Studies in Chemical Sciences*

*In partial fulfillment of requirements  
For the Degree of*

**DOCTOR OF PHILOSOPHY**

*of*

**HOMI BHABHA NATIONAL INSTITUTE**

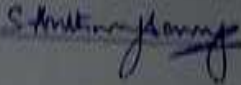


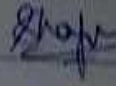
**November, 2012**

# Homi Bhabha National Institute

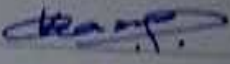
## Recommendations of the Viva Voce Board

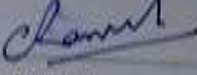
As members of the Viva Voce Board, we certify that we have read the dissertation prepared by **Girish Kumar Padhy** entitled "Study of diffusible hydrogen in steel welds using indigenously developed hot-extraction techniques" and recommend that it may be accepted as fulfilling the dissertation requirement for the Degree of Doctor of Philosophy.

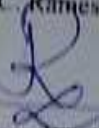
 Date: 21/8/13  
Chairman - Dr. S. Anthonysamy

 Date: 21.08.13  
Guide / Convener - Dr. Shaju K. Albert

 Date: 21/8/2013  
Member 1 - Dr. Arun Kumar Bhaduri

 Date: 21/08/2013  
Member 2 - Dr. V. Ganesan

 Date: 21/8/2013  
Technology Advisor - Mr. C. Ramesh

 Date: 21.08.13  
Examiner - Prof. D. Janakiram, IIT, Madras

Final approval and acceptance of this dissertation is contingent upon the candidate's submission of the final copies of the dissertation to HBNI.

I hereby certify that I have read this dissertation prepared under my direction and recommend that it may be accepted as fulfilling the dissertation requirement.

Date: 21-08-2013

Place: Indira Gandhi Centre for Atomic Research, Kalpakkam

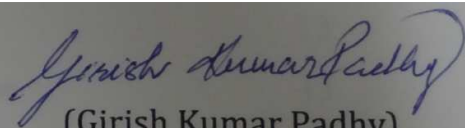
## STATEMENT BY AUTHOR

---

---

This dissertation has been submitted in partial fulfillment of requirements for an advanced degree at Homi Bhabha National Institute (HBNI) and is deposited in the Library to be made available to borrowers under rules of the HBNI.

Brief quotations from this dissertation are allowable without special permission, provided that accurate acknowledgement of source is made. Requests for permission for extended quotation from or reproduction of this manuscript in whole or in part may be granted by the Competent Authority of HBNI when in his or her judgment the proposed use of the material is in the interests of scholarship. In all other instances, however, permission must be obtained from the author.



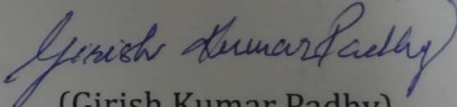
(Girish Kumar Padhy)

## DECLARATION

---

---

I, hereby declare that the investigation presented in this thesis has been carried out by me. The work is original and has not been submitted earlier as a whole or in part for a degree /diploma at this or any other Institution/ University.



(Girish Kumar Padhy)

*Dedicated To...*

*My Beloved Parents*

## ACKNOWLEDGEMENT

---

---

My dream about getting a doctoral degree turned into a reality. I would like to take this pleasant opportunity to express my heartfelt gratitude to those who helped and supported me during the course of this tune.

At first, I would like to express my deepest gratitude to my research guide, **Dr. Shaju K. Albert**, (Head, MTD, IGCAR) for his magnanimity in expending his valuable time and restless effort with his invaluable guidance, constant encouragement, unstinted inspiration and keen interest throughout my research work and in preparing this thesis. He has been a dream guide for me. I am grateful to **Dr. Arun Kumar Bhaduri** (Additional Director, MDTG, IGCAR) for making me motivated to take up this project and for extending his support and good wishes throughout. I am thankful to **Dr. C. Ravishankar** for his help in preparing this thesis.

It's my pleasure to thank my doctoral committee, **Dr. S. Anthonysamy** (Chairman), **Dr. V. Ganesan** (Member) and **Mr. C. Ramesh** (Member) for their meticulous evaluation of my work and their valuable suggestions. I thank all the **Professors of HBNI** who taught me various subjects during my course work.

I am privileged to thank **Dr. T. Jayakumar**, (Group Director, MMG, IGCAR), **Mr. S.C. Chetal**, (Director, IGCAR), **Dr. Baldev Raj**, (Ex-Director, IGCAR) for their trust and support on me. Furthermore, I sincerely thank the **Department of Atomic Energy** (DAE), India for providing the necessary financial support. I would like to thank **Dr. M. Saibaba** and **GSO, Kalpakkam** for providing a pleasant accommodation.

Words would be inadequate to express my gratitude to **Mr. V. Ramasubbu** and **Mr. N. Murugesan** for their help and support in carrying out diffusible hydrogen measurements. My Sincere thanks are again due to **Mr. C. Ramesh** for providing necessary laboratory facilities. I would like to acknowledge the help of **Dr. N. Parvathavarthini** and **Mr. Vinod Kumar** in preparing the hydrogen charged specimens.

I would like to thank **Mr. M. Arul**, **Mr. D. Manokaran** and **Mr. A. Yuvraj** (all MTD) for preparing weld specimens and to **Mr. Munnivel** for the transportation of equipments. I extend my thanks to **Mr. Hensonraj** (QAD, IGCAR) for helium leak tests, the **staff of Liquid Nitrogen Plant**, IGCAR and the **staff of Zonal Workshop**, IGCAR.

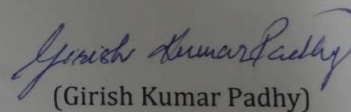
I would like to thank **Dr. Chitta Ranjan Das, Dr. Utpal Borah, Mr. V. Sunderajan, Mr. Hemant Kumar, Mr. N. Chandrasekhar, Mr. G. Srinivasan, Mr. V. Maduraimuthu, Mr. Harish Chandra De, Dr. B. Arivazhagan, Mr. Vasantharaja and Mrs. Divya** for the informative discussions, help and support during my research work. I would like to extend my thanks to the **whole staff of MTD** for their help and support in various ways.

My very-special thanks to my friends **Pradeep, Alok, Haribabu, Sudhansu & Smiti, Shaswat & Uma, Herojit, Maneesha, Pravati, Madhusmita, Subhra, Sudipta, Rajini Karunakara, Kalpataru, Bishnu, Sorb, Saravana Kumar, Sarath, Navin, Manas, and other fellow research scholars** for their help, support and enjoyable company. Additional thanks to **Mr. Haribabu Sata** for an unforgettable gift. I thank **all the members of MMG cricket team** for the funny, entertaining, exciting and winning moments we shared together in the open stadiums of Kalpakkam and Anupuram during the practice sessions and IGCAR Interlab Cricket Tournaments.

Finally, I would like to express my heartfelt gratitude to my parents, **Mr. Gouri Sankar Padhy** and **Mrs. Annapurna Padhy**, brother **Arun**, Sister **Archana**, other **family members** and **relatives** for their endless love, affection, support, and encouragement. A special mention is obvious to my very special teacher, **Mr. Krishna Chandra Panda** (My Uncle), who inspired and optimized my inquisitive-still-divergent mind throughout my childhood and adolescence. I would like to thank and share this achievement with my beloved wife **Sulata**, who was always with me creating a cheerful world filled with her love, affection, dedication, support and encouragement.

Above all, I thank **the Almighty**, without whose wish and blessing, this project would never have seen its successful accomplishment. He is the one who knows all the hardships, all my hard works and he is the one, whose satisfaction and acceptance I seek the most.

Date: 22-11-2012

  
(Girish Kumar Padhy)

Place: Indira Gandhi Centre for Atomic Research

# CONTENTS

---

---

S. No.	Title	Page No.
I	Synopsis	2
II	List of figures	
III	List of tables	

## CHAPTER 1

1	Introduction	2
	Reference	3

## CHAPTER 2

2	Literature Review	6
2.1	Hydrogen in steel	6
2.2	Origin of hydrogen in steel	7
2.3	Mode of hydrogen entry in steel during fabrication processes	7
2.3.1	Hydrogen Adsorption	8
2.3.1.1	Aqueous Solution	8
2.3.1.2	Gas Atmosphere	8
2.3.2	Hydrogen Recombination	8
2.3.3	Hydrogen absorption	9
2.4	Solubility of hydrogen in steel	9
2.5	Diffusion of hydrogen in steel	11
2.5.1	Dependence of diffusion on steel microstructure	12
2.5.2	Dependence of diffusion on temperature	13
2.5.3	Dependence of diffusion on applied stress	13
2.6	Trapping of hydrogen in steel	14
2.7	Hydrogen embrittlement	16
2.8	Theories of hydrogen embrittlement	18
2.8.1	Internal Pressure Model	18
2.8.2	Decohesion Model	18

2.8.3	Surface Energy Model	19
2.8.4	Hydride Phase Model	19
2.8.5	Dislocation Interaction/Slip softening Model	19
2.8.6	Corrosion Enhanced Plasticity (CEP) Model	20
2.9	Hydrogen Assisted Cracking (HAC) in Steel Weldments	21
2.10	Source of hydrogen in steel weldments	22
2.11	Solubility of hydrogen in steel weldments	23
2.12	Residual hydrogen and diffusible hydrogen	24
2.13	Distribution of hydrogen in weldments	26
2.14	Prevention of HAC in weldments	27
2.15	Classification of $H_D$ in welding consumables	30
2.16	Determination of $H_D$ in weldments	31
2.16.1	Glycerin Method	32
2.16.2	Mercury Method	34
2.16.3	Gas Chromatography/Carrier Gas Hot Extraction Method	35
2.16.4	Vacuum-Extraction methods	39
2.16.5	Other methods for diffusible hydrogen measurement	40
2.17	$H_D$ measurement using polymer hydrogen sensor	41
2.18	Effect of pre- and post-heating on diffusible hydrogen in weld	41
2.19	Determination of apparent diffusivity of hydrogen in steel	42
2.20	Scope of the present study	43
	Reference	44

## CHAPTER 3

<b>3</b>	<b>Experimental Details</b>	<b>61</b>
3.1	Determination of Diffusible Hydrogen ( $H_D$ )	61
3.1.1	Weld specimen preparation	62
3.1.1.1	Test assembly	62
3.1.1.2	Welding electrodes	63
3.1.1.3	Welding fixture/Copper jig	63
3.1.1.4	Preparation of specimen	64
3.1.2	Collection of $H_D$ from weld specimen	66
3.1.2.1	Chamber for $H_D$ collection at 25-45°C and its measurement using PEMHS (RT-PEMHS)	66

3.1.2.2	Chamber for hot extraction of H <sub>D</sub> and its measurement using PEMHS (HE- PEMHS)	67
3.1.2.3	Chamber for hot extraction of H <sub>D</sub> and its measurement using GCTCD (HE-GCTCD)	67
3.1.2.4	Collection of H <sub>D</sub>	70
3.1.3	Measurement of H <sub>D</sub>	70
3.1.3.1	Measurement of H <sub>D</sub> using PEMHS	70
3.1.3.1.1	Gas sampling valve	71
3.1.3.1.2	Proton exchange membrane hydrogen sensor (PEMHS)	72
3.1.3.1.3	Procedure for measurement of H <sub>D</sub> using PEMHS	75
3.1.3.2	Measurement H <sub>D</sub> using GCTCD	78
3.1.3.2.1	H <sub>D</sub> collection Unit	78
3.1.3.2.2	Gas Chromatography	78
3.1.3.2.3	Thermal Conductivity Detector (TCD)	79
3.1.3.1.4.	Procedure for measurement of diffusible hydrogen using GCTCD	79
3.1.4	Determination of H <sub>D</sub> using mercury method	80
3.1.5.	Measurement of H <sub>D</sub> with respect to time using PEMHS	82
3.2	Effect of preheat and post-heating on H <sub>D</sub> content	83
3.2.1.	Specimen Preparation	83
3.2.1.1	Preparation of specimens with preheating and preheating combined with post-heating	84
3.2.1.2	Measurement of H <sub>D</sub>	86
3.2.2	Measurement of hydrogen evolved from weld specimen during its post-heating	86
3.3	Study on apparent diffusivity of hydrogen in steel	87
3.3.1	Materials used and specimen	87
3.3.2	Hydrogen charging of the specimen	88
3.3.3	Measurement of hydrogen evolved at different temperatures	91
	Reference	92

## CHAPTER 4

<b>4</b>	<b>Measurement of <math>H_D</math> contents using indigenously developed techniques</b>	<b>96</b>
4.1	Results of $H_D$ measurement using PEMHS	96
4.1.1	Calibration of the PEMHS	96
4.1.2	Results of $H_D$ measurement using RT-PEMHS and their comparison with mercury method	98
4.1.3	Application of the RT-PEMHS to study hydrogen evolution with time	99
4.1.3	Results of $H_D$ measurement using HE-PEMHS and their comparison with mercury method	101
4.2	$H_D$ measurement using HE-GCTCD	103
4.2.1	Calibration of GCTCD	103
4.2.2	Results of measurement using HE-GCTCD and their comparison with mercury method	104
4.3	Statistical analysis of results	106
4.3	Discussion	110
	Reference	112

## CHAPTER 5

<b>5</b>	<b>Effects of preheat and post-heating on <math>H_D</math> content in welds</b>	<b>115</b>
5.1	Results	115
5.1.1	Cooling behavior	115
5.1.2	Comparison of $H_D$ obtained using mercury and HE-PEMHS	116
5.1.3	Effect of preheat on $H_D$ content	117
5.1.4	Effect of pre- and post-heating on $H_D$ content	121
5.1.5	Hydrogen evolution from specimen during post-heating	121
5.2	Discussion	125
	Reference	128

## CHAPTER 6

<b>6</b>	<b>Study on the apparent diffusivity of hydrogen in steel</b>	<b>131</b>
6.1	Diffusion through a cylinder	131
6.1.1	Equation for the diffusion through a finite cylinder	131
6.1.2	Solutions of the diffusion equation available in literature	133
6.1.3	Relationship between $D$ and $t_{0.5}$	134
6.2	Results	135
6.2.1	Hydrogen evolution profiles at different temperatures	135
6.2.2	Calculation of $t_{0.5}$ and apparent diffusivity, $D$	136
6.2.3	Calculation of the lost hydrogen content	140
6.3.2.1	Experimental verification of lost hydrogen content calculated	141
6.2.4	Calculation of time lags at 100, 200, 300 and 400°C	141
6.2.5	Calculation of $t_{0.5}$ and $D$ using corrected data	145
6.3	Discussion	147
6.3.1	Variation in apparent diffusivity by incorporating lost hydrogen	147
6.3.2	Comparison of apparent diffusivities obtained in the present study with the data in literature	148
6.3.3	Variation in apparent diffusivity with temperature and alloying	149
6.3.4	Hydrogen diffusivity and $H_D$ in the welds	151
	Reference	154

## CHAPTER 7

<b>7</b>	<b>Concluding remarks and scope for future research</b>	<b>157</b>
7.1	Conclusions	157
7.1.1	Measurement of $H_D$ using indigenously developed techniques	157
7.1.2	Study on effects of preheat and post-heating on $H_D$ content in welds	158
7.1.3	Determination of apparent diffusivity of hydrogen in steel	159
7.2	Scope for future research	159

7.2.1	Development of HE-PEMHS and HE-GCTCD for commercial application	159
7.2.2	Correlating diffusible hydrogen remaining in welds with cracking susceptibility	160
7.2.3	Study on hydrogen trapping in steels	161
	<b>Publications out of this work and Awards</b>	<b>163</b>

# **SYNOPSIS**

# Synopsis

---

---

## 1. Introduction

Hydrogen in steel is known to cause embrittlement [1, 2] and hydrogen assisted cracking (HAC) frequently reported during welding of steels or fabrication of steel structures or components is one of the manifestations of this form of embrittlement. HAC during welding is of a major concern because it is carried out on semifinished components and often this is carried out during the final stages of fabrication and cracking at this stage is unacceptable. Further, the probability of HAC in welded component is the maximum at ambient temperature [3]. Another aspect which is of concern is that HAC is often delayed for hours, or even days after welding and hence often not detected during inspection and hence, can lead to catastrophic failure in service.

Hydrogen enters into the steel weldment during arc welding processes and the sources for hydrogen include chemically bonded water in the constituents of flux used to produce the welding consumables, moisture absorbed by the consumables from atmosphere, and hydrocarbons on the surfaces of base metal or welding consumable. These hydrogenous compounds dissociate in the welding arc to form atomic hydrogen. Solubility of atomic hydrogen in molten metal is fairly high [3, 4]. However, immediate solidification of the molten weld pool due to rapid cooling leaves the weldment (weld metal and heat affected zone) supersaturated with hydrogen as solubility of hydrogen in steel in solid state is much less compared to its solubility in liquid metal. The supersaturated hydrogen diffuse within the weldment and during this diffusion transport, a portion of it is trapped in hydrogen traps which include grain boundaries, dislocations, microvoids, inclusions etc. and others diffuse out. There are two types of hydrogen traps reversible (Binding energy  $< 30\text{kJ/mole}$ ) and irreversible traps (Binding energy  $>$

50kJ/mole) in steel. Hydrogen, which is trapped in the reversible traps during its transport within the weldment is able to overcome the trap barrier at or near room temperature and continue its diffusion, is referred to as diffusible hydrogen ( $H_D$ ). It is this diffusible hydrogen which accumulates to a critical concentration in the potential crack sites and assists cracking [5]. However, residual hydrogen which is held in the irreversible traps requires higher energy (corresponding to temperatures  $\geq 650^\circ\text{C}$ ) to overcome the trap barrier for further transport. Therefore, at room temperature, residual hydrogen cannot contribute to the accumulated hydrogen at the potential crack sites thus is not responsible for HAC. Therefore, knowledge about diffusible hydrogen in steel welds is very important to assess the susceptibility of the weld joint to HAC and also to develop procedures to avoid cracking.

Several methods are available to measure  $H_D$  in steel welds produced using different welding consumables and welding procedures and welding consumables are classified based on the  $H_D$  content in the welds produced by them. Among methods available to determine the  $H_D$  contents in steel welds, only four methods namely Glycerin method, Mercury method, Gas Chromatography method or Carrier gas-Hot extraction method and Vacuum Extraction method have been recommended by different national and international standards [6-13]. However, none of these techniques are without limitations and there is scope for refining the existing methods and introducing new methods based on the techniques available for hydrogen detection and its measurement.

## **2. Objective of the present study**

The main objective of the present study is to indigenously develop techniques for  $H_D$  measurement by hot extraction method using newly developed proton exchange membrane hydrogen sensor (PEMHS) and conventional gas chromatography that uses

thermal conductivity detector (GCTCD). These systems have also been used to determine apparent diffusivity of hydrogen in three different steels at different temperatures. Further, system based on PEMHS has also been used to study the effect of preheating and post heating on steel welds on  $H_D$  remaining in the steel welds.

### **3. Organization of the thesis**

This thesis presents a broad idea on the development of two hot extraction methods, one based on a PEMHS and the other based on a GCTCD for  $H_D$  measurement, their application for other aspects of hydrogen in steel. This thesis consists of seven chapters.

#### ***Chapter 1***

This chapter briefly states the motivation for present work. It discusses the limitations of standards methods presently available and how the methods developed in the present work can be used for applications other than the standard determination of  $H_D$  content in welding consumables.

#### ***Chapter 2***

The second chapter provides a detailed survey on hydrogen assisted cracking in steel welds and  $H_D$  measurement. Different aspects of hydrogen in steel and steel weldments such as its sources, absorption, solubility, diffusion, trapping and their effects on hydrogen assisted cracking (HAC) has been presented. This chapter also discusses briefly the various theories and models proposed for HAC, the application of preheat as a measure to prevent HAC and the purposes of  $H_D$  measurement in welds. It also covers the concerns in  $H_D$  measurement, various standard and non-standard methods available for measurement of  $H_D$  in welds, their correlation, advantages, and limitations in using them. The chapter finally concludes with relevance of the present study in the context of the present understanding on  $H_D$  in steel welds and current practices of its determination.

### ***Chapter 3***

The third chapter gives details of the PEMHS sensor, principles of its operation, experimental set up used for  $H_D$  measurements and calibration procedure. Similarly, the details of  $H_D$  measurement using GCTCD has also been given. Details of design, fabrication and testing of the hot extraction chambers used for these techniques are also given here.  $H_D$  content determined using these methods was compared with standard mercury method, which is also discussed briefly in this chapter. Subsequently the experimental facility developed to study the effect of preheating and post heating in the  $H_D$  remaining in the weld and the preparation of specimens for this study has been discussed. For hydrogen diffusivity measurement, hydrogen charging was carried out on specimens prepared from three different steels using an electrochemical cell. Details of this set up and the experiments are also discussed in this chapter

### ***Chapter 4***

In the fourth chapter, initially, results of the calibration of the two measurement techniques using known volume/concentration of hydrogen in Ar-H<sub>2</sub> mixtures are presented. Subsequently, for the method using PEMHS, results of  $H_D$  measurements carried out using hydrogen collected at room temperature for 72 h are given and compared with those obtained from standard mercury method. Subsequently results of  $H_D$  measurements carried out with both the hot extraction techniques are presented and compared with those of the standard methods. A statistical analysis of these results are also presented to demonstrate that the one to one correlation obtained for the results from these techniques and with those obtained from standard mercury method is not by chance. This chapter concludes by demonstrating that these two methods can be used for  $H_D$  measurements of steel welds with same accuracy and reliability offered by the

standard mercury methods. It also presents various advantages of these newly developed methods over the presently available ones.

### ***Chapter 5***

The fifth chapter presents a systematic investigation the effects of pre- and post-heating on the  $H_D$  contents of welds using hot extraction-PEMHS method. This study was carried out with weld specimens prepared by depositing E7018 electrodes on standard mild steel specimens and E9015-B3 electrodes on modified 9Cr-1Mo specimen. The results clearly show both preheating and post heating brings down the  $H_D$  content in the weld considerably. However, it is found that a combination of preheating and post heating at lower temperature is more effective in reducing the  $H_D$  content than using preheating alone at higher temperature. Further, for comparing the effect of preheating temperature on  $H_D$  measurements, it is shown that specimens shall be taken for measurements after it is cooled down to 100°C ( $t_{100}$ )

### ***Chapter 6***

This chapter presents the results of the apparent diffusivity of hydrogen estimated in three different steels; modified 9Cr-1Mo steel, 2.25Cr-1Mo steel and mild steel in the temperature range 25-400°C based on the hydrogen diffused out from the specimens pre-charged with hydrogen electrochemically up to the saturation level. From the hydrogen evolution data obtained from these measurements, at various temperatures and durations, apparent hydrogen diffusivity was measured for different temperatures by using standard solutions of diffusion equations for a finite cylinder described in literature. A numerical procedure for estimating of the volume of hydrogen lost from the specimen before the measurement has also been proposed in this chapter. Hydrogen diffusivity data has been subsequently modified by adding hydrogen lost thus estimated with hydrogen measured. The calculated apparent diffusivities of hydrogen in all the above specified steels with

and without incorporating the modifications for the above specified temperatures are given in table 1.

The apparent diffusivities in table 1 were found to be in good agreement with the literature data which has been claimed to be accurate [14, 15]. From the apparent diffusivity data of hydrogen in the three steels in table 1, the effect of alloying/composition on the apparent diffusivity of hydrogen is discussed along with its relevance to HD measurement in steel welds [16].

Table 1: Apparent diffusivity of hydrogen in steel within 25-400°C

Temperature (°C)	Apparent diffusivity $\times 10^{11}$ (m <sup>2</sup> /s)					
	Modified 9Cr-1Mo		2.25Cr-1Mo		Mild steel	
	Without modification	With modification	Without modification	With modification	Without modification	With modification
25	2.6	4.18	8.31	18	17.6	42.6
100	29.5	36.4	91.3	110	111	150
200	104	127	208	224	256	283
300	261	313	691	727	822	904
400	700	744	945	1310	1280	1710

## Chapter 7

In this chapter, a summary of the whole investigation is discussed and scope for future research based on this work is proposed.

### 4. Summary

To summarise the whole investigation, two hot extraction methods, one based on proton exchange membrane based electrochemical sensor (HE-PEMHS) and the other based on thermal conductivity detector (HE-GCTCD) were proposed for rapid determination of diffusible hydrogen in welding consumables. Both these methods are found to be reliable and valid with respect to the accuracy and precision in their measurements. Using the HE-PEMHS based method, a systematic study on the effects of

preheat and post heating on the diffusible hydrogen contents in welds was carried out successfully. Further, these methods were employed in determining the apparent diffusivities of hydrogen in mild steel, 2.25Cr-1Mo steel and Modified 9Cr-1Mo steel. The apparent diffusivities determined using both these methods agree well with the literature data. In addition, the variation in apparent diffusivities with composition is used to discuss the effect of composition on  $H_D$  values measured using standard techniques.

## Reference

1. R.A.Oriani, Hydrogen Assisted Cracking of High Strength Alloys, In: *Comprehensive Structural Integrity*, 2003, Vol. 6, Elsevier Science, New York, NY, pp. 31-101.
2. R. A. Oriani, Hydrogen-The Versatile Embrittler, *Corrosion*, 1987, Vol. 43, No. 7, 390-397.
3. G. E. Linnert, *Welding Metallurgy: Carbon and Alloy Steels. Fundamentals*, Vol.1, American Welding Society, 1965.
4. M. Johnson, Effect of hydrogen on weld metal properties and Integrity, *State of the Art Report on Welding and Inspection*, SAC Joint Venture, Federal Emergency Management Agency, 355B, September, 2000.
5. E. Quadrini, Factors in hydrogen embrittlement of high strength steels, *Materials Chemistry and Physics*, 1989, Vol.21, 437-446.
6. *ISO 3690:2008, ISO 3690:2000*, Welding and allied processes – Determination of hydrogen in ferritic steel arc weld metal.
7. *ANSI/AWS A4.3: 1993 (R2006)*, Standard methods for determination of diffusible hydrogen content of martensitic, bainitic and ferritic steel weld metal produced by arc welding. American Welding Society, Miami, FL.
8. *BS 6693-5: 1988*, Diffusible hydrogen. Primary method for the determination of diffusible hydrogen in MIG, MAG, TIG or cored electrode ferritic steel weld metal.

9. *JIS Z 3118: 2007*, Method for measurement of amount of hydrogen evolved from steel welds.
10. *JIS Z 3113: 1975*, Method for measurement of *hydrogen* evolved from deposited *metal*.
11. *DIN 8572: 1981 Part 1*, Determination of diffusible hydrogen in weld metal- Manual Arc Welding.
12. *AS/NZS 3752: 2006* Welding and allied processes - Determination of hydrogen content in ferritic steel arc weld.
13. *BIS IS 11802:1986 (R2003)*, Method of determination of diffusible hydrogen content of deposited weld metal from covered electrodes in welding mild and low alloy steels.
14. R.C. Brouwer: 'Hydrogen diffusion and solubility in vanadium modified pressure vessel steels', *Scripta Metallurgica et Materialia*, 1992, 27(3), 353-358.
15. Th. Boellinghaus, H. Hoffmeister, A. Dangeleit, C Middel Scatterbands for hydrogen diffusion coefficients in steels having a ferritic or martensitic microstructure and steels having an austenitic microstructure at room temperature, *Welding in the World*, 1996, Vol. 37, No.1, 16–23.
16. S.K. Albert, V. Ramasubbu,, N. Parvathavarthini, and T.P.S. Gill: Influence on alloying on hydrogen assisted cracking and diffusible hydrogen content in Cr-Mo steel welds, *Sadhana*, vol-28, Parts 3& 4, June/August 2003, pp. 383-393.

# LIST OF FIGURES

---

---

<b>S. No.</b>	<b>Figure Caption</b>	<b>Page No.</b>
Fig. 2.1	Critical hydrogen concentration causing HAC in steel microstructures	7
Fig. 2.2	Solubility of hydrogen in iron as a function of temperature and pressure	11
Fig. 2.3	Schematic of the interaction energy of atomic hydrogen and trap sites	15
Fig. 2.4	Schematic representation of traps on the basis of their effect on hydrogen	16
Fig. 2.5	Variation of overall/apparent hydrogen diffusivity with temperature in steels	17
Fig. 2.6	Locations of delayed cracks in weldment	22
Fig. 2.7 a	Absorption of hydrogen in the weld pool following Seivert	23
Fig. 2.7 b	Absorption of hydrogen in the weld pool following Gedeon	23
Fig. 2.8 a	Solubility of hydrogen in weld pool exposed to monatomic hydrogen as per Gedeon	24
Fig. 2.8 b	Solubility of hydrogen in weld pool exposed to diatomic hydrogen as per Sievert	24
Fig. 2.9	Schematic representation of diffusion of hydrogen to HAZ	27
Fig. 2.10	Classification of steels to choose between hardness or hydrogen control approach to determine safe preheat temperature	28
Fig. 2.11 a	Photograph of glycerin apparatus for diffusible hydrogen measurement	33
Fig. 2.11 b	Schematic of glycerin apparatus for diffusible hydrogen measurement	33
Fig. 2.12 a	U-tube Apparatus for diffusible hydrogen measurement using mercury method	35
Fig. 2.12 b	Y-tube Apparatus for diffusible hydrogen measurement	35

	using mercury method	
Fig. 2.13	GC setup for diffusible hydrogen measurement	37
Fig. 2.14 a	Schematic of Carrier gas hot extraction for diffusible hydrogen measurement	38
Fig. 2.14 b	Photograph of Carrier gas hot extraction for diffusible hydrogen measurement	38
Fig. 2.15 a	Vacuum extraction apparatus for diffusible hydrogen measurement at room temperature	39
Fig. 2.15 b	Vacuum extraction apparatus for hot extraction of diffusible hydrogen and its measurement	39
Fig. 3.1	Schematic of test assembly	63
Fig. 3.2	Photograph of Copper jig holding the test assembly	65
Fig. 3.3	Schematic of copper jig used	65
Fig. 3.4	Chamber for collecting $H_D$ at room temperature	66
Fig. 3.5	Hot extraction chamber along with the temperature controller	68
Fig. 3.6	Schematic of heater with enclosure in the hot extraction chamber	68
Fig. 3.7	Hydrogen collection chamber for GCTCD technique	69
Fig. 3.8 a	Schematic of sampling valve: Valve in Mode 1 for sampling the gas	71
Fig. 3.8 b	Schematic of sampling valve: Valve in Mode 2 for injection of sampled gas onto the PEMHS	72
Fig. 3.9	Schematic of PEMHS	74
Fig. 3.10	Photographs of PEMHS and Data acquisition unit	75
Fig. 3.11	Schematic of measurement of $H_D$ using PEMHS	76
Fig. 3.12	Photograph of measurement of $H_D$ using PEMHS	77
Fig. 3.13	Photograph of GCTCD setup for measurement of $H_D$	80
Fig. 3.14	Mercury apparatus used for $H_D$ measurement	82
Fig. 3.15	Heater unit for pre- and post-heating	84
Fig. 3.16	Time-Temperature profile of post heating	85
Fig. 3.17	Photograph of specimen for hydrogen charging	88
Fig. 3.18	Schematic of electrochemical cell for hydrogen charging	89

Fig. 3.19	Photograph of hydrogen charging set up	90
Fig. 4.1	Response of the PEMHS during calibration	97
Fig. 4.2	Calibration plot of PEMHS	97
Fig. 4.3	Correlation between RT-PEMHS and Mercury method	98
Fig. 4.4	Variation in Rate of hydrogen evolution with time	101
Fig. 4.5	Cumulative $H_D$ content obtained with time	101
Fig. 4.6	Correlation between HE-PEMHS and mercury method	102
Fig. 4.7	Response of GCTCD on injection of hydrogen	103
Fig. 4.8	Calibration plot of GCTCD	104
Fig. 4.9	Correlation between HE- GCTCD and Mercury method	105
Fig. 4.10	Representation of t-Distribution	107
Fig. 5.1	Cooling behavior of preheated weld specimen	116
Fig. 5.2	Comparison of $H_D$ contents obtained from preheated and post-heated specimens in HE-PEMHS and mercury method	117
Fig. 5.3 a	Effect of preheat on the $H_D$ content (mild steel)	120
Fig. 5.3 b	Effect of preheat on the $H_D$ content (modified 9Cr-1Mo steel)	120
Fig. 5.4	$H_D$ obtained after post heating	124
Fig. 5.5	Hydrogen diffused during post-heating	124
Fig. 5.6	Hydrogen diffused out of weld during post-heating + $H_D$ after post-heating	125
Fig. 6.1	Cylinder co-ordinate system	132
Fig. 6.2 a	Hydrogen evolution profiles as a function of time at different temperatures for modified 9Cr-1Mo steel	138
Fig. 6.2 b	Hydrogen evolution profiles as a function of time at different temperatures for 2.25Cr-1Mo steel	138
Fig. 6.2 c	Hydrogen evolution profiles as a function of time at different temperatures for mild steel	138
Fig. 6.3 a	Fraction of remaining hydrogen as a function of time in modified 9Cr-1Mo steel	139
Fig. 6.3 b	Fraction of remaining hydrogen as a function of time in 2.25Cr-1Mo steel	139
Fig. 6.3 c	Fraction of remaining hydrogen as a function of time in	139

	mild steel	
Fig. 6.4 a	Rate of hydrogen evolution at 25°C as a function of corrected time in modified 9Cr-1Mo steel	144
Fig. 6.4 b	Rate of hydrogen desorption at 25°C as a function of corrected time in 2.25Cr-1Mo steel	144
Fig. 6.4 c	Rate of hydrogen desorption at 25°C as a function of corrected time in mild steel	144
Fig. 6.5 a	Fraction of remaining hydrogen as a function of corrected time in modified 9Cr-1Mo steel	146
Fig. 6.5 b	Fraction of remaining hydrogen as a function of corrected time in 2.25Cr-1Mo steel	146
Fig. 6.5 c	Fraction of remaining hydrogen as a function of corrected time in Mild steel	146
Fig. 6.6	Variation of apparent diffusivity of hydrogen in different steels with temperature	147
Fig. 6.7	Comparison of apparent diffusivity of hydrogen obtained from present study with Bollinghaus scatterbands	148
Fig. 6.8	Comparison of apparent diffusivity of hydrogen obtained from present study with that in literature	149
Fig. 6.9 a	Microstructure of modified 9Cr-1Mo steel after heat treatment	150
Fig. 6.9 b	Microstructure of 2.25Cr-1Mo steel after heat treatment	150
Fig. 6.9 c	Microstructure of mild steel after heat treatment	150

# LIST OF TABLES

---

---

S. No.	Table Caption	Page
Table 2.1	Hydrogen trapping energies and detrapping temperatures	15
Table 2.2	Classification of consumable based on $H_D$ content	31
Table 2.3	Efficiency of $H_D$ collection over different collecting fluids	40
Table 3.1	Chemical composition of mild steel and modified 9Cr-1Mo	62
Table 3.2	Baking and welding conditions of different electrodes	64
Table 3.3	Chemical composition of steels used in this study	87
Table 3.4	Heat treatment conditions of of steels used in this study	88
Table 3.5	Optimization of time duration for hydrogen charging	
Table 4.1	$H_D$ contents obtained using RT-PEMHS and mercury method	99
Table 4.2	Diffusible hydrogen evolution with time	100
Table 4.3	$H_D$ contents obtained using HE-PEMHS and mercury method	102
Table 4.4	$H_D$ contents obtained by HE-GCTCD and mercury method	105
Table 4.5	Sample size, degree of freedom and choice of $t_{statistical}$ at 95% confidence	108
Table 4.6	t-Test of means of $H_D$ obtained from RT-PEMHS and mercury methods	108
Table 4.7	t-Test of means of $H_D$ obtained from HE-PEMHS and mercury methods	109
Table 4.8	t-Test of means of $H_D$ obtained from HE-GCTCD and mercury methods	109
Table 5.1	$H_D$ collected from preheated weld specimens using HE-PEMHS	119
Table 5.2	Total $H_D$ measured during and after post heating in HE-PEMHS chamber	123
Table 6.1	Normalized solutions for the diffusion equation of finite cylinder	134
Table 6.2	Bessel's roots for $m = 0$	135
Table 6.3	$t_{0.5}$ and apparent diffusivity of hydrogen, $D$ at different temperatures	137
Table 6.4	Volume of lost hydrogen 25°C estimated from experiment	143

Table 6.5	Calculated amount of hydrogen lost at 25°C	143
Table 6.6	Time lags calculated for different steels	143
Table 6.7	Revised $t_{0.5}$ and apparent diffusivity of hydrogen from corrected data	145
Table 6.8	$H_D$ contents measured at standard temperature + time durations	152

# CHAPTER **1**

## INTRODUCTION

# Introduction

---

---

Hydrogen is absorbed in steel welds during welding. Major source of this hydrogen is the moisture present in the electrode coating. Hydrogen thus absorbed remains in steel welds either as residual hydrogen or as diffusible hydrogen. Residual hydrogen is permanently trapped in steel and not free to diffuse. Therefore, it has no effect on the properties or performance of steel at ambient temperature. However, diffusible hydrogen ( $H_D$ ) is mobile at room temperature.  $H_D$  in steel welds causes hydrogen assisted cracking which can occur few hours after welding. Therefore,  $H_D$  content needs to be controlled to avoid hydrogen cracking in steel weldments. Measurement of diffusible hydrogen in weldments is the first step in the attempts to control it. Unlike other elements, diffusivity of hydrogen in steel is high even at room temperature, and hence, difficulties exist in its accurate measurement.

At present, standard methods that are widely used for  $H_D$  measurement in steel welds include the International Institute of Welding (IIW) method (ISO 3690) [1], the AWS standard (ANSI/AWS A4.3-93) [2], Japanese standards (JIS Z 3113-1975 and JIS Z 3118-2005) [3, 4] etc. These standards recommend hydrogen collection over fluids like glycerin, mercury and its volumetric measurement and gas chromatography. However, these methods suffer from various drawbacks. Glycerin method requires at least 48 hours for completion of diffusible hydrogen collection. Therefore this method is time consuming and always results in  $H_D$  contents lower than those obtained by mercury and gas chromatography methods [5]. Further, variations in the purity and viscosity of glycerin vary the  $H_D$  contents obtained with glycerin method. Mercury method is accurate and precise in its measurements. However, it requires at least 72 h or more for

completion of hydrogen collection from a weld specimen. Therefore, it is time consuming. Mercury is considered to cause potential health hazards and its use is banned in many countries. In addition, the leak tightness of the apparatus used in mercury method for such longtime is an issue. Further, both the glycerin and mercury methods are not suitable for  $H_D$  measurement in the improved duplex stainless steel welds [6-8]. Gas chromatography method for measuring diffusible hydrogen is as accurate as mercury method. It allows  $H_D$  collection at 150°C, therefore reduces the collection time substantially to 6 hours. However, consumable manufacturers, who require carrying out  $H_D$  measurements routinely for every batch of the production, even 6-8 h for  $H_D$  measurement is considered to be time consuming [9]. Recently, a hot extraction procedure which extracts hydrogen from weld specimen at 400°C and its subsequent measurement was introduced in some standards [1, 2]. This procedure reduces the collection time of diffusible hydrogen to 20-30 minutes. Results obtained in this method are found to be precise and comparable to other standard techniques. However, the cost of the equipment is unreasonably high and its availability is also limited.

From the above, it is clear that technique for  $H_D$  measurement is being continuously developed with an objective of reducing time and cost of measurement. Hence, it is relevant to develop new techniques which use hot extraction techniques and new hydrogen sensors. This was the motivation to develop new techniques for  $H_D$  measurement. The aim of this study was to develop techniques which are rather simple to use, less time consuming, accurate in measurement and cost effective.

Before developing the new techniques, a broad literature survey was carried out. This survey covers the basic aspects of hydrogen in steel and its weldments, need for  $H_D$  measurement in welds and details of various methods available for this purpose. This is provided in the next chapter along with the scope of the present work.

## Reference

1. *ISO 3690:2012 (E), ISO 3690:2000 (E)*, Welding and allied processes – Determination of hydrogen in ferritic steel arc weld metal.
2. *ANSI/AWS A4.3: 1993 (R2006)*, Standard methods for determination of diffusible hydrogen content of martensitic, bainitic and ferritic steel weld metal produced by arc welding. American Welding Society, Miami, FL.
3. *JIS Z 3113: 1975*, Methods for measurement of hydrogen evolved from steel welds
4. *JIS Z 3118: 2007*, Methods for measurement of amount of hydrogen evolved from steel welds
5. M. A. Quintana, A critical evaluation of glycerin test, *Welding Journal*, 1984, Vol. 63, No. 5, 141s-149s.
6. Y. Kikuchi, C. D. Lundin and K. K. Khan, Measurement of diffusible hydrogen content and hydrogen effects on the cracking potential of duplex stainless steel weldments (Part 1), *Transactions of JWRI*, 1991, Vol. 2, No. 1, 95-104
7. R. B. Hutchings, A. Turnbull and A. T. May, Measurement of hydrogen transport in a duplex stainless steel, *Scripta Metallurgica et Materialia*, 1991, Vol. 25, 2657-2662
8. S. Brauser and Th. Kannengiesser, Hydrogen absorption of different welded duplex steels, *International Journal of Hydrogen Energy*, 2010, Vol. 35, 4368 – 4374
9. R. Ravi and D. S. Honnaver, Hydrogen in steel weldments – A review, *Proceedings of National welding seminar*, 26-28 Nov. 1987, Bangalore, E23-E43

**CHAPTER 2**

**LITERATURE REVIEW**

# Literature Review

---

---

## 2.1 Hydrogen in steel

The damaging effects of hydrogen in iron and steel are recognized for over a century [1]. Hydrogen in structural steel causes hydrogen assisted cracking (HAC) of the steel. This is a form of hydrogen embrittlement that occurs at temperatures in the range of -50 to 150C° when hydrogen in steel is accompanied with favorable conditions such as crack susceptible martensitic microstructure and sufficient tensile stress [2-4]. Hydrogen is absorbed in steel during its processing, fabrication and also while in service. The fact that HAC occurs several hours or days after absorption of hydrogen often results in unexpected catastrophic failure while components are in service or storage. The delay in hydrogen cracking is due to the time required for hydrogen to be accumulated to a critical level at potential crack sites (such as the regions of high triaxial stress) in the steel microstructure. This accumulation takes place by diffusion of hydrogen through the lattice. Critical size of the site (where hydrogen is accumulated) which can cause cracking varies with steel microstructure. Similarly, concentration of hydrogen required to cause cracking also depends on microstructures as shown in Fig. 2.1 [5]. From this figure, it is clear that critical concentration of hydrogen that can cause cracking in steel is lower for martensitic microstructure. Hence, martensitic microstructure is highly susceptible to HAC. With increasing strength of the martensite, critical concentration of hydrogen required to cause HAC still decreases. Several theories and models were proposed in the past to understand and explain the role of hydrogen in causing HAC. Before going to these theories, a brief review of some of the mechanisms related to hydrogen in steels, like entry, solubility, trapping, diffusion etc. is essential.

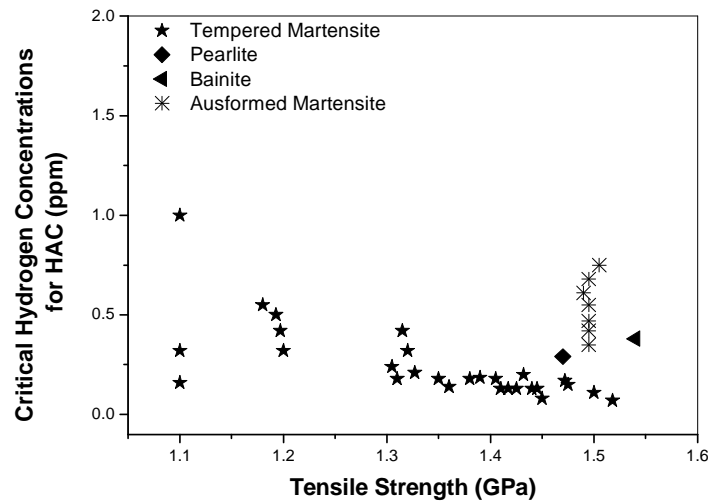


Fig. 2.1 Critical hydrogen concentration causing HAC in steel microstructures [5]

## 2.2 Origin of hydrogen in steel

During steel production, the main source of hydrogen is the hydrogenous impurities in raw materials [6-9]. Processing operations such as pickling [10, 11], electrolytic cleaning, cathodic polarization protection [12], electroplating [13-15] and electrochemical machining [16] contribute to hydrogen absorption in steel. During the welding of steel components, main source of hydrogen is the welding consumable. Moisture or any other hydrogenous material present in the welding consumables dissociate in the welding arc producing atomic hydrogen which dissolves in liquid weld metal. In service, hydrogen may be picked up when steel components are subjected to heating or pressurizing in hydrogenous environments [17, 18] or exposed to sulphide or chloride environments as in oil and petrochemical industries.

## 2.3 Mode of hydrogen entry in steel during fabrication processes

The entry of hydrogen in iron and steels is widely studied by several authors [12, 19-24]. In general, hydrogen atom or ion enters into steel through adsorption, recombination and absorption. These processes are given below.

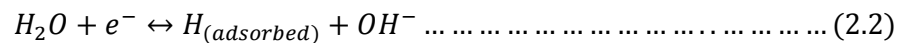
### 2.3.1 Hydrogen Adsorption

Hydrogen can be adsorbed in steel from two types of environments

1. Aqueous/Electrochemical solution ( $H_{(hydrated)}^+$  ion)
2. Gas atmosphere ( $H - atom$ )

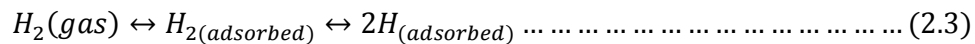
#### 2.3.1.1 Aqueous Solution

Steel, under cathodic polarisation, is in contact with the hydrated hydrogen cations,  $H_{(hydrated)}^+$  or  $H_3O^+$  in an aqueous solution.  $H_{(hydrated)}^+$  migrates towards steel cathode and undergoes reduction to form hydrogen atom. Hydrogen atom so formed is electroadsorbed on the steel surface, ( $H_{(adsorbed)}$ ). This electroadsorption follows Volmer's adsorption [25, 26] as given in equations 2.1 and 2.2:



#### 2.3.1.2 Gas Atmosphere

Hydrogen molecules ( $H_2$ ), when used in contact with metallic surfaces can dissociate to hydrogen atoms. Atomic hydrogen so formed is adsorbed on the steel surface. This model was proposed by Wang [27]. The reaction involved in this adsorption is given in equation 2.3

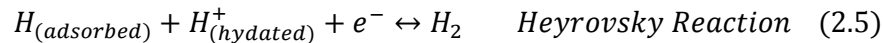


These adsorbed hydrogen atoms are absorbed into the bulk of the steel in the presence of recombination inhibitors, As,  $S^{2-}$  etc. In the absence of recombination inhibitors, hydrogen atoms recombine to form hydrogen molecule,  $H_2$  and escape from the surface.

### 2.3.2 Hydrogen Recombination

In the absence of hydrogen recombination inhibitors, a considerable fraction of hydrogen atoms adsorbed on the steel surface recombine to form hydrogen molecule

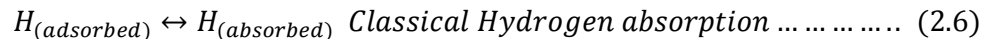
which evolves out of the surface. This recombination reaction follows Tafel [28, 29] and Heyrovsky [30-32] mechanisms at low and high overpotentials which are given in equation 2.4 and 2.5 respectively



Combining the Volmer's electroadsorption with the recombination reactions, the evolution of hydrogen at the steel cathode follows either Volmer-Tafel-Pathway at low overpotentials or Volmer-Heyrovsky-Pathway at high overpotentials.

### 2.3.3 Hydrogen absorption

A fraction of the total adsorbed hydrogen atoms have propensity to be absorbed in the bulk of steel by diffusion if there is a concentration gradient between the surface and the bulk. Presence of recombination inhibitors on the surface of steel suppresses the hydrogen evolution by inhibiting the formation of hydrogen molecule. This causes concentration gradient to increase which results in higher amounts of hydrogen absorption. This reaction is given below:



Recently, another mechanism for hydrogen absorption in steel is proposed by Crolet et al [33-36]. This mechanism suggests that hydrated hydrogen ion ( $H_{(hydrated)}^+$ ) in contact with steel losses its water and proceeds directly to the surface-bulk interface of steel and absorbed as ion. The reaction is presented as follows:



## 2.4 Solubility of hydrogen in steel

Hydrogen atom, which enters into steel, remains inside as a solute atom. In an isothermal and closed system, solubility of hydrogen in steel is governed by Sievert's

law [37] under the equilibrium conditions. The equilibrium reaction for absorption of hydrogen in steel is



And the corresponding equation for equilibrium solubility of hydrogen in steel is

$$\bar{H} = K_S \sqrt{P_{H_2}} \dots \dots \dots (2.9) \text{ in which}$$

$$K_S \propto \exp\left(-\frac{\Delta H_S}{RT}\right) \dots \dots \dots (2.10)$$

In the above relation,

$\bar{H}$  = Concentration of hydrogen atom in the liquid metal

$P_{H_2}$  = Partial pressure of hydrogen in gas atmosphere

$K_S$  = The equilibrium constant, exponentially decreases with temperature,

$\Delta H_S$  = Enthalpy of dissolution of hydrogen in the metal

$R$  = Gas Constant

$T$  = Temperature in K

Hirth [19], based on a compendium of experimental data, suggested that, for iron and its alloys,

$$K_S = 0.00185 \exp\left(-\frac{3440}{T}\right) \dots \dots \dots (2.11)$$

At room temperature, hydrogen dissolved in steel occupies the tetrahedral site of ferrite phase ( $\alpha$ -iron with BCC lattice) and octahedral site in austenite phase ( $\gamma$ -iron with FCC lattice) depending on the free volume and void size [38-40]. The solubility of hydrogen depends on temperature, pressure, and the crystal structure of steel [41]. This is evident from Fig. 2.2, which shows the solubility of hydrogen in different phases of steel as a function of temperature and pressure. The figure reveals a sudden increase in solubility when ferrite ( $\alpha$ ) transforms to austenite ( $\gamma$ ) upon heating. The solubility drops again at higher temperatures when austenite ( $\gamma$ ) transforms to delta-ferrite ( $\delta$ ). In liquid iron, the

solubility of hydrogen is reported to be as high as 34wppm at 1600°C and 1 atm. [42, 43]. When cooled to room temperature under nonequilibrium conditions, hydrogen retained in the microstructure can be much above the solubility limit since the solubility of hydrogen in steel at room temperature is quite low. In the martensite phase, this solubility is reported to be lower (0.4wppm) than that in the austenite phase but is higher than that in ferrite ( $3 \times 10^{-4}$ wppm) [44].

From the above, it is clear that in liquid iron, the solubility of hydrogen is much higher than that in its different crystallographic forms in solid state. Therefore, during solidification of steel, hydrogen solubility decreases. This makes steel supersaturated with hydrogen in the solid state if hydrogen has entered in the steel in the molten state.

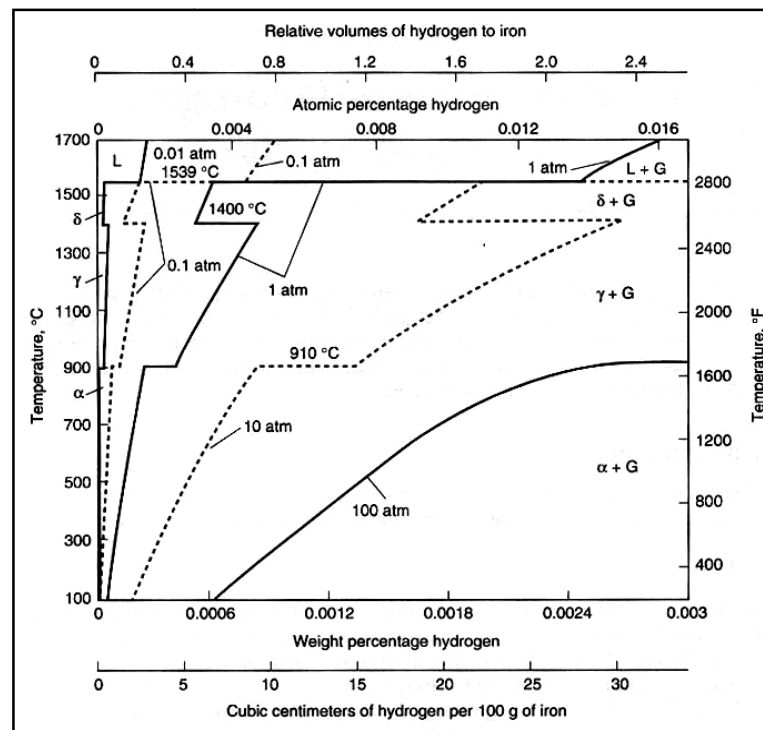


Fig. 2.2 Solubility of hydrogen in iron as a function of temperature and pressure [41]

## 2.5 Diffusion of hydrogen in steel

Hydrogen dissolved in steel is free to diffuse and due to the small size of hydrogen atom, hydrogen diffusivity is highest in steel among all the elements. This

diffusion is governed by Fick's laws [45]. Fick's first law for steady state diffusion postulates that the magnitude of flux diffusing from regions of higher concentration to lower concentration is proportional to the concentration gradient between the two regions. This is expressed as follows:

$$J = -D\nabla C \dots \dots \dots (2.12)$$

Where,  $J$  = Magnitude of flux, measures the amount of substance flowing through unit area per unit time,

$D$  = Diffusion coefficient or diffusivity,

$C$  = Concentration and

$$\nabla = \frac{\partial}{\partial x} + \frac{\partial}{\partial y} + \frac{\partial}{\partial z} = \text{Gradient operator}$$

$x, y, z$  = Position or distance [length]

$$\frac{\partial C}{\partial x} = \text{Concentration gradient along } x \text{ direction}$$

Diffusion of hydrogen in steel follows the non steady state. It is governed by Fick's second law of diffusion which is expressed as follows

$$\frac{\partial C}{\partial t} = D(\nabla^2 C) \dots \dots \dots (2.13)$$

Where,

$$\nabla^2 = \text{Laplace operator} = \nabla \cdot \nabla = \frac{\partial^2}{\partial x^2} + \frac{\partial^2}{\partial y^2} + \frac{\partial^2}{\partial z^2}$$

$$\frac{\partial C}{\partial t} = \text{Change in concentration with respect to time}$$

Diffusion of hydrogen in steel depends upon various factors such as microstructure of steel, temperature and external stress applied to steel.

### **2.5.1 Dependence of diffusion on steel microstructure**

Diffusion of hydrogen through steel lattice is significantly influenced by the crystal structure of the material. Hydrogen diffuses with high mobility in ferrite ( $\alpha$ -Fe

with BCC structure, 32% free space) than in austenite ( $\gamma$ -Fe with FCC structure, 26% free space) due to higher free space and lower packing fraction in ferrite. Also, the diffusivity of hydrogen in austenite is lower by an order of magnitude than in martensite with BCT or distorted BCC unit cells [46].

### 1.5.2 Dependence of diffusion on Temperature

Diffusivity is exponentially related to temperature according to an Arrhenius type relation as follows:

$$D = D_0 \exp\left(-\frac{E_a}{kT}\right) \dots \dots \dots (2.14)$$

Where,  $D_0$  = Diffusion constant or lattice diffusivity

$E_a$  = Activation Energy for diffusion at temperature T

$k$  = Boltzman Constant

### 2.5.3 Dependence of diffusion on applied stress

When a stress is applied to the steel, hydrogen diffuses under stress gradient toward the regions of high stress. The diffusion flux depends not only on the concentration gradient, but also on the stress gradient according to equation [47]:

$$J = -D \left( \frac{\partial C}{\partial x} - \frac{c\bar{V}}{3RT} \frac{\partial \sigma_h}{\partial x} \right) \dots \dots \dots (2.15)$$

Where,

$D$  = Apparent Diffusivity

$\sigma_h$  = Stress

$\frac{\partial \sigma_h}{\partial x}$  = Stress Gradient

$c$  = Concentration of hydrogen and

$\bar{V}$  = Partial Molar Volume

From the equation, it is clear that, the diffusion of hydrogen can take place under the stress gradient, even when hydrogen distribution is uniform inside the material. This is because, even if the concentration gradient diminishes i.e.,  $\left(\frac{\partial C}{\partial x} = 0\right)$ , there will be still diffusion under the stress gradient.

## 2.6 Trapping of hydrogen in steel

During the diffusion of hydrogen in the bulk of steel, its mobility can be hindered at various sites called traps. A trap is a barrier where hydrogen is preferentially retained and the activation energy required to overcome this barrier is much higher than the activation energy of normal lattice sites otherwise occupied by hydrogen atoms. Fig. 2.3 schematically represents free energy levels of the trapping sites, which is lower than that of the normal site by a quantity of  $\Delta E_X$  and is bound by a high energy barrier, whose energy is the sum of the energy in the normal site  $E_a$  and the additional energy  $E'$ . This means that hydrogen requires energy equal to  $E_a + E'$  to overcome the barrier before arriving at the trapping site, and it requires much more energy to escape from the trapping site. This is the reason for the accumulation of hydrogen at the trapping sites [48]. The traps in the steel microstructure are classified in several ways based on the binding energies and the type of hindrance they offer to the hydrogen transport. Based on binding energies, they are categorized as reversible and irreversible traps [49, 50]. Reversible traps such as dislocations, grain boundaries, vacancies, substitutional atoms and interstitial sites are weak traps with lower binding energies and can accommodate only a finite number of atoms [38, 51] hence are saturable in nature. Irreversible traps, which include voids, particle matrices and inclusions, have higher binding energies. Davison has extended this classification by proposing a very reversible trap [38, 52, 53]. Binding energies and detrapping temperatures for these traps are shown in Table 2.1.

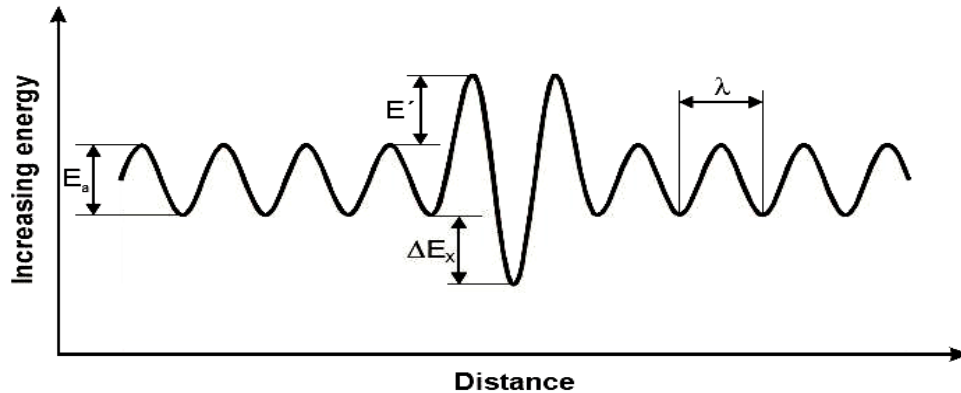


Fig. 2.3 Schematic of the interaction energy of atomic hydrogen and trap sites [48]

Table 2.1 Hydrogen trapping energies and detrapping temperatures

Type of Hydrogen trap	Binding Energy (kJmol <sup>-1</sup> )	Detrapping Temperature (°C)
<u>Very Reversible</u> Interstitial Lattice sites, Elastic stress field, Dislocations	≤ 7.7	30
<u>Reversible</u> Ti-Substitutional atom, Grain Boundary, Dislocation, Fe-C and Fe- Cementite Interface, Martensite	17 - 36	112 - 270
<u>Irreversible</u> Microvoids, Inclusions and particle matrices like : Fe <sub>2</sub> O <sub>3</sub> , Fe <sub>3</sub> O <sub>4</sub> , MnS, Al <sub>2</sub> O <sub>3</sub> , SiO <sub>2</sub> , TiC, Ce <sub>2</sub> O <sub>3</sub>	37-112 129	305-750 >750

Traps, based on the kind of hindrance they offer, are classified into attractive traps, physical traps, repellers and obstacles [54, 55]. Attractive traps exert an attractive force upon the hydrogen atom. Hydrogen atoms fall randomly into a physical trap. A repeller is a region which exerts repulsive forces for hydrogen. An obstacle is a region of discontinuity through which hydrogen cannot diffuse. It is noteworthy that attractive

traps and repellers exert mutually opposite effects on hydrogen and so does physical traps and obstacles. Schematic presentation of these traps is shown in Fig. 2.4.

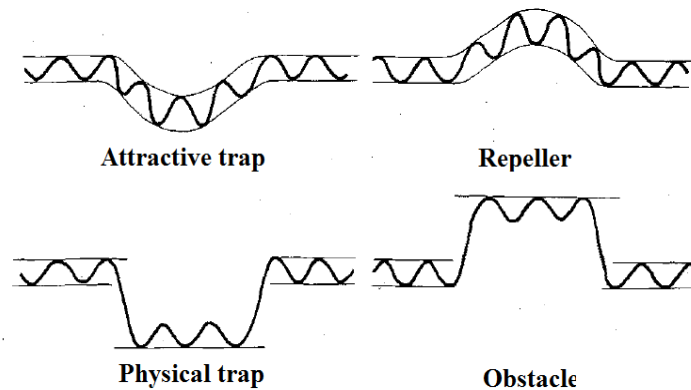


Fig. 2.4 Schematic representation of traps on the basis of their effect on hydrogen [55]

Due to trapping of hydrogen in the various kinds of traps in steel, its lattice diffusion is hindered. As a result, there is a decrease in diffusivity of hydrogen in steel. The variation of overall or apparent diffusivity (lattice diffusivity hindered by traps) of hydrogen in different steels as a function of temperature is reported by Coe et al summing up different studies in literature [56] which is shown in Fig. 2.5. This figure also shows the lattice diffusivity of hydrogen in steel. It is clear from the figure that, at 30°C, lattice diffusivity of hydrogen in steel is  $\sim 10^5 \text{ cm}^2 \text{ s}^{-1}$  whereas its apparent diffusivity (which is experimentally determined) is reduced to  $10^{-9} \text{ cm}^2 \text{ s}^{-1}$  in presence of traps. Even at higher temperatures, the apparent diffusivity is several orders lower than the lattice diffusivity. Therefore presence of traps results in decrease of the apparent diffusivity of hydrogen. Also, it causes an increase in the apparent solubility of hydrogen due to the accumulation of hydrogen at the trap sites.

## 2.7 Hydrogen Embrittlement

It is clear from the above discussion that traps in steel reduce the apparent diffusivity of hydrogen or increase the apparent solubility. Further, diffusivity is affected by stress. Hence, there is a tendency for hydrogen atoms to get accumulated at locations

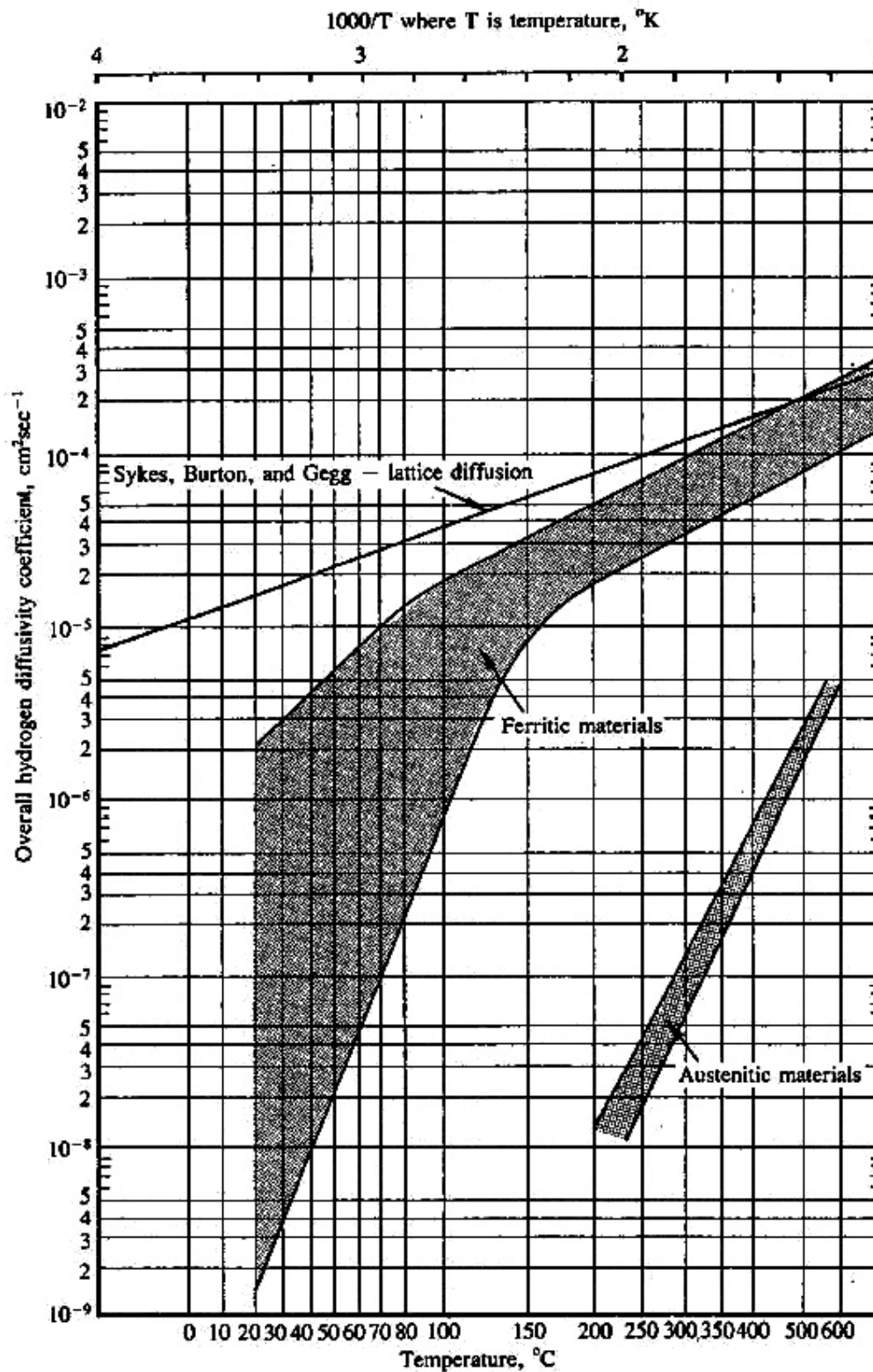


Fig. 2.5 Variation of overall/apparent hydrogen diffusivity with temperature in steels

of stress concentration in steel lattice. If the concentration of accumulated hydrogen reaches a critical level, it interacts with the lattice and causes reduction/loss of ductility of the steel leading it to fracture. This phenomena is popularly known as hydrogen embrittlement or hydrogen assisted cracking (HAC). To sum up, hydrogen embrittlement of steel takes place if the following are present in steel:

1. Crack susceptible microstructure,
2. Residual tensile stress,
3. Sufficient amount of hydrogen

Although many theories/models were proposed to explain the interaction of hydrogen trapped in the steel lattice structure, and its effects resulting hydrogen embrittlement, the actual mechanism is still not clear. Various theories proposed for hydrogen embrittlement are briefly given in the following section.

## **2.8 Theories of hydrogen embrittlement**

### ***2.8.1 Internal Pressure Model***

Internal pressure model [57, 58] is based on the approach that, molecular hydrogen is trapped within the voids or defects such as interfaces, carbides and non-metallic inclusions in steel generating large internal pressure. The pressure of hydrogen molecules in such defects increases according to the solubility law. This large internal pressure causes void growth and crack propagation in steel. Blister formation is an example of this model [59].

### ***2.8.2 Decohesion Model***

Decohesion model, initially proposed by Troiano [60] and modified by Oriani [61, 62], suggests that that electrons from hydrogen atoms enter the d-band (conduction band) of iron and raise the inter-atomic spacing and reduces the cohesive strength of iron atoms at the regions of hydrogen accumulation. Troiano supposed this region to be the

region of triaxial stress whereas Oriani supposed this to be a region at a few atomic distances from the crack tip. The reduction of the cohesive strength results in a brittle crack nucleation, which rejoins the crack front continuing the crack propagation. Troiano considered this process to be repetitive, producing a discontinuous propagation while Oriani considered this as a continuous and non-intermittent phenomenon.

### ***2.8.3 Surface Energy Model***

Surface energy model is proposed by Petch *et al* [63, 64]. It suggests that hydrogen adsorbed on the surface of steel decreases the cohesive strength of iron atoms on the surface, thermodynamically leading to a reduction in the energy required to produce brittle fracture. Also, interaction of adsorbed hydrogen with strained bonds at the crack tip involves a reduction in bond strength [65]. The difference between the adsorption model and decohesion model is the site of embrittlement. In this case, hydrogen will be preferentially adsorbed on the surface itself rather than at ‘few atomic distances’ below the surface.

### ***2.8.4 Hydride Phase Model***

The hydride induced cracking model proposed by Westlake *et al* [66] suggests the formation of a brittle hydrogen enriched phase (iron hydride) at regions of high triaxial stress such as the crack tip. This hydride phase affects the mechanical properties of the metal leading to a brittle crack. However, for iron it was found that no stable hydrides are formed up to hydrogen pressure of 2 GPa.

### ***2.8.5 Dislocation Interaction/Slip softening Model***

Dislocation Interaction model was proposed by Beachem *et al* [67]. This model suggests that hydrogen would enter in the metal matrix at the crack tip, the deformed surface and the regions of higher triaxial stress, dissolved at a region just ahead of the crack tip and helps the crack propagation entirely by microscopic plastic flow at the tips

of cracks. This model presents three different modes of fracture, microvoid coalescence, quasicleavage and intergranular fracture. The cracking modes are determined by microstructure, crack tip intensity or stress intensity factor and concentration of hydrogen. Further developments to this model is provided by Lynch [68] who suggested that adsorption of hydrogen at crack tip results in weakening of interatomic bonds. This weakening facilitates injection of dislocations from crack tips thus promotes coalescence of cracks (microvoids) with voids ahead of existing crack fronts which is accompanied by plastic flow. These result in crack growth. An advanced version of dislocation interaction model is hydrogen enhanced localized plasticity (HELP) model proposed by Beacham [69]. Further, high resolution fractographic examinations of Binbaum and Sofronis [70-74] provided experimental evidence in favour of HELP model showing that the hydrogen related fracture is due to the “locally enhanced plasticity at the crack tip” rather than “loss of macroscopic ductility”. Presence of hydrogen in steel decreases the barriers to dislocation motion i.e., increases the dislocation motion, thereby increasing the deformation that occurs in a localized region adjacent to the fracture surface. Final fracture is a highly localized ductile rupture. The enhanced dislocation mobility is due to the shielding or reduction of the elastic interactions between dislocations and obstacles by the hydrogen solutes.

### ***2.8.6 Corrosion Enhanced Plasticity (CEP) Model***

Corrosion Enhanced Plasticity (CEP) Model proposed developed by Magnin et al [75] takes into account the generation of vacancies due to localized anodic dissolution and hydrogen evolution by cathodic reaction at the newly depassivated crack tip. Thus, corrosion produces an enhanced localized plasticity. The activated dislocations along slip bands form pile-ups interacting with obstacles. The resulting high local stress can initiate cracking.

Though there are many theories on hydrogen embrittlement or HAZ, it is reported that none of them could explain all aspects of this phenomena because of its diversified nature [76].

## **2.9 Hydrogen Assisted Cracking (HAC) in steel weldments**

Most of the carbon and alloy steel welding is carried out using arc welding processes and the arc temperature is very high; typically around 10,000°C. Such a high temperature produces arc plasma dissociating almost all the molecules present in the arc column to ions. In arc welding processes, especially those that employ flux to protect the molten metal during welding, like shielded metal arc welding (SMAW) or submerge arc welding (SAW), hydrogen is present in the welding arc. Due to the high solubility of hydrogen in the molten weld pool, large amount of this hydrogen dissolve in the molten weld metal prior to its solidification. As solubility of hydrogen decreases significantly on solidification and cooling of weld is quite fast, sufficient time is not available for hydrogen to diffuse out of the weld. Hence, at the end of welding, weld metal remains supersaturated with hydrogen. As the application of heat during welding is highly localized and cooling after welding is very rapid, localized expansion and contraction in a weld joint produces tensile residual stresses in the weld joints. In the case of steel welding, high cooling rate of the weld and the adjacent heat affected zone of the base metal can, depending on composition and cooling rate, also produce hard bainitic or martensitic microstructures. Therefore, all the criteria for HAC, sufficient hydrogen, high tensile residual stresses and susceptible microstructure, are satisfied in the case of steel welds, making them highly prone to HAC. Cracks may appear in several locations of a weldment as shown in Fig. 2.6 but mostly in the heat-affected zone (HAZ). These cracks develop over a period after welding is completed.

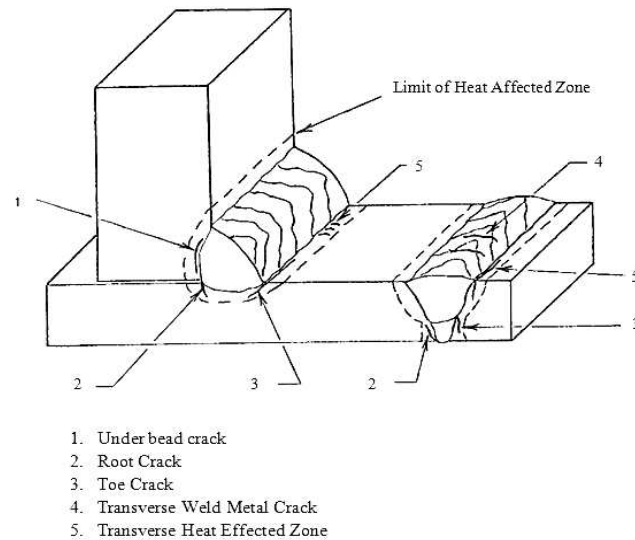


Fig. 2.6 Locations of delayed cracks in weldment

## 2.10 Source of hydrogen in steel weldments

Various sources of hydrogen in different arc welding processes are divided into two categories, major and minor sources depending on amount of hydrogen they release and contribute to the total hydrogen of the weld metal.

Major sources of hydrogen in weld include hydrogen from chemically bonded water in the hydrocarbon and non-hydrocarbon ingredients in the electrode flux coating (SMAW), powder flux (SAW) and hydrogen in shielding gas (GTAW and GMAW) [77-80], incidental hydrogenous materials on electrode surface. Hydrogen in some of these sources is stable up to 900°C and contributes largely to the hydrogen in weld.

Minor sources of hydrogen in weld include moisture, oil, primer, paint, grease and oxide layers on the base metal surface, moisture absorbed by the powdery electrode core and flux coating from humid air, residual hydrogen in the bulk of the base metal, moisture from the surrounding of welding atmosphere. These sources can be reduced or eliminated by baking the electrode in the temperature range of 100-350°C.

## 2.11 Solubility of hydrogen in steel weldments

Based on a careful analysis of literature data and experimental results, Sievert's law appears insufficient to explain of solubility of hydrogen during welding [81]. Several investigations which are based on Sievert's law reported that temperature of the surface of weld pool for hydrogen absorption is greater than 2500°C [82-86]. However, this temperature on the surface of weld pool was predicted as impossibly high in several investigations [87-91]. Further, some investigations based on Sievert's law predicted the hydrogen absorption to be maximum at the center of the weld pool as shown in Fig. 2.7(a). Also, this law does not take into account the monoatomic hydrogen solubility and ionization of hydrogen in the welding arc.

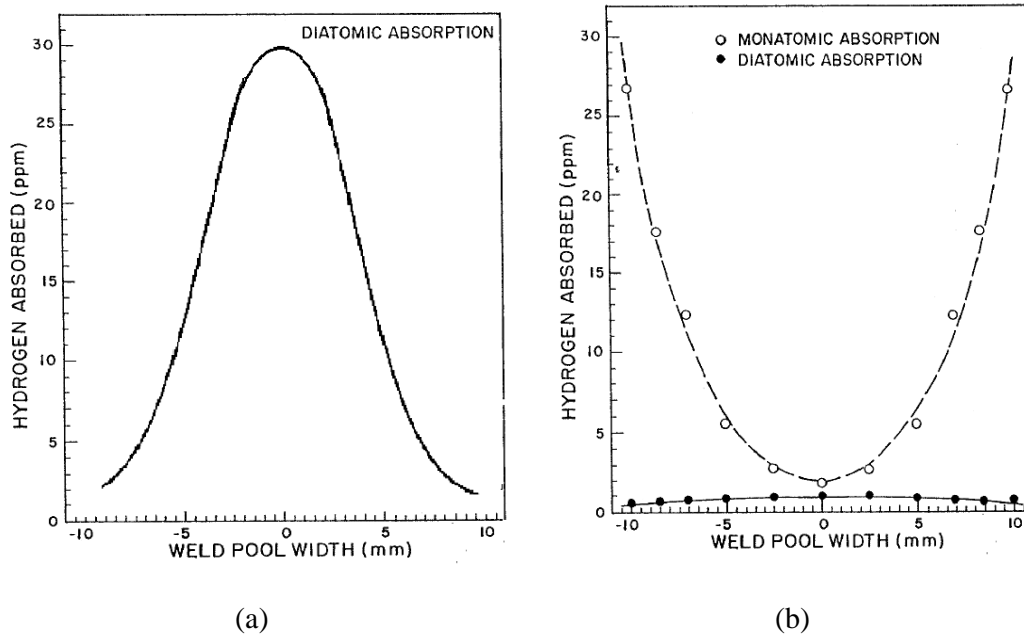


Fig. 2.7 Absorption of hydrogen in the weld pool following (a) Sievert (b) Gedeon

The above insufficiencies were considered in a model proposed by Gedeon at al for hydrogen solubility in weld pool [81, 91, 92]. This model assumed that, during welding, hydrogen dissociation and absorption depends on the reaction temperature of cathode boundary layer and the surface temperature of weld pool respectively, and

predicted that maximum hydrogen distribution is at the trailing edges of the weld pool as shown in Fig. 2.7(b). This model also predicted that, at a given reaction temperature, hydrogen solubility in the weld pool increases linearly as a function of partial pressure of monatomic hydrogen. However, in a fixed hydrogen atmosphere, hydrogen solubility decreases monotonically with increase in absorption reaction temperature as shown in Fig. 2.8 (a). These are different from the solubility patterns obtained by Sievert's law as shown in Fig. 2.8 (b). A further investigation [93] on hydrogen solubility provided necessary experimental support to Gedeon's model. The amount of hydrogen absorbed, diffused and trapped in the weld depends upon the thermal cycles of the weld pool. Variation in temperature significantly affects the diffusion and trapping behaviour of hydrogen in steel discussed earlier in this chapter. These discussions are valid in a similar way for hydrogen in steel weldments.

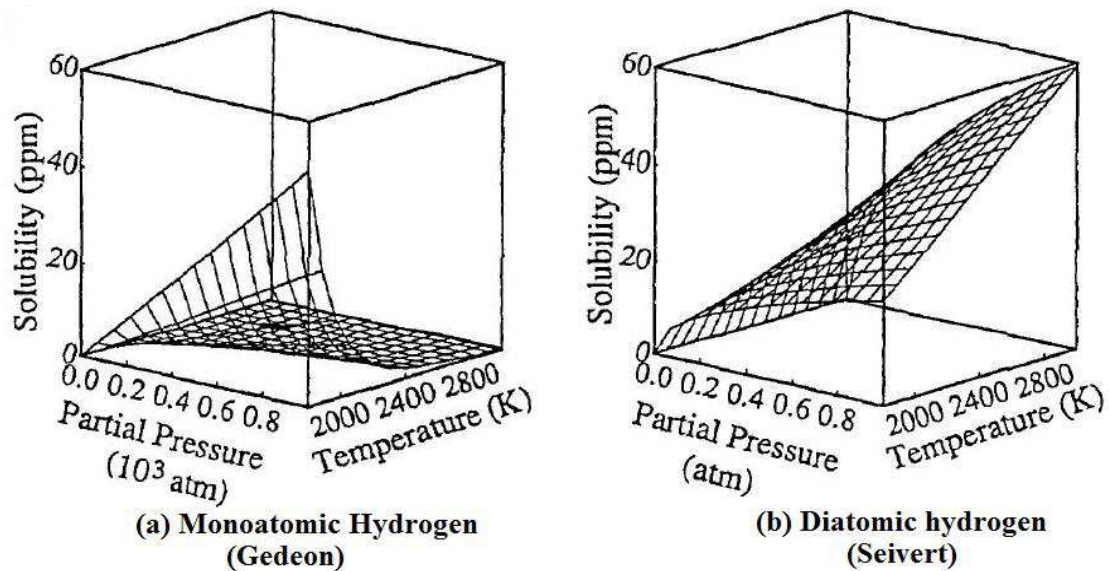


Fig. 2.8 Solubility of hydrogen in weld pool [93]

## 2.12 Residual hydrogen and diffusible hydrogen

Hydrogen dissolved in steel is divided into two categories namely residual hydrogen, and diffusible hydrogen ( $H_D$ ). Residual hydrogen is trapped in the irreversible

traps in the weldments. These traps have higher binding energy for hydrogen and temperatures higher than 600°C are required to make hydrogen released from these traps. Therefore, residual hydrogen can not diffuse at the lower temperatures at which HAC takes place and thus does not contribute to HAC.

Diffusible hydrogen is trapped in the weak very reversible or reversible sites in the lattice. These traps have lower binding energy which can be overcome at temperatures nearby the ambient temperature. Therefore, diffusible hydrogen is able to diffuse at or near room temperature (i.e., in the vicinity of 45°C) and is considered as potentially responsible for HAC. Diffusible hydrogen present in the weldment is related to sources of hydrogen in the welding consumable as follows [94]:

$$H_D = [\alpha^2(\eta_1 a_1 + \eta_2 a_2) + \beta^2 b]^{\frac{1}{2}} \dots \dots \dots (2.16)$$

For 50% carbonate in the coating of a basic coated electrode, equation 2.16 reduces to the empirical relation as follows

$$H_D = [260a_1 + 30a_2 + 0.9b - 10]^{\frac{1}{2}} \dots \dots \dots (2.17)$$

In the above relations,

$H_D$ : Diffusible hydrogen content

$a_1$ : Coating moisture in AWS A5.5 Coating moisture test after baking electrode (Wt%)

$a_2$ : Moisture absorbed by the coating after baking the electrode until the time of welding

$b$ (mm Hg): Partial pressure of water vapor in the ambient atmosphere

$\eta_1$  and  $\eta_2$ : Efficiency of moisture transfer from coatings into atmosphere

$\alpha$ : A constant indicating activity of moisture in the coating on hydrogen content dissolved into weld metal, (ml/100g\*wt %) <sup>1/2</sup>:

$\beta$ : A constant indicating the activity of humidity in ambient atmosphere on hydrogen content dissolved into weld metal, in (ml/100g) (mm Hg) <sup>1/2</sup>

The empirical equation 2.17 reveals that the chemically bonded water contributes much higher to the diffusible hydrogen content in weld metal than the absorbed moisture [95].

### 2.13 Distribution of hydrogen in weldments

Hydrogen absorbed in the weld pool has propensity to diffuse within the weldment. This diffusion depends upon temperature, microstructure of the material, solubility, trapping and stress effects. Diffusion and accumulation of hydrogen in the heat affected zone (HAZ) of weldment has been first explained by Granjon [96] and is modified for carbon steels by Kou [97] based on the transformation temperatures of weld metal and HAZ in the weldment during welding. In the case of carbon steel welds, composition of the consumables are such that the microstructure of the weld metal in the as welded condition is predominantly ferritic. However, HAZ microstructure can be ferritic or bainitic or martensitic depending of the composition and cooling rate experienced during welding. Consider a typical case in which weld metal transforms to ferritic and HAZ to martensitic/ bainite. Transformation of austenite to ferrite occurs at higher temperature ( $T_F$ ) than transformation of austenite to martensite/bainite ( $T_B$ ). As a result, during cooling of the weldment, weld metal transforms into ferrite at high temperature while HAZ still remains austenite as shown in Fig. 2.9.

As solubility of hydrogen in the ferrite is lower than that in austenite, hydrogen is rejected from the weld metal ferrite to HAZ austenite just adjacent to the fusion line. The higher diffusivity of hydrogen in ferrite also favours this process. Consequence of this is accumulation of hydrogen in the HAZ adjacent to the fusion line. Upon transformation of austenite to martensite, hydrogen solubility in the HAZ matrix decreases and hydrogen becomes supersaturated in the HAZ. This re-distribution of hydrogen in the weldment due to difference in the transformation behaviour of weld metal and HAZ make HAZ more susceptible to cracking than the weld metal in the case of carbon steel

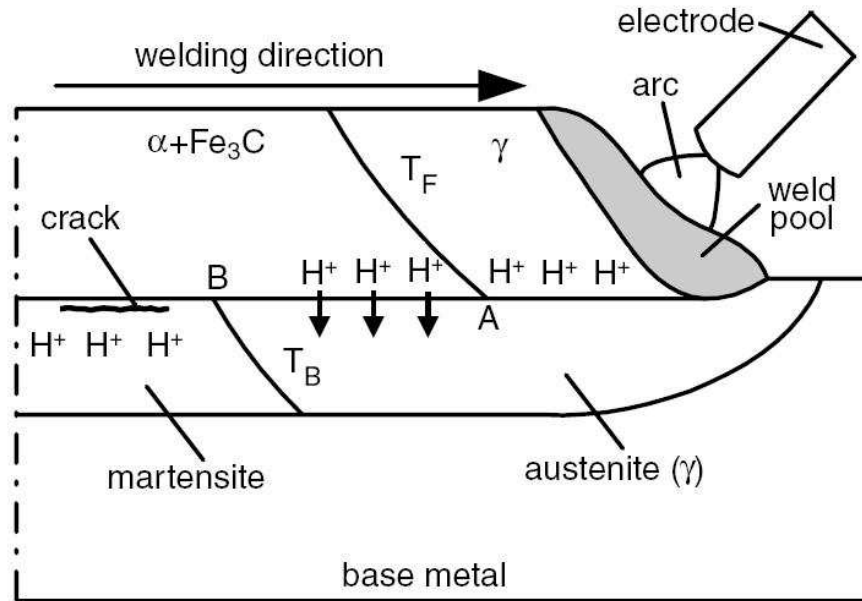


Fig. 2.9 Schematic representation of diffusion of hydrogen to HAZ [97]

welds. The above concept is further verified by Wang et.al [98] by calculating the hydrogen concentrations across the weldment.

Nevertheless, cracking need not always confined to HAZ in all steel welds. In case of alloy steels, composition of the welding consumables and base metal are similar and hence transformations that occur in HAZ and weld metal are similar. In this case, hydrogen distribution within HAZ and weld metal may not differ much and hence both would be equally susceptible to cracking. . In the case of high strength low alloy steels in which carbon content is reduced and strength is achieved by microalloying and microstructural modification using thermomechanical processing, both HAZ and weld metal remains ferritic [99, 100] and weld metal is more susceptible to HAC than HAZ.

## 2.14 Prevention of HAC in weldments

The underlying principle to reduce HAC in a weldment is to reduce or remove one of the following three from the weldment. These are i) Crack susceptible microstructure, ii) Residual stress, and iii)  $H_D$  content. As the main source of hydrogen in

weldment is the moisture in the electrode covering, hydrogen can be reduced by baking of the welding electrodes. However, the hygroscopicity of the flux coating quickly picks up moisture from the ambient. Also, electrodes with cellulose coating produces gaseous shield rich in hydrogen in the welding arc. However, cellulose coated electrodes are not used for welding steels susceptible to HAC.

Probably, reducing the cooling rate of the weld, when it cools down after completion of welding is the most practical way of reducing the risk of HAC. Slow cooling of the weld provides more time for hydrogen to diffuse out of the weld when it is hot and also facilitate formation of ferritic and pearlitic microstructure, which are less susceptible to HAC, than martensite or bainite. Increasing the weld heat input is one of the ways to reduce the cooling rate of the weld; but this may have adverse effect on mechanical properties of the weld joint. Hence, the simplest and the most widely used technique to reduce the risk of cracking is preheating of the parts to be welded to a specified temperature so that after welding, the joint cools down slowly [101, 102].

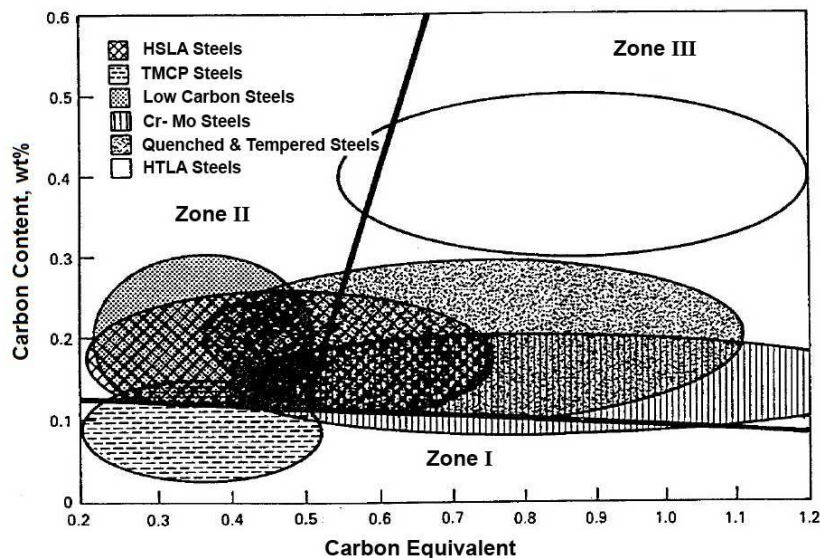


Fig. 2.10 Classification of steels to choose between hardness or hydrogen control

approach to determine safe preheat temperature [103]

There are two approaches recommended in literature to estimate safe preheat temperatures of welding of steels. One considers the importance of changing the microstructure or hardness of the HAZ from more susceptible to less susceptible (hardness control approach) and another gives emphasis to reducing the  $H_D$  content (hydrogen control approach). The choice of the approach would depend on the carbon and alloy content of the steel. In all studies related to HAC, alloy content is represented by carbon equivalent (CE), which normalizes the influence of various alloying elements on HAC to that of carbon [104]. There are many CE proposed by various investigators and valid for different range of composition of the steels. In general, with increase in CE, susceptibility to HAC increases. Important point to be noted is that with increase in alloy content CE will increase and even steels with low carbon content would be susceptible to HAC.

Graville diagram proposed by Graville, in which carbon content of a steel is plotted against CE is used to explain the choice between hardness control and hydrogen control approach for choosing preheat temperature [103, 105]. This diagram, shown in Fig. 2.10 places different classes of steels in three different zones of the diagram based on their carbon content and CE. From this figure, one can find out the susceptibility of various steels to HAC as well as the approaches to be chosen for its prevention. Steels falling in Zone I have least susceptibility to HAC. Steels falling in Zone II have high carbon content and low CE (low alloy content) and for these steels hardness control is used for selection of preheat temperature. This considers four factors: combined thickness, hydrogen content of electrode, carbon equivalent and weld heat input to arrive at minimum preheat temperature that would prevent cracking. For steels in this zone, HAZ hardness can be varied by changing the heat input and preheat temperature. For steels falling in Zone III, CE and carbon content are high as a result, weld microstructure

is always susceptible to HAC, Application of preheating or increasing the weld heat input can not alter the microstructure; hence, the only option to avoid HAC is to ensure diffusible hydrogen in the weld is below the critical level required for cracking. Hence, hydrogen control is adopted for steels falling in this zone.

Many other investigations proposed different cracking parameters to determine a safe preheat temperature and time durations to be employed for preheating [106-120]. Summary of these observations was that preheat temperature is a function of diffusible hydrogen content of the weld.

$$\text{i.e. } T_{preheat}(^{\circ}C) = f(H_D) \dots \dots \dots (2.18)$$

In other words, knowledge of  $H_D$  levels provides the starting point to determine safe preheat temperature. This fact holds the primary motivation for the determination of  $H_D$  content of weld metal.

## 2.15 Classification of $H_D$ in welding consumables

As consumables are the major sources of hydrogen in steel welds, they are classified in various national and international standards based on the diffusible hydrogen that they can introduce into the weld metal produced by them [121-124]. Although these standards have many similarities in definitions and formulations for calculating the hydrogen levels, historically these have adopted different hydrogen levels, as given in table 2.2

It should be noted that, while IIW adopted a linear scale increment of hydrogen levels by units of 5 (5-10-15 ml/100g), AWS uses logarithmic scale (4-8-16 ml/100g) based on the correlation of diffusible hydrogen levels with critical cracking stress, critical preheat temperature, and the like, for avoiding hydrogen cracking [43]. From these correlations, AWS logarithmic system of hydrogen classification is claimed to be more logical than the IIW linear system of hydrogen classification.

Table 2.2: Classification of consumables based on  $H_D$  content

Type of Hydrogen Control	Weld metal diffusible hydrogen (ml/100g)			
	ISO 2560 & IIW	AWS A 5.1	AS/NZ S 3752	JIS Z – 3211* & JIS Z - 3212
Very low	$\leq 5$	$\leq 4$ $\leq 2 \ddagger$	$\leq 5$	$\leq 6$ (780) $\dagger$
Low	$\leq 10$	$\leq 8$	$\leq 10$	$\leq 7$ (750) $\dagger$ $\leq 9$ (610 & 690) $\dagger$ $\leq 10$ (570) $\dagger$
Medium	$\leq 15$	$\leq 16$	$\leq 15$	$\leq 12$ (520) $\dagger$ $\leq 15$ (420* & 490) $\dagger$
High	$> 15$	$> 16$	-	-

$\dagger$  Tensile strength of steel (MPa),  $\ddagger$  under consideration

Unlike the AWS and IIW, Japanese standards, JIS Z 3211 (for mild steel electrodes), and JIS Z 3212 (for high tensile strength electrodes) establish a single maximum diffusible hydrogen limit for each tensile strength level. However, in these standards, the step from low to very low  $H_D$  levels differ by 1 ml/100g of hydrogen content with a decrease from  $\leq 7$  to  $\leq 6$  ml/100g. Considering the reproducibility of the diffusible hydrogen tests to be  $\pm 1$  ml/100g, JIS scale seems impractical [125]. Regardless this factor,  $H_D$  content is an essential variable in standards like ANSI/AWS D1.1–2000 and AS/NZ S 1554.1-2000.

## 2.16 Determination of $H_D$ in weldments

The role of  $H_D$  in HAC of carbon and low alloy steel weldments has been understood for past 70 years and the need for measurement of  $H_D$  has been realized since it provides the first step in the estimation of safe preheat temperature for reduction of  $H_D$  in weldments. Apart from this,  $H_D$  levels are needed to be measured for classification of welding consumables based on their  $H_D$  content. However, determination of  $H_D$  is

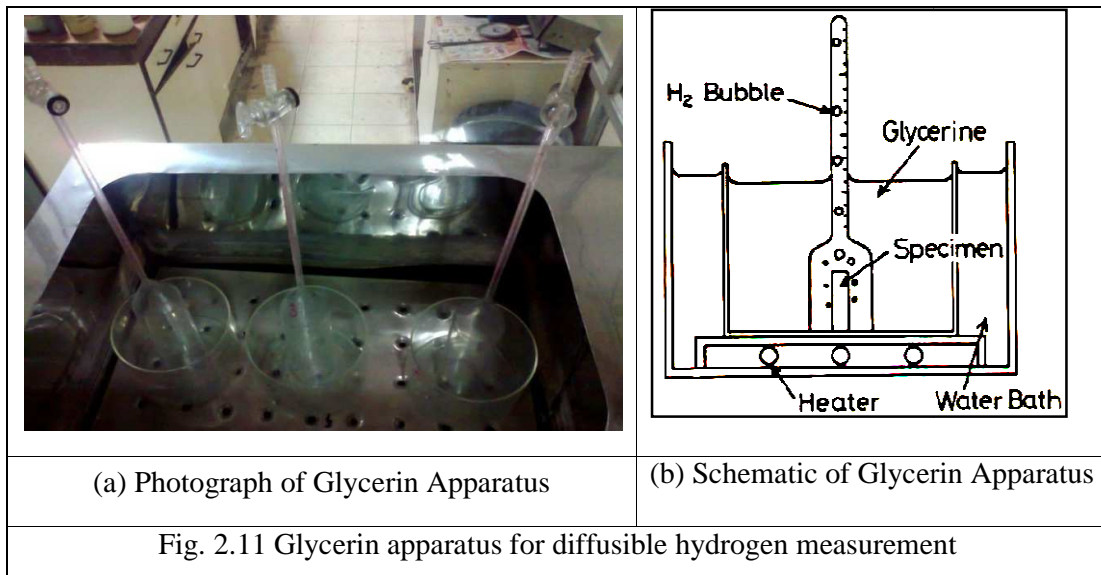
difficult since hydrogen is a transient element in steels. It continuously escapes from the weld even below 0°C. Therefore, it is virtually impossible to prepare reference standards for hydrogen in steels as done for other elements for their analysis [43].

There are several methods for the determination diffusible hydrogen in weldments. Among these, only four methods are recommended by various standards such as IIW/ISO [126], AWS [127], BS [128], JIS [129, 130], DIN [131], AS/NZ [132], GOST [133] and BIS IS [134]. These include glycerin and mercury methods in which collection and measurement of hydrogen is carried out at room temperature, and gas chromatography method and/or carrier gas-hot extraction method and vacuum hot extraction methods for rapid determination of  $H_D$ . All these methods aim to determine  $H_D$  levels under extreme welding conditions. This procedure includes a specimen of carbon steel ( $C \leq 0.2\%$ ) of dimension specified by these standards. Immediately after welding, the specimen is quenched down to -78°C or less and stored at that temperature until it is used for  $H_D$  measurement. The various standard methods recommended for determination of  $H_D$  are discussed below.

### ***2.16.1. Glycerin Method***

Glycerin method is probably the earliest method for determination of  $H_D$  in welds. Principle of measurement of  $H_D$  in this method is the displacement of glycerin by hydrogen and subsequent volumetric measurement of  $H_D$ . Measurement using this method consists of two parts: preparation of weld specimen and collection of hydrogen evolved from the specimen over glycerin. In this method, four test specimen blanks, each of dimensions  $125 \times 25 \times 12 \text{mm}^3$  are used. A single bead is deposited along the 25 mm length with a total of 100mm for four specimens using a prebaked 4mm diameter and 150mm long electrode. The welding conditions are short arc and current, 150A. Immediately after deposition, samples are quenched in water at approximately 20°C and

individual specimens are separated. They are stored in dry ice or liquid nitrogen until measurement.



For measurement of  $H_D$ , each specimen is introduced in an apparatus containing glycerine as shown in Fig. 2.11. Glycerine is maintained at 45°C and hydrogen is collected from the weld sample for 48 hours. Hydrogen evolved from all the four specimens are collected simultaneously in four different apparatus. The amount of gas collected over glycerine is measured to the nearest 0.05 ml and the average estimated is corrected for STP using the following relation:

$$H_{Glycerin} = V_t \left( \frac{273}{273 + T} \right) \left( \frac{P}{760} \right) \left( \frac{100}{W_f - W_i} \right) \frac{ml}{100g} \text{ of deposited metal} \dots \dots (2.19)$$

In the above relation,  $H_{Glycerin}$  = Diffusible hydrogen measured in glycerin method

$V_t$  = Volume of hydrogen measured at temperature  $T$  and pressure  $P$

$W_i$  = Weight specimen before welding

$W_f$  = Weight of specimen after welding

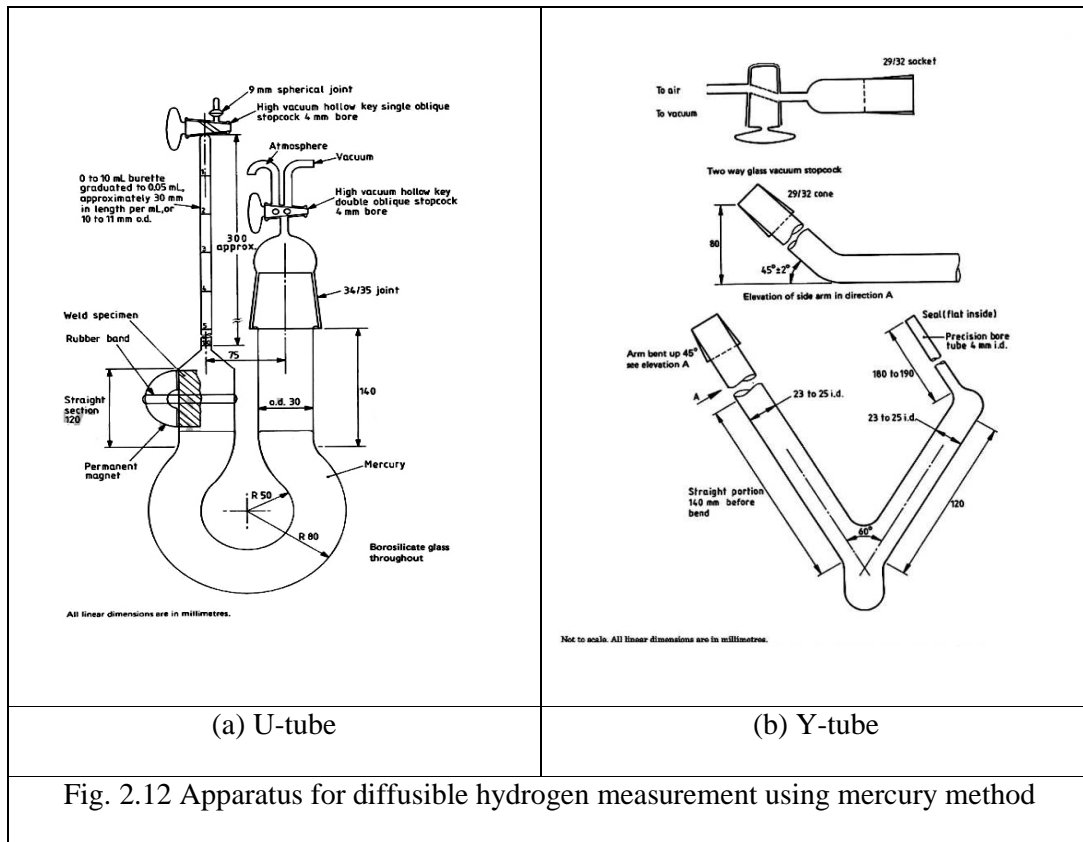
Glycerin method was introduced for short time duration in the AWS Specification A5.5-48T (ASTM A316-48T) in 1948 [135]. Stern *et al* suspected the

accuracy of this method [136] as more gas was collected over mercury than that over glycerin from similar weld specimens. This inaccuracy was attributed to the fact that hydrogen is partially soluble in glycerin. Therefore, this method was removed from AWS A5.5 specification by 1954. Also, many other drawbacks like the dissolution of water vapour, oxygen and nitrogen in glycerin which would contribute to the total gas collected, change in its purity and viscosity with time which would affect its efficiency of hydrogen collection and variation in collected hydrogen contents with varied shapes of glassware are reported over a period of time [137]. Therefore, it is concluded that, this method is not suitable for measurement of lower levels of hydrogen because of significant loss of hydrogen, underestimation and wide scatter (50-90%) in the measurements [138]. However, this method is still in use.

### ***2.16.2. Mercury Method***

The principle of hydrogen measurement using mercury method is the displacement of mercury by hydrogen and subsequent volumetric analysis of hydrogen. The materials, apparatus, procedures of specimen preparation,  $H_D$  collection and its analysis using this method are detailed in many standards mentioned above. Historically, the apparatus is designed for collection of hydrogen in mercury method is either U-shape or Y-shaped. Schematic of these apparatus are shown in Fig. 2.12 (a) and 2.12 (b). Since this method is used in the present study, details on the determination of diffusible hydrogen using this method are given in Chapter 3. The volume of gas collected over mercury is corrected for STP conditions and reported in ml per 100 grams of deposited metal.

Mercury has been tested as a collection medium for hydrogen since the disqualification of glycerin method as a standard for measurement of  $H_D$  in welds [136] and was adopted by IIW in 1977 in the standard, ISO 3690:1977 [43]. It is also included



in AWS A4.3, AS/NZ S3572, BIS IS 11082, BS 6693, DIN 8572. In spite of the toxicity and associated health hazards associated with the use of mercury, this method is retained in the recent revision of IIW, ISO 3690:2012 due to its accuracy precision and reliability in  $H_D$  measurement. This method is recommended as the primary standard for  $H_D$  measurement. Though this method is to be used only for measurement at room temperature, recently, possibility of using this method at higher temperatures up to 180°C has also been reported [139].

### 2.16.3. Gas Chromatography/ Carrier gas hot extraction Method

Gas chromatography and carrier gas hot extraction methods are rapid methods for  $H_D$  measurement. These methods are also included in various standards, ISO 3690: 2000, AWS A4.3-93, AS/NZ S3752, JIS Z 3118, BS 6693 etc. Both these methods use a thermal conductivity detector for the analysis of hydrogen collected. However, these

methods differ in the temperatures and time durations of  $H_D$  collection. Gas chromatography method allows  $H_D$  collection at 150°C for 6 h where as carrier gas hot extraction method allows it at 400°C for 0.5 h [140]; accordingly, these methods use different  $H_D$  collection units.  $H_D$  from weld specimen is collected by holding the weld specimen in a separate closed chamber. In gas chromatography, an aluminium chamber is used for collection where as a quartz or fused silica tube serves this purpose in hot extraction method [141]. After collection of  $H_D$ , its analysis is carried out using a thermal conductivity detector (TCD).

Before the measurement of  $H_D$  collected in the chamber, TCD is calibrated. In principle, TCD uses the difference in thermal conductivity between the analyte hydrogen gas and the carrier gas used in the process. This difference is manifested as a response recorded by an analyser. The amount of hydrogen collected in the chamber is proportional to the area under the response and is estimated by comparing this area with the calibration.

A set of photographs and the schematic of GC method are shown in Fig. 2.13. Detailed description of  $H_D$  measurement using this method is given by Quintana [142] and Pokhodnya [143]. Though results obtained using this method agrees well with mercury method, there remains several limitations. Although this method allows heating the specimen up to 150°C and reduces the collection time to 6 hours, with today's increased demand on quality control and batch testing for product release, still shorter analysis times are called for [144]. Also, this method demands calibration before each analysis [81]. Incomplete purging of the collection chamber, traces of moisture in the carrier gas and moisture contamination in the dehumidifier or in the column significantly affect its results [143].

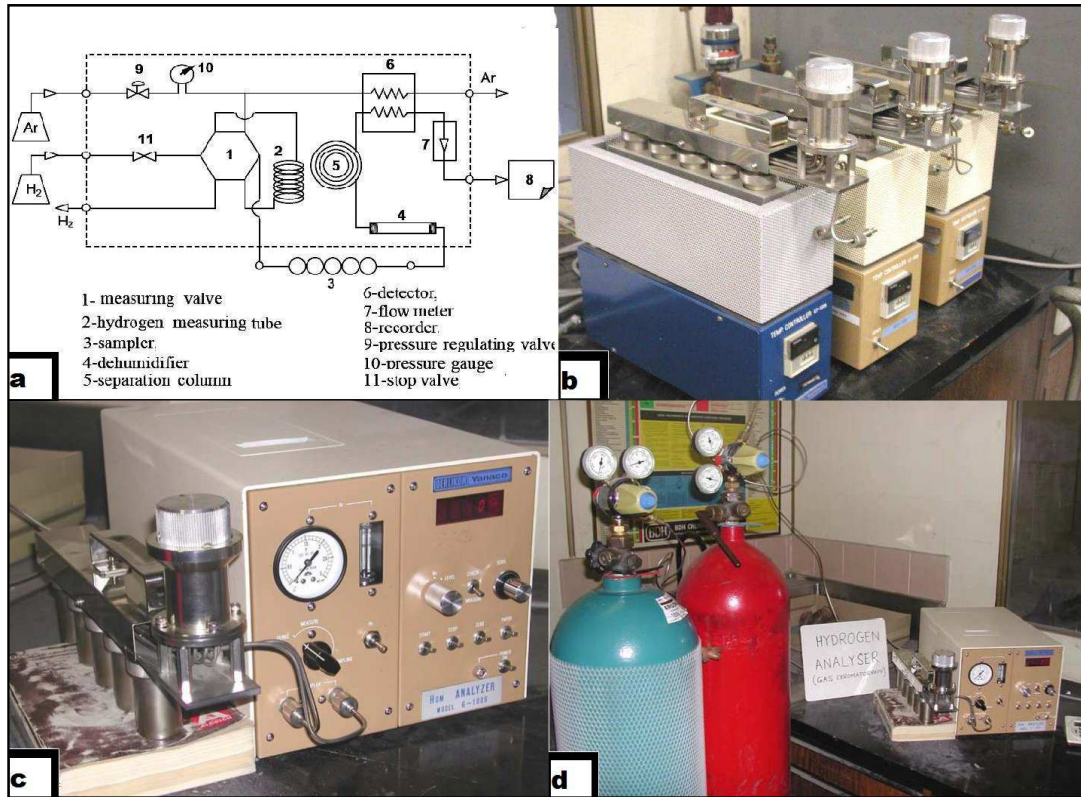
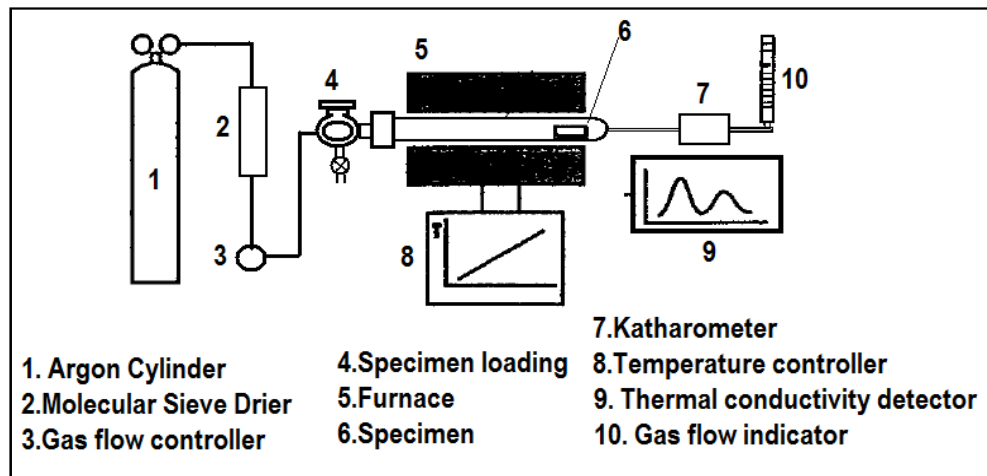


Fig. 2.13 GC setup for diffusible hydrogen measurement (Courtesy: [125])

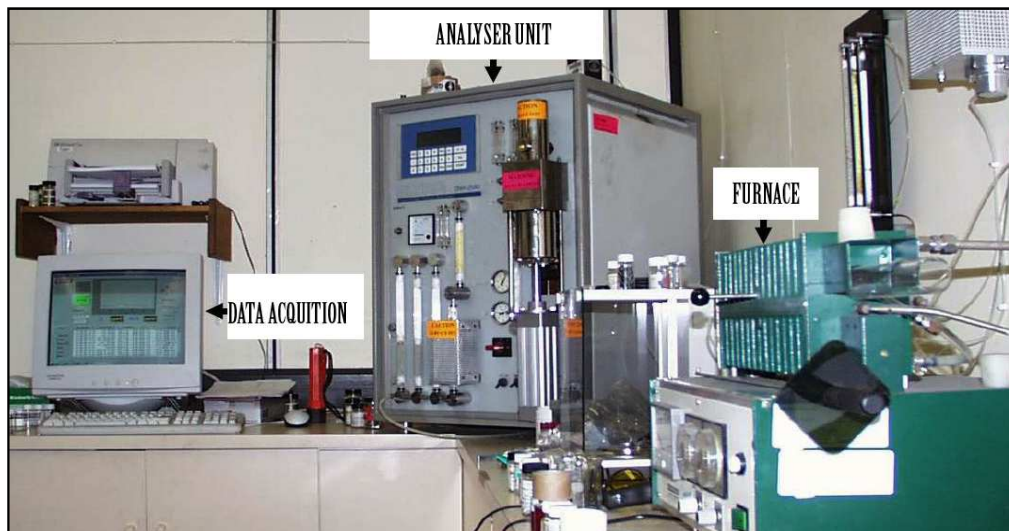
- a) Flow Diagram of GC apparatus      b) Electric Furnaces to heat chamber  
c) Chambers Connected to GC analyser      d) Carrier gas connected to GC analyser

Keeping the limitations of gas chromatography method in mind, hot extraction of  $H_D$  from welds has been investigated for more than 20 years [145, 146]. Schematic and photograph of carrier gas hot extraction are shown in Fig. 2.14 (a) and (b). Collection of  $H_D$  in this method is accomplished within 0.5 h because it allows the collection at 400°C. This method is accurate and its results are reproducible thus reliable. However, it is costly and its availability is too limited. Besides this, there were two principal objections to this method. First, the potential loss of hydrogen through reactions with oxide layers present on the specimen surface [147]. To remove these oxide layers, full sample cleaning by wire brushing was proposed [148]. Second issue was the risk of residual hydrogen

release at higher temperatures which would lead to overestimation of  $H_D$ . However, residual hydrogen release up to 400°C was either found to be insignificant [149] or neglected [150] in view of environmental and safety benefits associated in using this method. Further, many investigations concluded that diffusible hydrogen contents measured in hot extraction method are precise, reproducible, repeatable and are in good agreement with other alternative standard methods, therefore reliable [146, 148-153].



- Schematic of Carrier gas hot extraction setup

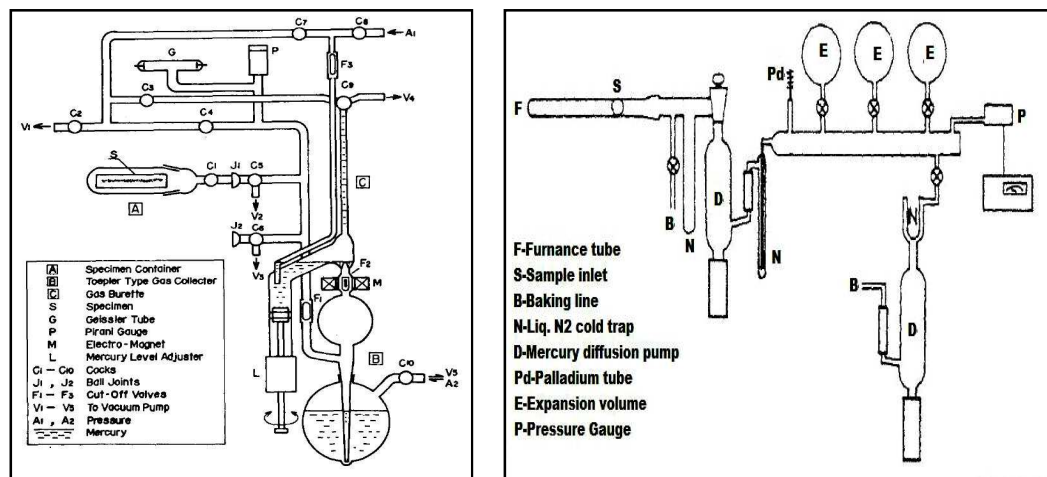


(b) Photograph of carrier gas hot extraction setup (Courtesy: [125])

Fig. 2.14 Carrier gas hot extraction facility for diffusible hydrogen measurement

### 2.16.4 Vacuum-Extraction methods

Literature studies reveal two types of vacuum extraction methods; one measures hydrogen near room temperatures [147] and the other at high temperatures [154]. Schematics of these two methods are in Fig. 2.15. The investigator of room temperature vacuum extraction method claims that the method measures  $H_D$  at a better accuracy than glycerin method. In the vacuum hot extraction method, the weld specimen is heated at higher temperatures in a silica furnace tube for extraction of  $H_D$ . Hydrogen along with any other gas so extracted is passed through two nitrogen cold traps into an expansion volume where condensable gases freeze out. Combined pressure of hydrogen and other gases reaching the expansion volume is monitored by a pressure gauge till the hydrogen evolution ceases. Hydrogen is removed through the palladium/silver osmosis tube and pressure of rest of the gases is measured. The difference in these two pressures is the pressure of  $H_D$ . The  $H_D$  contents obtained in this method are on the lower side as compared to that using the carrier gas hot extraction method [154].



a)At room temperature [147]

b)With hot extraction [154]

Fig. 2.15 Vacuum extraction apparatus for diffusible hydrogen measurement

### 2.16.5 Other methods for diffusible hydrogen measurement

Apart from the above mentioned methods, there are many other methods which are neither included in any standard nor are in wide practice either because of serious drawbacks or because of limited investigation and availability. Most of these methods are similar to mercury or glycerin methods in principle which is based on volumetric displacement of a liquid/fluid by the diffusible hydrogen evolved from the weld specimen and subsequent volume measurement. These differ only with respect to the type of fluids over which diffusible hydrogen is collected. The liquids which are employed in these methods include silicone oil [155], water [156], 10N K<sub>2</sub>CO<sub>3</sub> [157], ethyl alcohol, ethylene glycol, paraffin and carbon tetrachloride [137]. The percentage of diffusible hydrogen collection over these fluids in comparison to mercury is given in Table 2.3.

Table 2.3 Efficiency of H<sub>D</sub> collection over different collecting fluids [137]

Collecting mediums	Efficiency of H <sub>D</sub> collection (%)	Remark
Mercury	100	Widely Accepted
‡ 10N K <sub>2</sub> CO <sub>3</sub>	100	Insufficient investigation
*Water	100	Insufficient investigation
Silicone oil	100†, 5-32	Insufficient investigation
Glycerin	79-88	Poor accuracy
Ethyl alcohol	23-39	Poor accuracy
Distilled water	58-72	Poor accuracy
Ethylene glycol	18-32	Poor accuracy
Paraffin	10-19	Poor accuracy
Carbon tetrachloride	10-20	Poor accuracy

†[155], \*[156], ‡[157]

Olson et al and Smith have developed three methods namely laser ablation/mass spectrometry [158], tungsten oxide based optoelectronic sensor method [159] and a Seeback hydrogen instrument based on the measurement of thermoelectric coefficient

[160] for diffusible hydrogen measurement in welds. Further, Lasseigne et al [161, 162] have developed a real time non-contact hydrogen sensor based on low frequency impedance measurements. However, at present, these methods are not adopted for diffusible hydrogen measurement in welds.

### **2.17 H<sub>D</sub> measurement using polymer electrolyte hydrogen sensor**

Measurement of diffusible hydrogen in steel welds using polymer electrolyte based hydrogen sensor was first reported by Albert et al [163]. The sensor was an electrochemical fuel cell [164]. It worked in amperometric mode i.e., current is measured as a function of time. The principle of its operation was proton exchange through its conducting polyvinyl alcohol based polymer electrolyte. The conducting polymer was coated with palladium on its either side as anode and cathode. Weld specimens for this measurement were autogenous bead-on-plate welds made on UT-modified HST specimens. Hydrogen was introduced into the weld metal by mixing it with argon in varied proportions. Hydrogen was collected in stainless steel collection chambers at room temperature as a mixture of hydrogen in argon. The Ar-H<sub>2</sub> Mixture was analyzed using the sensor to obtain the concentration of hydrogen collected in the chamber. Results obtained in this method showed good correlation with the gas chromatography analysis. Therefore, the authors proposed this sensor as an additional method for measurement of diffusible hydrogen. However, the sensor was reported to have poor long term stability with its response behavior [165].

### **2.18 Effect of pre- and post-heating on diffusible hydrogen in weld**

As already discussed, preheating during welding is employed to reduce the cooling rate of a weldment thereby providing more time for hydrogen to diffuse out of the weldment before it is cooled down to ambient temperatures. Post-heating of the weldment soon after welding also serves the purpose of reducing the diffusible hydrogen

content in the welds and this is employed especially for alloyed steels where preheating alone is not adequate to ensure freedom from HAC. In a recent study carried out on high strength (1100MPa) steels, it was found that preheating alone could not bring down the  $H_D$  levels below the critical levels to prevent HAC. Instead, it increased the residual stress in the welded components and thus increased the risk of cracking [166-169]. Preheat combined with post-heating is found to reduce both  $H_D$  content and residual stress and thus prevent cracking. However, choice of preheating and post heating temperature and duration are important [119, 170, 171]. A reduction in post heating temperature was reported with the increase in duration of post heating [172] which can be explained by the temperature dependence of apparent diffusivity of hydrogen in steel. However, a systematic study on  $H_D$  content remaining in the weldment after preheating and post heating and its comparison with the  $H_D$  content originally present in the welding consumable has not been reported.

### **2.19 Determination of apparent diffusivity of hydrogen in steel**

Hydrogen diffusion in steel is affected by its interaction with traps, which in turn depends on steel composition, microstructure, processing history etc. Hence, extensive studies on estimation of apparent diffusivity of hydrogen have been carried out on wide range steels as this data is important to understand various forms of hydrogen embrittlement in different alloys and to develop methods to overcome them. Diffusivity data available from these studies have been reported in two reviews of Boellinghaus et al [173, 174]. These reviews present data from about 300 different studies and has constructed scatter bands for apparent hydrogen diffusivities considering the effect of various parameters that affect diffusivity measurements. Kiuchi et al also report a number of studies carried out on apparent diffusivity of hydrogen in well annealed and deformed iron. This report also includes the various techniques used to determine the

apparent diffusivity of hydrogen in steel [175]. The various measurement techniques are electrochemical permeation, thermal desorption, transient technique etc. Another study by Brower claims the apparent diffusivities of hydrogen obtained in his study to be accurate as it takes into account the hydrogen lost prior to the start of the measurement [176].

## 2.20 Scope of the present study

From the broad literature review presented above on hydrogen in steel and its weldments, it is clear that diffusible hydrogen in steel weldment is an important parameter in studying HAC in steel welds. There is a need to ensure that  $H_D$  is controlled in welding consumables and hydrogen is allowed to diffuse out from steel welds before they are cooled to ambient temperatures to prevent cracking.  $H_D$  measurement is an important step in achieving this objective. Though many techniques are available for  $H_D$  measurements, new techniques are being developed for various reasons like improving the accuracy, reducing the measurement duration, avoiding the use of hazardous chemicals etc.

Keeping in view of the above facts, this thesis presents the development of two techniques, an indigenously developed proton exchange membrane hydrogen sensor (PEMHS) and a gas chromatography facility (GCTCD) which uses a thermal conductivity detector for measurement of  $H_D$  in steel welds. This involves procedure development for hot extraction of  $H_D$  and its measurement using these two techniques. These techniques are validated against the standard mercury method. After employing for  $H_D$  measurement, these techniques were further used in studying the effects of preheating and post-heating on the  $H_D$  content of welds. These techniques were also used to estimate the apparent diffusivity of hydrogen in steel. The details of these techniques, their applications and the results are presented in the later chapters of this thesis.

## Reference

1. W. H. Johnson, Some remarkable changes produced in iron by the action of hydrogen and acids, Proceedings of the Royal Society (London), 1875, Vol. 23, 168-179
2. P. G. Bastien, Welding Journal, 1960, Vol.39, 546-557
3. A. E. Flanigan and J. L. Kaane, Welding Journal, 1964, 43, 80s-85s
4. A. E. Flanigan and M. S. Tucker, Welding Journal, 1966, 45, 368s-373s
5. S. Yamasaki, Hydrogen trapping in steels: Modelling the precipitation of carbides in martensitic steels,  
Web Source: <http://www.msm.cam.ac.uk/phase-trans/2001/shingo/img6.htm>
6. S. M. Carter, Effect of melting practice on hydrogen, 1950, Journal of Metals AIME, Vol. 188, 30-40.
7. S. M., Carter Effect of melting practice on hydrogen II, 1950, Journal of Metals AIME, Vol. 188, 245-255
8. C. Sykes, H. H. Burton, and C. C. Gegg, Hydrogen in steel manufacture, Journal of Iron Steel Institute, 1947, Vol. 156, 155 -180
9. G. M. Pressouyre, C. G. Interrante, International Conference of Current Solutions to Hydrogen Problems in Steel, American Society for Metals, Washington, DC, 1982, 3-8.
10. C. A. Edwards, Pickling or the action of acid solution on mild steel and the diffusion of hydrogen through the metal, Journal of Iron and Steel Institute, 1924, Vol. 110, 9-60
11. C. A. Zapffe and M. E. Haslem, Acid composition, concentration temperature and pickling time as factors in the hydrogen embrittlement of mild steel and stainless steel wire, Transactions of ASM, 1947, Vol. 39, 213-236
12. H. W. Pickering, Analysis of hydrogen evolution and entry into metals for the discharge-recombination process, contract no. N00014-84-K-0201, Annual technical report, January, 1989, The Pennsylvania State University.
13. J. R. Gustafson, Some of the effects of cadmium, zinc, and tin plating on springs, Proceedings of ASTM, Vol 47, 1947, 782.

14. K. B. Valentine, Stress Cracking of Electroplated Lockwashers, Transactions of ASM, Vol. 38, 1947, 488–504.
15. C.A. Zapffe. and M.E. Haslem, Measurement of embrittlement during chromium and cadmium electroplating and the nature of recovery of plated articles, Transactions of ASM, Vol. 39, 1947, 241–258.
16. R.P. Gangloff, "Hydrogen assisted cracking of high strength alloys", in Comprehensive Structural Integrity, 2003, Vol. 6, Elsevier Science, New York, NY, 31-101.
17. N. Mabho, Determination of diffusible and total hydrogen concentration in coated and uncoated steel, M.Sc. Thesis, universität duisburg-essen, September, 2010
18. R. Ramachandran, R. K. Menon, An overview of industrial uses of hydrogen, International Journal of Hydrogen energy, 1998, Vol. 23, No. 7, 593-598.
19. J. P. Hirth, Effects of hydrogen on the properties of iron and steel, Metallurgical Transactions A, 1980, Vol. 11, No. 6, 861-890.
20. M. A. V. Devanathan and Z. Stachurski, The mechanism of hydrogen evolution on iron in acid solutions by determination of permeation rate, Journal of electrochemical society, Vol. 111, No. 5, 619-623.
21. H. W. Pickering, A review of the mechanism and kinetics of electrochemical hydrogen entry and degradation of metallic systems, Annual report to office of naval research, Contract no.00014-84-K-0201, The Pennsylvania State University, January 1990
22. T. Kushida, Hydrogen Entry into Steel by Atmospheric Corrosion, ISIJ International, 2003, Vol. 43, No. 4, 470–474,
23. T.Tsuru, Y. Huang, M. R. Ali, A. Nishikata, Hydrogen entry into steel during atmospheric corrosion process, Corrosion Science, 2005, Vo. 47, 2431–2440
24. R. N. Iyer, H. W. Pickering, A review of the mechanism and kinetics of electrochemical hydrogen entry and degradation of metallic systems, Annual Review of Material Science, 1990, Vol. 20, 299-338

25. T. E. Grúz and M. Volmer, Zur theorie wasserstoffüberspannung, Zeitschrift für physikalische Chemie, Abteilung A, Chemische Thermodynamik, Kinetik, Elektrochemie, Eigenschaftslehre, 1930, Vol. 150A, 203-213,
26. T. E. Grúz and M. Volmer, Zur Frage der Elektrolytischen Metallüberspannung, Zeitschrift für physikalische Chemie, Abteilung A, Chemische Thermodynamik, Kinetik, Elektrochemie, Eigenschaftslehre, 1931, Vol. 157A, 165-181,
27. J. S. Wang, On the diffusion of gases through metals. Mathematical Proceedings of the Cambridge Philosophical Society, 1936, Vol. 32, 657-662.
28. J. Tafel, Über die Polarisation bei kathodischer Wasserstoffentwicklung, Zeitschrift für physikalische Chemie, Stöchiometrie und Verwandtschaftslehre, 1905, Vol. 50, 641-712,
29. J. Tafel and K. Naumann, Beziehungen zwischen Kathodenpotential und elektrolytischer Reduktionswirkung, Zeitschrift für physikalische Chemie, Stöchiometrie und Verwandtschaftslehre, 1905, Vol. 50, 713-752.
30. J. Heyrovsky, Researches with the dropping mercury cathode, Recueil des Travaux Chimiques des Pays Bas, 1925, Vol. 44, 488.
31. J. Heyrovsky, Transactions of Faraday Society, 1924, 19, 692 and 789.
32. H. P. Hack, Galvanic Corrosion, ASTM STP 978, 1988
33. M. E. Stroe, Hydrogen embrittlement of ferrous materials, Ph.D Thesis, The Université Libre de Bruxelles, Belgium, 2006.
34. J. L. Crolet and M. R. Bonis, Revisiting hydrogen in steel, Part II: Experimental Verifications, paper No. 01072, CORROSION NACE, March 11 - 16, 2001, Houston, TX
35. J. L. Crolet and M. R. Bonis, Revisiting hydrogen in steel, Part I, paper No. 01067, CORROSION NACE, March 11 - 16, 2001, Houston, TX
36. J. L. Crolet and G. G. Maisonneuve, Revisiting mechanisms of hydrogen charging and hydrogen stress cracking, Eurocorr 2000, London UK, The Institute of Materials, 2000.
37. A. Sieverts and W. Krumbhaar, Über die löslichkeit von gasen in metallen und legierungen, Ber. Deutsch. Chem. Ges., 1910, vol. 40, No.1, 893-900

38. H. M. Krom and A. D. Bakker, Hydrogen trapping models in steel, *Metallurgical and Materials Transactions B*, 2000, Vol. 31, No.10, 1475-1482.
39. D. Landolt in *Traité des Matériaux*, vol. 12 : Corrosion et Chimie de Surfaces des matériaux, Presses Polytechniques et Universitaires Romandes, Lausanne, pp. 413 – 462, 1993
40. E. Viyanit, Numerical simulation of hydrogen assisted cracking in supermartensitic stainless steel welds, M.Engg. Dissertation, Universität der Bundeswehr Hamburg, 2005
41. C. G. Interrante, and G. M. Pressouyre, Basic Aspects of the Problems of Hydrogen in Steels. Washington D.C.: American Society for Metals, 1982. Current Solutions to Hydrogen Problems in Steels. pp. 3-16
42. N. Eliaz and A. Shachar, 'Characteristics of hydrogen embrittlement, stress corrosion cracking and tempered martensite embrittlement in high-strength steels', *Engineering Failure Analysis*, No.9, 167-184, 2002
43. D. J. Kotecki, Hydrogen measurement and standardisation, Proceedings of the Joint Seminar on Hydrogen Management in steel Weldments, Melbourne, October, 1996, 87-102.
44. R. L. S. Thomas, D. Li, Trap-governed hydrogen diffusivity and uptake capacity in ultrahigh-strength AerMet®100 steel, *Metallurgical and Materials Transactions A*, 2002, Vol. 33, 1991-2004.
45. A. Fick, Ueber Diffusion, *Ann. der. Physik*, 1855, Vol. 170, No.1, 59-86
46. R. Padmanabhan, W. E. Wood, Stress corrosion cracking behaviour of 300M steel under different heat treated conditions, *CORROSION NACE*, Vol. 41, No. 12, 688-699, 1985
47. J. Philbert, *Diffusion and mass transport in solid*, Edition Du Physique, Paris, 1991
48. R. A. Oriani, The diffusion and trapping of hydrogen in steel, *Acta Metallurgica*, Vol.18, 1970, pp.147-157
49. I. M. Bernstein and A.W. Thompson, The Role of Microstructure in Hydrogen Embrittlement, *Hydrogen Embrittlement and Stress Corrosion Cracking*, R. Gibala and R.F. Hehemann (ed.), ASM, 1995, 135-152

50. G. M. Pressouyre and I. M. Bernstein, A quantitative analysis of hydrogen trapping, *Metallurgical Transactions A*, 1978, Vol. 9, No.11, 1571-1580
51. H. H. Johnson and R.W. Lin: in *Hydrogen Effects in Metal*, I.M. Bernstein and A.W. Thompson, eds., TMS AIME, New York, NY, 1981, pp. 3-23.
52. J. L. Davidson, S. P. Lynch, A. Majumdar, The relationship between hydrogen-induced cracking resistance, microstructure and toughness in high strength weld metal, *Proceedings of the Joint Seminar on Hydrogen Management in steel Weldments*, Melbourne, October, 1996, 21-34
53. D. L. Olson, I. Maroef, C. Lensing, R. D. Smith, W. W. Wang, S. Liu, T. Wilderman and M. Eberhart, Hydrogen management in high strength steel weldments, *Proceedings of the Joint Seminar on Hydrogen Management in steel Weldments*, Melbourne, October, 1996, 1-19
54. G. M. Pressouyre, A classification of hydrogen traps in steel, *Metallurgical Transactions A*, 1979, Vol. 10, No.10 -1571
55. G. M. Pressouyre, Hydrogen traps, repellers, and obstacles in steel: Consequences on hydrogen diffusion, solubility and embrittlement, *Metallurgical Transactions A*, 1983, Vol. 14, No.10 -2189-2193
56. F. R. Coe, *Welding steels without hydrogen cracking*, The Welding Institute, Cambridge, United Kingdom, 1973, 68 p
57. C. A. Zapffe and C. E. Sims, Hydrogen embrittlement, internal stress and defects in steel, *Transactions AIME*, TP.1307, Vol.145, 225-261, 1941.
58. A. S. Tetelman and W. D. Robertson, Mechanism of hydrogen embrittlement observed in iron-silicon single crystals, *Transactions AIME*, 1962, Vol.224, No.4 775-783
59. M. Smialowski, in *Stress corrosion cracking and hydrogen embrittlement of iron base alloys*, 1977, Editors R.W. Staehle, J. Hochmann, R.D. Mc.Cright and J.E. Slater, *Conference Proceedings of Unieux- Firminy*, 12-16 June 1973, NACE-5, Houston, TX, 405

60. R. Troiano, The role of hydrogen and other interstitials in the mechanical behaviour of metals, Transactions ASM, 1960, Vol. 52, 54-80.
61. R. A. Oriani, A decohesion theory for hydrogen-induced crack propagation, In Stress Corrosion Cracking and Hydrogen Embrittlement of Iron Base Alloys, Editors R.W. Staehle, J. Hochmann, R.D. Mc.Cright and J.E. Slater, Conference Proceedings of Unieux-Firminy, 12-16 June 1973, NACE-5, 351-358, 1977
62. R. A. Oriani, A mechanistic theory of hydrogen embrittlement of steels, Berichte der Bunsen-Gesellschaft, 1972, Vol.76, No.8, 848-857
63. N. J. Petch and P. Stables, Delayed fracture of metals under static load, Nature, Vol.169, 1952, 842-843
64. N. J. Petch, Lowering of the Fracture Stress Due to Surface Adsorption, Philosophical Magazine (Ser.8), 1956, Vol. 1, No. 4, 331-335.
65. E. N. Pugh, A post conference evaluation of our understanding of the failure mechanisms, Stress Corrosion Cracking and Hydrogen Embrittlement of Iron Base Alloys, Editors R.W. Staehle, J. Hochmann, R.D. Mc.Cright and J.E. Slater, Conference Proceedings of Unieux-Firminy, 12-16 June 1973, NACE-5, 37-51, 1977
66. D. G. Westlake, A generalised model for hydrogen embrittlement, Trans. ASM, Vol.62, 1000-1006, 1969.
67. C. D. Beachem, A new model for hydrogen-assisted cracking (Hydrogen Embrittlement), Metallurgical Transactions, Vol.3, 437-451, 1972.
68. S. P. Lynch, Environmentally assisted cracking: Overview of evidence for an adsorption-induced localised-slip process, Acta Metallurgica, 1988, Vol. 36, No.10, 2639-2661
69. C. D. Beachem, Electron fractographic support for a new model for hydrogen-assisted cracking, Stress Corrosion Cracking and Hydrogen Embrittlement of Iron Base Alloys, Editors R.W. Staehle, J. Hochmann, R.D. Mc.Cright and J.E. Slater, Conference Proceedings of Unieux-Firminy, 12-16 June 1973, NACE-5, 376-381, 1977

70. P. Sofronis and H. K. Birnbaum, Mechanics of the hydrogen dislocation impurity interactions-I. Increasing shear modulus”, J. Mech. Phys. Solids, Vol.43, No.1, 1995, pp.49-90.
71. P. Sofronis: The influence of mobility of dissolved hydrogen on the elastic response of a metal, J. Mech. Phys. Solids, Vol.43, No.9, 1995, pp.1385-1407.
72. H.K. Birnbaum, I. M. Robertson, P. Sofronis, D. Teter, Mechanisms of hydrogen related fracture-A review, In: Corrosion Deformation Interactions CDI'96, T. Magnin, Editor. 1997, The Institute of Materials, Great Britain.: Nice, France. p. 172-195
73. H. K. Birnbaum and P. Sofronis Hydrogen-enhanced localized plasticity--a mechanism for hydrogen related fracture, Materials Science and Engineering A, 1994, Vol. 176, 191-202
74. H. K. Birnbaum, Mechanisms of hydrogen related fracture of metals, Technical Report, Office of Naval Research, Contract USN 00014 - 83 - K - 0468, May 1989
75. Th. Magnin, Advances in corrosion-deformation interactions, Materials Science Forum, Trans Tech Publications, Volume 202, 1996.
76. W. W. Wolkow, Measurements of diffusible hydrogen in weld metal, Welding Research Abroad, 1987, No.3, 32-35
77. D. McKeown, Hydrogen and its control in weld metal, Metal Construction, 17, 1985, 655-661
78. B. Chew, Hydrogen control of basic coated MMA welding electrodes – The relationship between coating moisture and weld hydrogen, Metal Construction, 1982, Vol. 14, No. 7, 373-377
79. Y. Hirai, T. Hiro, J. Tsuboi, Behaviour of hydrogen in arc welding-Report 2, Sources of hydrogen in the shielded metal arc welding, Transactions of Japan Welding Society, 1974, Vol.5, 111-116
80. H. Li, T. H. North, Hydrogen absorption and hydrogen cracking in high strength weld metal, Key Engineering Materials, 1992, Vols. 69-70, 95-112
81. S. A. Gedeon, T. W. Eagar, Thermochemical analysis of hydrogen absorption in welding, Welding Journal, 1990, Vol. 69, No. 7, 264s-271s

82. G. R. Salter, and D. R. Milner, Gas absorption from arc atmosphere, *British Welding Journal*, 1960, February, 89-100
83. D. R. White, In-process measurement of hydrogen in welding, Ph.D. Thesis, University of Illinois, Champaign, IL, 1986
84. W. F. Savage, E. F. Nippes and E. I. Husa, Hydrogen-assisted cracking in HY-130 weldments, Final Report to the Office of Naval Research, Contract No. N00014-75-C-0944, NR 031-780, January 1981
85. B. Chew, and R. A. Willgoss, Weld metal hydrogen absorption during TIG-welding with argon-hydrogen gas shield, *Proceedings of Weld Pool Chemistry and Metallurgy International Conference*, London, April 1980, 155-165
86. The anode boundary region in argon shielded tungsten arcs, 11W Doc. 212-640-86, 1986
87. Block-Bolten, and T. W. Eagar, Metal vaporization from weld pools, *Metallurgical Transactions B*, 1984, Vol. 15, No. 3, 461-469
88. D. G. Howden, and D. R. Milner, Hydrogen absorption in arc welding, *British Welding Journal*, 1963, June, 304-316
89. M. B. C. Quigley, P. H. Richards, D. T. Swift-Hook,, and A. E. F. Gick, Heat flow to the work piece from a TIG welding arc, *J. Phys. D: App. Phys.*, 1973 Vol. 6, , 2250-2258
90. M. B. C. Quigley, Physics of the welding arc, *Welding and Metal Fabrication*, 1977, December, 619-626
91. H. G. Krause, Experimental measurement of thin plate SS 304 GTA weld pool surface temperatures, *Welding Journal*, 1987, Vol. 66, No. 12, 353s-359s
92. D. Suh, T. W. Eagar, Mechanistic understanding of hydrogen in steel welds, *Proceedings of International workshop conference on hydrogen management in welding applications*, Ottawa, Ontario, Canada, 6-8 October, 1998, CANMET, 1998, 105-110
93. K. Mundra, J. M. Blackburn, and T. Debroy, Absorption and transport of hydrogen during gas metal arc welding of low alloy steel, *Science and Technology of Welding and Joining*, 1997, Vol. 2, No.4, 174-184

94. D. J. Kotecki, and R. A. La Fave, AWS A5 Committee Studies of weld metal diffusible hydrogen, *Welding Journal*, 1985, Vol. 64, No. 3, 31-37
95. Y. Hirai, S. Minakawa and J. Tsuboi, Prediction of diffusible hydrogen content in deposited metals with basic covered type electrodes, IIW Document II-929-80
96. H. Granjon, Cold cracking in welding of steels, Intl. Symposium on Cracking and Fracture in Welds, Conference Proceedings Japan Welding Society, (1971), IB, 1.1
97. S. Kou, *Welding Metallurgy*, Second Edition, New York: John Wiley & Sons, Inc., 2002
98. W. W. Wang, R. Wong, S. Liu, and D.L. Olson, in Conference Proceedings of Welding and Weld Automation in Shipbuilding", Oct 29- Nov. 2, 1995, eds: R. DeNale, TMS, Warrendale PA, 1996, pp. 17-31
99. J. Vuik, An update of the state-of-the-art of weld metal hydrogen cracking, IIW Doc. IXJ-175-92, 1992, American Council, AWS, Miami, FL.
100. J. Adamczyk, Development of the microalloyed constructional steels, *Journal of Achievements in Materials and Manufacturing Engineering* 14 (2006), 9-20
101. R. Scott Funderburk, Key concepts in welding engineering- Postweld heat treatment, *Welding Innovation*, 1998, Vol. XV, No. 2
102. R. Hornberger, Assuring accurate preheat temperatures, *The American Welder*, April 2007, 104-107
103. B.A. Graville, Welding of HSLA (microalloyed) structural steels, Proceeding of International. Conference on welding of HSLA (microalloyed) structural steels, American Society for Metals, November 9-12, Rome, Italy, 1976, 85-101
104. S. Birch, What is the difference between the various carbon equivalent formulae used in relation to hydrogen cracking?, TWI FAQ, Web Source: <http://www.twi.co.uk/technical-knowledge/faqs/material-faqs/faq-what-is-the-difference-between-the-various-carbon-equivalent-formulae-used-in-relation-to-hydrogen-cracking/#References>
105. N. Bailey, F. R. Coe, T. G. Gooch, P. H. M. Hart, N. Jenkins and R. J. Pargeter, *Welding steels without hydrogen cracking*, ASM International and Abington Publishing house, Cambridge, UK

106. Y. Ito, K. Bessyo, Cracking parameter of high strength steels related to heat affected zone cracking, Journal of Japan Welding Society, 1968, Vol. 37, No. 9, 983-991
107. Y. Ito, K. Bessyo, Cracking parameter of high strength steels related to heat affected zone cracking (Report 2), Journal of Japan Welding Society, 1969, Vol. 38, No. 10, 1134-1144
108. H. Suzuki, Cold Cracking and its prevention in steel welding, Transactions of Japan Welding Society, 1978, Vol. 9, No. 2, 140-149
109. H. Suzuki, Root Cracking analyzed with a New Cracking Parameter  $P_H$ , Journal of Japan Welding Society, 1980, Vol. 49, No. 11, 737-741
110. H. Suzuki, Cracking parameter  $P_H$  considering welding heat input and restraint intensity, Journal of Japan Welding Society, 1981, Vol. 50, No.5, 478-482
111. H. Suzuki , N. Yurioka and M. Okumura, A new cracking parameter for welded steels considering local accumulation of hydrogen, Transactions of Japan Welding Society, 1982, Vol. 13, No. 1, 3-12
112. H. Suzuki and N. Yurioka, Prevention against cold cracking by hydrogen accumulation cracking parameter, Transactions of Japan Welding Society, 1983, Vol. 14, No. 1, 40-52
113. H. Suzuki, Revised cold cracking parameter  $P_{HA}$  and its application, Transactions of Japan Welding Society, 1985, Vol. 14, No. 1, 40-49.
114. N. Yurioka, H. Suzuki, S. Ohshita and S. Saito, Determination of necessary preheating temperature in steel welding, Welding Journal, 1983, 62 (6), 147s-153s
115. K. Satoh, S. Matsui, K. Horikawa, K. Bessyo and T. Okumura, JSSC Guidance report on determination of safe preheating conditions without weld cracks in steel structures, Transactions of JWRI, 1973, 2(2), 117-126
116. N. Yurioka and T. Kasuya, A chart method to determine necessary preheat temperature in steel welding, Quarterly journal of Japan Welding Society, 1995, 13(3), 347-357
117. AWS D1.1 2004: Structural Welding Code – Steel, Appendix XI, Guideline on alternative methods for determining preheat, 299-308
118. R. Gaillard, S. Debiaz, M. Hubert and J. Defourny, Methods for optimizing preheat temperature in welding, Welding in the world, 1988, 26(9/10), 216-230

119. P. K. Ghosh and U. Singh, Influence of pre- and post-weld heating on weldability of modified 9Cr–1Mo(V–Nb) steel pipe under shielded metal arc and tungsten inert gas welding processes *Sci. Technol. Weld. Join.*, 2004, 9(3), 229–236
120. D. Uwer and H. Hohne, Determination of suitable minimum preheating temperatures for cold-crack-free welding of steels, *Welding and Cutting*, 1991, Vol.5; IIW Doc. IX-1631-91, 1991
121. ANSI/AWS A5.1-91, Specification for carbon steel electrodes for shielded metal arc welding, Miami, Florida, American Welding Society.
122. ISO 2560: 2009, Welding consumables — Covered electrodes for manual metal arc welding of non-alloy and fine grain steels — Classification
123. JIS Z 3212-2000, Covered electrodes for high tensile strength steel
124. JIS Z 3211: Covered electrodes for mild steel, high tensile strength steel and low temperature service steel
125. M. Pitrun, The effect of welding parameters on levels of diffusible hydrogen of weld metals deposited using gas shielded rutile cored electrodes, Ph.D Thesis, University of Wollongong, 2004.
126. ISO 3690:2008, ISO 3690:2000, Welding and allied processes – Determination of hydrogen in ferritic steel arc weld metal.
127. ANSI/AWS A4.3: 1993 (R2006), Standard methods for determination of diffusible hydrogen content of martensitic, bainitic and ferritic steel weld metal produced by arc welding. American Welding Society, Miami, FL.
128. BS 6693-5: 1988, Diffusible hydrogen. Primary method for the determination of diffusible hydrogen in MIG, MAG, TIG or cored electrode ferritic steel weld metal.
129. JIS Z 3118: 2007, Method for measurement of amount of hydrogen evolved from steel welds.
130. JIS Z 3113: 1975, Method for measurement of hydrogen evolved from deposited metal.
131. DIN 8572: 1981 Part 1, Determination of diffusible hydrogen in weld metal- Manual Arc Welding.

132. AS/NZS 3752: 2006 Welding and allied processes - Determination of hydrogen content in ferritic steel arc weld.
133. GOST 23338-91, Welding of metals. Methods for determination of diffusible hydrogen in deposited weld metal and fused metal.
134. BIS IS 11802:1986 (R2003), Method of determination of diffusible hydrogen content of deposited weld metal from covered electrodes in welding mild and low alloy steels.
135. D.J. Kotecki, Hydrogen reconsidered, *Welding Journal*, 1992, Vol. 71, No. 8, 35-43.
136. I.L. Stern, I. Kalinsky, and E.A. Fenton, Gas evolution from weld metal deposits, *Welding Journal*, 1949, Vol. 28, No.9, 405s-413s.
137. M. A. Quintana, A critical evaluation of glycerin test, *Welding Journal*, 1984, Vol. 63, No. 5, 141s-149s.
138. Determination of hydrogen in weld metal using the glycerin method, *Materials and NDE Book J MQPS 11-7*, Lloyd's Register of shipping, Rev.1, 2002.
139. T.S. Senadheera, and W.J.D. Shaw, Improvements in the mercury displacement method for measuring diffusible hydrogen content in steels, *Journal of Testing AND Evaluation*, 2009, Vol. 37, No.3, 275-282.
140. N. Jenkins, P.H.M.H. Hart, D.H. Parker, An evaluation of rapid methods for diffusible weld hydrogen, *Welding Journal*, 1997, vol. 76, no. 1, pp. 1s-10s.
141. Y. Kikuta, T. Araki, A. Ookubo, and H. Ootani, A study on method of measurement for diffusible hydrogen in weld metal (Report 1): Property of collecting solution for measurement of evolved hydrogen, *Journal of the Japan Welding Society*, 1976, Vol. 45, No.2, 1008-1015.
142. M. A. Quintana and J. R. Dannecker, Diffusible hydrogen testing by gas chromatography, In: *Hydrogen Embrittlement: Prevention and Control*, ASTM STP 962, 1988, Editor: L. Raymond, ASTM, Philadelphia, PA, 247-268.
143. I. K. Pokhodnya, and A. P. Pal'tsevich, A chromatographic method for the determination of the amount of diffusible hydrogen in welded joints, *Automatic Welding*, 1980, vol. 33, no. 1, pp. 30-32.

144. R. Ravi, D. S. Honnover, Hydrogen in steel weldments – A review, Proceedings of National welding seminar, 26-28 Nov. 1987, Bangalore, India, E23-E43
145. B. Sohrman, S. Budgifvars, H. Dahlskog, J. Elvander and G. Nilsson, A new method for measuring diffusible hydrogen in weld metal, Svetsaren, 1985, No. 1, 8-10.
146. D. Nolan and M. Pitrun, Diffusible hydrogen testing in Australia, Doc. IIW-1616, Welding in the World, 2004, vol. 48, no. 1/2, pp. 14-20.
147. S. Ohno and M. Uda, Vacuum-extraction method for hydrogen determination in weld metals- An analysis of hydrogen behavior in the JIS type weld specimen, Journal of the Japan welding society, 1980, Vol. 49, No. 11. 747-745
148. J. Elvander, Experiences from accelerated test methods at elevated temperatures, IIW Doc II-1633-07, 2007.
149. V. van der Mee, Round robin on effect of atmospheric storage condition on weld metal diffusible hydrogen content of gas shielded cored wires – A study for IIW Subcommission IIA, IIW Doc. II-1523-04, 2004.
150. T. Kannengiesser and N. Tiersch, Comparative study between hot extraction methods and mercury method – A national round robin test, Doc. IIW-2136, Welding in the World, 2010, vol. 54, n° 5/6, pp. R108-R114.
151. T. Kannengiesser and N. Tiersch, Measurements of diffusible hydrogen contents at elevated temperatures using different hot extraction techniques - An international round robin test, Doc. IIW-2135, Welding in The World, 2010, Vol. 54, No. 5/6, pp. R115-R122
152. P. H. M. H. Hart, D. H. Parker, Rapid methods for diffusible hydrogen measurements in standard test welds. Final report part 1, TWI report 5612/6A/92, 1992.
153. C. Ström, J. Elvander, Calibration and verification of the hot extraction method including a comparison with the mercury method, IIW Doc. II-1543-04, 2004.
154. N. Jenkins, P. H. M. H. Hart, D.H. Parker, An evaluation of rapid methods for diffusible weld hydrogen, Welding Journal, 1997, vol. 76, no. 1, pp. 1s-10s.

155. D. J. Ball, W.J. Gestal, and E. F. Nippes, Determination of diffusible hydrogen in weldments by the RPI Silicone- Oil Extraction method, *Welding Journal*, 1981, Vol. 60, No. 3, 50s-56s
156. G. C. Schmid, R. D. Rodabaugh, A water displacement method for measuring diffusible hydrogen in welds, *Welding Journal*, 1980, Vol. 59, No. 8, 217s-225s
157. Y. Kikuta, T. Araki, A. Ookubo, and H. Ootani, A study on method of measurement for Diffusible hydrogen in weld metal (Report 1): Property of Collecting Solution for Measurement of Evolved Hydrogen, *Journal of the Japan Welding Society*, 1976, Vol. 45, No.2, 1008-1015.
158. R. D. Smith II, G. P. Landis, I. Maroef, D. L. Olson and T. R. Wildeman, The determination of hydrogen distribution in high-strength steel weldments Part 1: Laser ablation methods, *Welding Journal*, 2001 Vol. 80, No.5, 115s-121s
159. R. D. Smith II, D. K. Benson, I. Maroef, D. L. Olson and T. R. Wildeman, The determination of hydrogen distribution in high-strength steel weldments Part 1: Optoelectronic diffusible hydrogen sensor, *Welding Journal*, 2001 Vol. 80, No.5, 122s-125s
160. D.L. Olsen: High strength steel weldment reliability, Report documentary page, P.O. Report Number: CSM-MT-CWJCR-001-022, U. S. Army office, August, 2001 (46 Pages)
161. N. Lasseigne, J. D. McColskey, K. Koenig, J.E. Jackson, D. L. Olson, B. Mishra, and R.H. King, Advanced non-contact diffusible hydrogen sensors for steel weldments, *Trends in Welding Research, Proceedings of the 8th International Conference*, Editors: S. A. David, T.S. DebRoy, J. N. DuPont, T. Koseki, AND H. B. Smartt, 424-429
162. K. Koenig, A. N. Lasseigne, J. W. Cisler, B. Mishra, R.H. King, and D. L. Olson, Non contact, nondestructive hydrogen and microstructural assessment of steel welds, *International Journal of Pressure Vessels and Piping*, 2010, Vol. 87, 605-610
163. S. K. Albert, C. Ramesh, N. Murugesan, T. P. S. Gill, G. Periaswamy, S. D. Kulkarni, A new method to measure the diffusible hydrogen content in steel weldments using a

- polymer electrolyte based hydrogen sensor, *Welding Journal*, 1997, Vol. 76, No.7, 251s-255s
164. C. Ramesh, G. Velayutham, N. Murugesan, V. Ganesan, K. S. Dhathathreyan, G. Periaswami, An improved polymer electrolyte based amperometric hydrogen sensor, *Journal of Solid State Electrochemistry*, 2003, Vol. 7, No. 8, 511–516
165. S.K. Albert: Some aspects of weldability of Cr Mo steels, Ph.D Thesis, 1996, Indian Institute of Technology, Bombay.
166. P. Wongpanya , Th. Boellinghaus and G. Lothongkum, Ways to reduce the cold cracking risk in high strength structural steel welds. International Conference of International Institute of Welding, 25-29 May 2008, Johannesburg, South Africa
167. P. Wongpanya , Th. Boellinghaus and G. Lothongkum, Effects of hydrogen removal heat treatment on residual stresses in high strength structural steel welds, *Welding in the World*, Volume 50, Special Issue, 2006
168. P. Wongpanya , Th. Boellinghaus and G. Lothongkum, Numerical simulation of hydrogen removal heat treatment procedures in high strength steel welds, *Mathematical modeling of weld phenomena* 8, 743-765
169. P. Wongpanya , Th. Boellinghaus and G. Lothongkum, Heat treatment procedures for hydrogen assisted cold cracking avoidance in S 1100 QL steel root welds, *Welding in the world*, 52, 2008, pp-671-678
170. R. Kume, H. Okabayashi and T. Naiki, Effect of pre and post heating on weld cracking of low alloy steels, *Transactions of Japan Welding Society*, 1974, Vol. 5, No. 2, 62-71
171. P. K. Ghosh, P. C. Gupta, N. B. Potluri and Y. Gupta, Influence of pre and post weld heating on weldability of modified 9Cr–1MoVNb steel plates under SMA and GTA welding processes, *ISIJ International*, 2004, Vol. 44, No. 7, 1201–1210
172. Y. Nishio, K. Kito and S. Kanemitsu, Effect of continuous post heating time on reduction of preheating temperature, *Quarterly Journal of the Japan Welding Society*, 1991, Vol. 9, No. 3, pp. 124-127.

173. Th. Boellinghaus, H. Hoffmeister, A. Dangeleit, A Scatterband for Hydrogen Diffusion Coefficients in Micro-Alloyed Low Carbon Structural Steels, *Welding in the World* (1995), Vol. 35, No. 2, 83-96
174. Th. Boellinghaus, H. Hoffmeister, A. Dangeleit, C. Middel, Scatterbands for hydrogen diffusion coefficients in steels having a ferritic or martensitic microstructure and steels having an austenitic microstructure at room temperature, *Welding in the World*, 1996, Vol. 37, No.1, 16-23
175. K. Kiuchi and R. B. McLellan, The solubility and diffusivity of hydrogen in well-annealed and deformed iron, *Acta Metallurgica*, 1983, Vol. 31, No. 7, pp. 961-984,
176. R. C. Brouwer, Hydrogen diffusion and solubility in vanadium modified pressure vessel steels, *Scripta Metallurgica*, 1992, Vol. 27, No. 3, 353-358

**CHAPTER 3**

**EXPERIMENTAL DETAILS**

## Experimental Details

---

---

### 3.1 Determination of Diffusible Hydrogen ( $H_D$ )

Two techniques were developed indigenously for diffusible hydrogen ( $H_D$ ) measurement in weldments. One of the techniques uses a Nafion based proton exchange membrane hydrogen sensor (PEMHS) and the other a gas chromatograph with thermal conductivity detector (GCTCD) as hydrogen sensor. Since PEMHS was being used first time for  $H_D$  measurement, the  $H_D$  collection was carried out at room temperature and its feasibility for measurement was demonstrated. This measurement process is henceforth referred to as RT-PEMHS. Subsequently, a facility for hot extraction of  $H_D$  was made. This facility was combined with PEMHS and further measurements were carried out. This technique is referred as HE-PEMHS. Similarly, the combination of hot extraction of  $H_D$  and its measurement using gas chromatography facility is referred to as HE-GCTCD in this thesis.

In general, all the above techniques involve three basic steps for determination of  $H_D$  from weld specimen. They are weld specimen preparation,  $H_D$  collection and its measurement. For collection of  $H_D$ , each weld specimen was introduced into a separate chamber. The chamber along with specimen was filled with argon to a known pressure. Hydrogen from weld sample was collected as a mixture consisting of argon and hydrogen (Ar-H<sub>2</sub>) gases. In PEMHS based measurements, concentration of hydrogen in the gas mixture is measured. In GCTCD based measurement, total hydrogen collected in the chamber is measured.

$H_D$  obtained using the indigenous hot extraction techniques was compared with the standard mercury method given in ISO 3690:1977 [1]. For this comparison,  $H_D$  measurements were carried out using the mercury method with weldments identical to

that used in the indigenous techniques. Various materials, equipment and procedures adopted for the above study are given in the following sections.

### **3.1.1 Weld specimen preparation**

For all the above techniques of  $H_D$  measurement, weld specimens were prepared as per ISO 3690: 2000 [2]. The base metals, welding electrodes, welding procedure employed for the preparation of weld specimen are detailed below.

#### **3.1.1.1 Test Assembly**

For  $H_D$  measurement, test assembly consisting of a specimen piece of dimensions 30×15×10mm and run-on and run-off pieces of dimensions 45×15×10mm were prepared from mild steel and modified 9Cr-1Mo steel. The compositions of both these steels are given in Table 3.1.

Table 3.1: Chemical composition of mild steel and modified 9Cr-1Mo in Wt%

Elements	Mild steel	Modified 9Cr-1Mo
Carbon	0.205	0.114
Chromium	-	8.838
Molybdenum	-	0.860
Manganese	0.553	0.403
Nickel	-	-
Silicon	0.062	0.309
Phosphorous	0.039	0.014
Sulphur	0.047	-
Niobium	-	0.080
Vanadium	-	0.027
Copper	0.324	-
Aluminium	0.01	-
Iron	Balance	Balance

Each constituent of the test assembly was degassed at 650°C for 1 h to remove any bulk hydrogen present and cooled in the furnace. Their surfaces were ground to

remove the oxide scale formed during degassing treatment. These were finished at right angles to ensure good contact between the adjacent pieces, cleaned with acetone followed by warm air and stored in desiccators until they were used for welding. During welding, the specimen was placed in between the run on and run off pieces. The run-on piece was used for arc striking and run-off piece for arc extinction during welding so that a stable arc and uniform shape of the deposit could be obtained on the specimen. The schematic of a test assembly after deposition of bead is shown in Fig. 3.1.

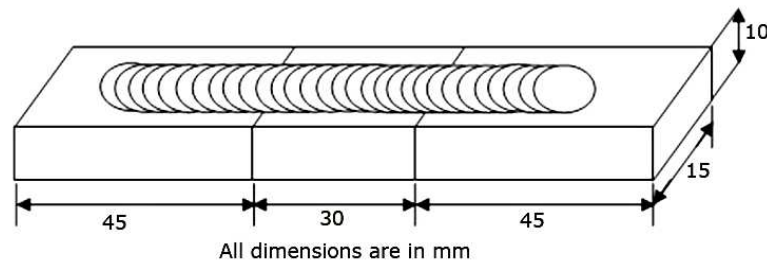


Fig. 3.1 Schematic of test assembly [2]

### 3.1.1.2 Welding electrodes

$H_D$  measurements using the new indigenous techniques were carried out for a variety of welding electrodes having cellulose, rutile and basic coating.  $H_D$  content in these electrodes varied from 2 to 31ml/100g. This range includes all the levels of  $H_D$  as per IIW and AWS benchmarks [3]. The electrodes were appropriately baked prior to deposition. Details of the electrodes, baking treatment they were subjected to, and the welding parameters employed for their deposition are given in Table 3.2. P91M is an electrode for welding modified 9Cr- 1Mo steel with a composition modified from that of AWS Specification E9015- B3. For this electrode, two separate sets of  $H_D$  measurements were carried out: one using test assembly prepared from mild steel and another prepared from modified 9Cr-1Mo steel.

### 3.1.1.3 Welding fixture/Copper jig

Following the procedures from ISO 3690:2000, bead was deposited on the test assembly held in a copper jig. The dimensions of the jig were such that during welding,

Table 3.2: Baking and welding conditions of different electrodes

Electrode	Diameter (mm)	Baking	Welding Current (A)	Voltage(V)
E6010	3	80°C/0.5 h	80	28
E6010	4	80°C/0.5 h	120	25
E6013	3.5	125°C/1 h	110	27
E6013	4	125°C/1 h	140	27
E7016	3.5	250°C/2 h	120	28
E7018	3.5	250°C/2 h	110	28
E 7018	4	250°C/2 h	150	25
E7018-A1	3.5	250°C/2 h	110	27
E7018-A1	4	250°C/2 h	150	23
E7018 redried	4	250 °C /2 h	100	26
E8016-C2	4	250 °C /2 h	120	26
E8018-B2	4	250 °C /2 h	150	24
E8018-W2	4	250 °C /2 h	150	24
E9018-G	4	250 °C /2 h	150	32
E9018-B3	4	250 °C /2 h	150	34
E11018-M	4	250 °C /2 h	150	35
Modified E9015-B3 (P91M)	3	300°C/2 h	90	28

the heat was immediately conducted away from the test assembly to the copper jig. Apart from facilitating the test assembly for faster cooling, the jig also holds it firmly as shown in the photograph in Fig. 3.2. A schematic of the jig is also shown in Fig. 3.3. Weld metal was deposited on different test assemblies clamped to the copper jig using different welding electrodes and shielded metal arc welding (SMAW) process.

#### **3.1.1.4 Preparation of specimen**

Immediately after the deposition, the test assembly was removed from the copper jig, and immersed in cold water for 4-6 seconds and subsequently in liquid nitrogen.

After holding for 5 minutes in liquid nitrogen, the middle weld specimen was separated from the run-on and run-off pieces with a hammer. Any slag remaining on the weld specimen was removed within 20s and the specimen stored in liquid nitrogen till it is taken for measurement.

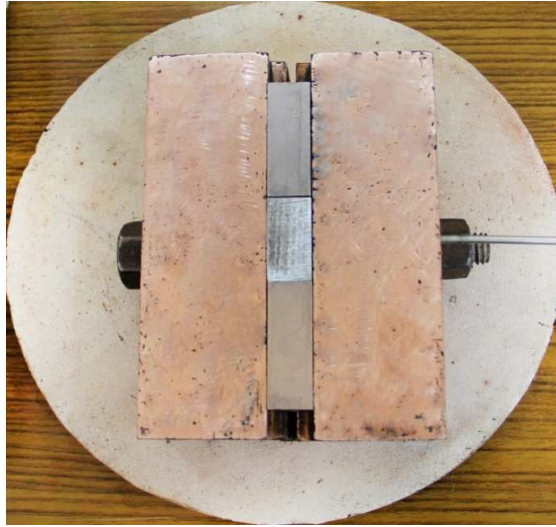


Fig. 3.2 Photograph of Copper jig holding the test assembly

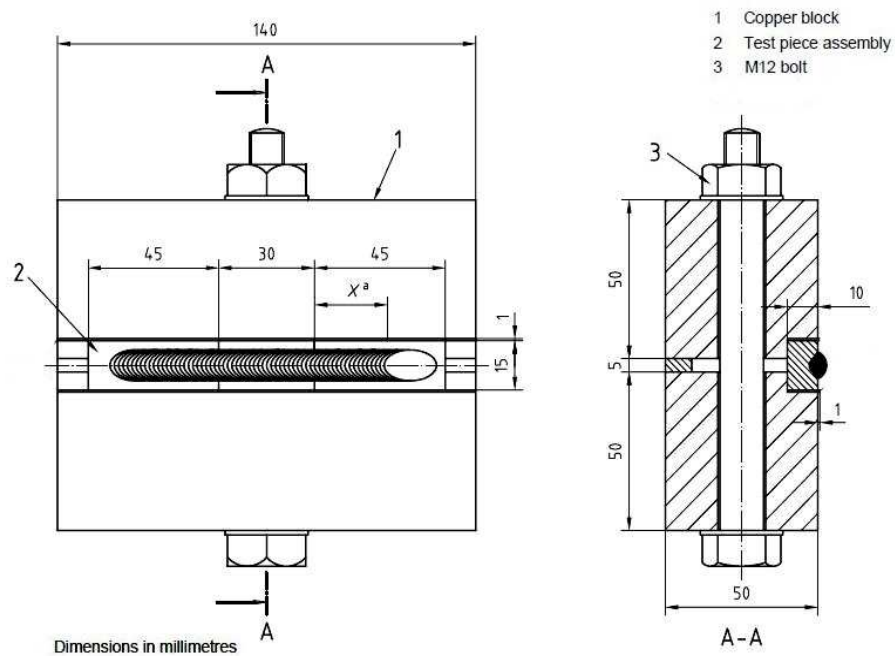


Fig. 3.3 Schematic of copper jig used [1]

### **3.1.2 Collection of $H_D$ from weld specimen**

For the measurement of  $H_D$  using the indigenous PEMHS technique,  $H_D$  from the weld specimen was collected at 25°C for 72 h, the time and temperature recommended in ISO 3690: 1977. In the hot extraction technique, it was collected by heating the weld specimen at 400°C for 0.5 h. For such collection, new chambers were designed. The design and construction of collection chambers for each of these techniques are discussed below.

#### **3.1.2.1 Chamber for $H_D$ collection at 25-45°C and its measurement using PEMHS (RT-PEMHS)**

This chamber was used in an earlier study by Albert et al [4, 5]. Fig. 3.4 shows a photograph of the chamber along with plug. The volume of the chamber is measured by filling it with distilled water and draining the water completely into a measuring jar. The volume of water in the measuring jar is equal to the volume of the chamber.

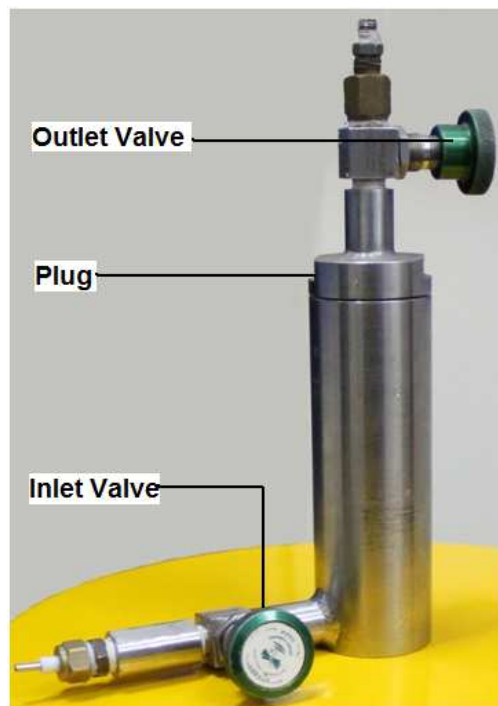


Fig. 3.4 Chamber for collecting  $H_D$  at room temperature

### ***3.1.2.2 Chamber for hot extraction of $H_D$ and its measurement using PEMHS (HE-PEMHS)***

The chamber consists of a stainless steel cylinder of length 240mm and ID 75mm. The cylinder can be opened /closed from both ends by two CF75 flanges [6, 7]. The flanges have knife edge grooves for copper/viton gaskets to ensure leak-tightness of the chamber. A tubular furnace of 20mm ID is fixed to one of the CF75 flanges for holding and heating the weld specimen. A photograph of the hot extraction chamber is shown in Fig. 3.5. The furnace is capable of heating the specimen up to 500°C. The furnace has a 70 mm long uniform temperature zone within which the test specimen is heated. Temperature of the furnace is measured using a K-type thermocouple. In addition, temperature of the furnace can be controlled using a 8 step programmable PID temperature controller. The chamber is provided with inlet and outlet nozzles fit with diaphragm valves. In order to prevent excessive heating of the chamber during operation, it is provided with a double walled design for water cooling, as shown in Fig. 3.6. Before using the chamber for collection of  $H_D$ , the entire chamber was helium-leak tested in vacuum. Its leak rate was found to be less than  $10^{-8}$ std cc/min. This chamber was used for hot extraction of  $H_D$  in the HE-PEMHS technique.

### ***3.1.2.3 Chamber for hot extraction of $H_D$ and its measurement using GCTCD (HE-GCTCD)***

For  $H_D$  collection from weld specimen in GCTCD based measurement, a different collection chamber was used. A photograph of the chamber is shown in Fig. 3.7. For reliable response of the TCD, the volume of the gas introduced into the system should be small and accordingly the volume of the chamber was kept as small as possible. It is a stainless steel tube of 90 mm length and 25 mm diameter with bottom end closed (machined out from a rod) and provided with a plug on the top. The leak tightness of the

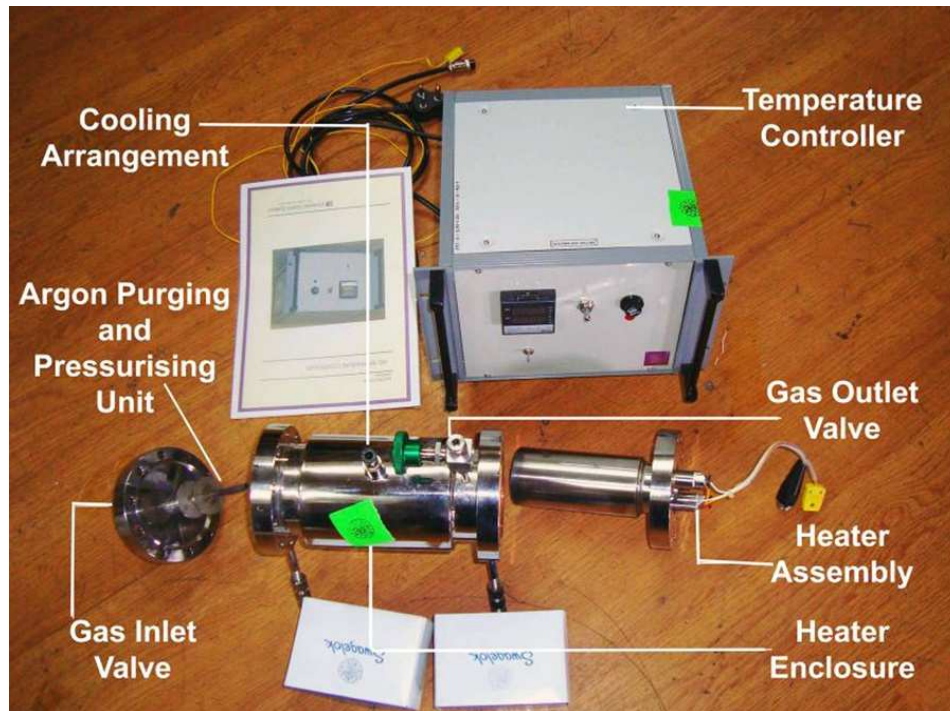


Fig. 3.5 HE chamber along with the temperature controller

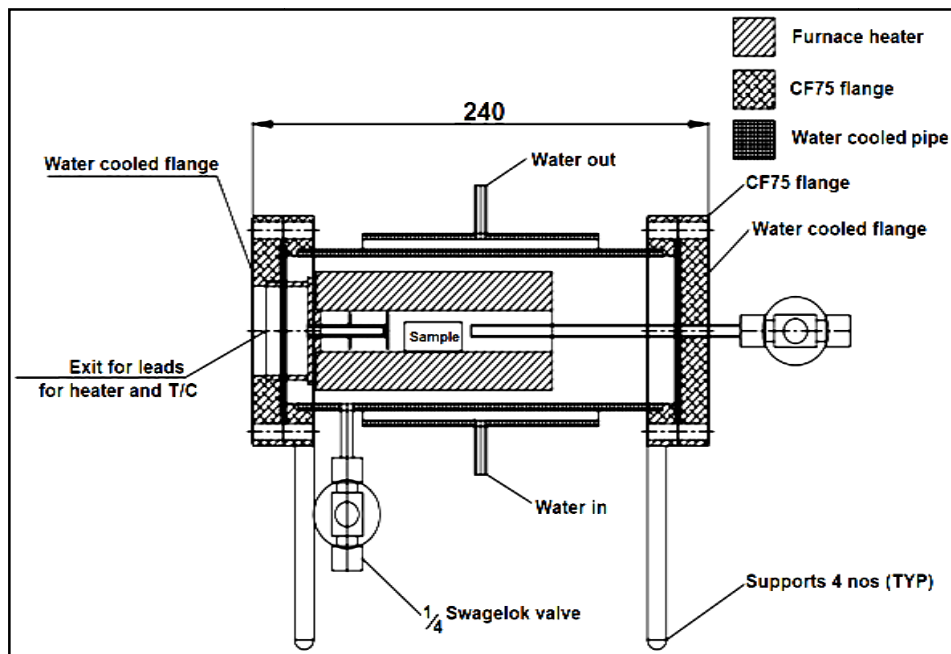


Figure 3.6 Schematic of heater with enclosure in the HE chamber

chamber along with plug assembly is ensured with the help of an O-ring as shown in Fig. 3.7. Helium leak testing showed the leak rate of chamber to be less than  $10^{-9}$  std cc/min. The plug contains the inlet and an outlet tubes for the passage of carrier/sample gas

through the chamber. The inlet and outlet are connected to a 6-Port valve arrangement to control the passage of carrier gas into the chamber. Apart from this, the chamber has a septum through which known amount of hydrogen can be injected. This septum is provided for hydrogen injection during calibration of measuring device, GCTCD. The chamber can be heated to desired temperature (in the present case 400°C) in a furnace. Heating of the chamber inside the furnace can be controlled with a temperature controller. The temperature inside the chamber is calibrated with respect to the furnace temperature by inserting a thermocouple in the chamber. The chamber, the 6-port valve arrangement and the furnace are together referred to as the  $H_D$  collection unit.

The collection of  $H_D$  in the technique which uses this chamber involves hot extraction of  $H_D$  from the weld specimen in the chamber followed by its estimation of  $H_D$  using the GCTCD. Therefore, this technique is referred to as HE-GCTCD in this thesis.

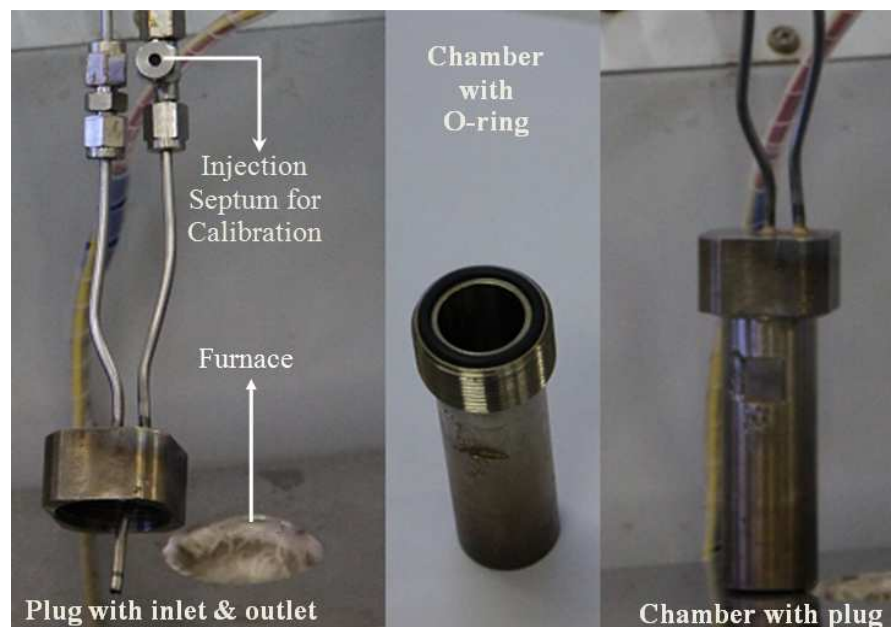


Figure 3.7 Hydrogen collection chamber for GCTCD technique

### **3.1.2.4 Collection of $H_D$**

For the collection of  $H_D$  from the weld specimen, the specimen is removed from liquid nitrogen, cleaned with water, followed by acetone. Specimen was subsequently dried with a stream of dry air. The cleaning of the specimen is completed within 60 s and immediately after that, the specimen is transferred to the hydrogen collection chamber and the chamber is closed.

For measurements using RT-PEMHS, the chamber with the specimen in it is flushed and pressurized with argon gas to a known pressure. For collecting  $H_D$  at room temperature, weld specimen inside the chamber is allowed to evolve hydrogen for 72 h while in HE-PEMHS, the specimen inside the chamber was heated to 400°C and is held at this temperature for 0.5h. The temperatures and time durations of heating is controlled using the programmable temperature controller. Since the chambers are pressurized with argon gas,  $H_D$  evolved from the specimen is collected as mixture of hydrogen in argon ( $Ar-H_2$ ). The concentration of hydrogen in the mixture is estimated using the PEMHS.

In GCTCD based  $H_D$  measurement, the weld specimen is inserted into the chamber. The chamber is immediately closed and initially flushed with pure argon gas for 10-15 seconds. After flushing, the inlet and the outlet of the chamber are closed using the 6-port valve arrangement. The chamber along with the weld specimen inside is inserted into the furnace. For the collection of  $H_D$ , it was heated to 400°C and held at this temperature for 0.5h.  $H_D$  collected inside the chamber was estimated using the GCTCD.

### **3.1.3 Measurement of $H_D$**

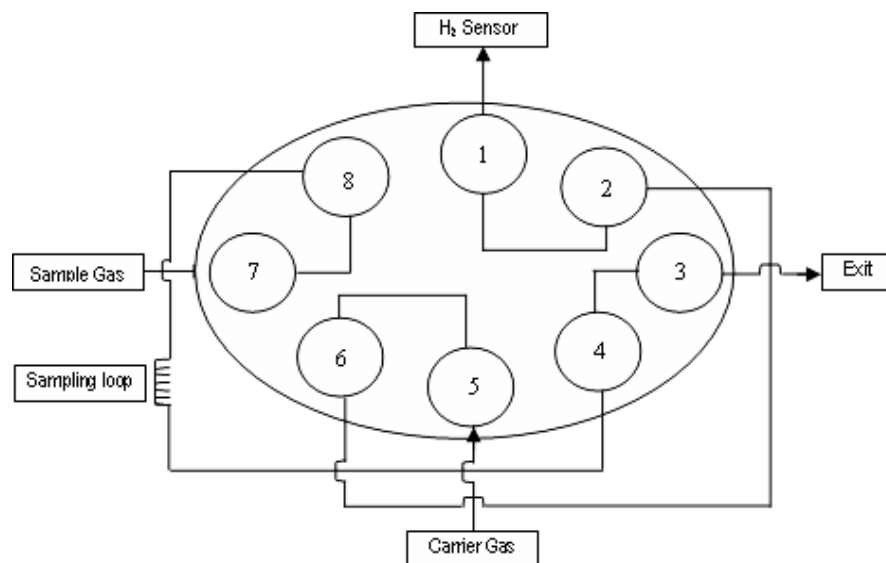
#### **3.1.3.1 Measurement of $H_D$ using PEMHS**

$H_D$  collected from weld specimens as per sections 3.1.2.1 and 3.1.2.2 is estimated using PEMHS. First, the concentration of  $H_D$  in the  $Ar-H_2$  mixture collected in the chamber is measured. From this concentration, volume of  $H_D$  /100g of weld is calculated.

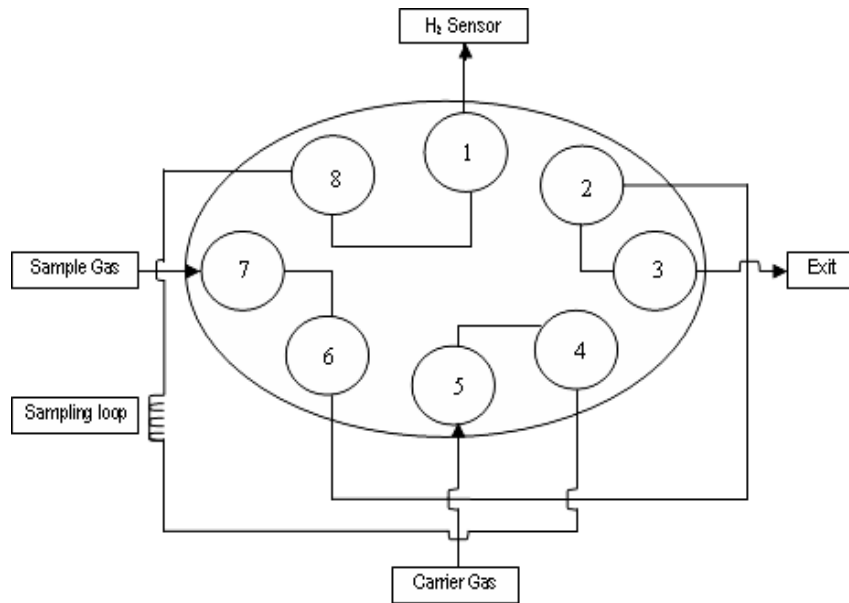
The procedure of estimation and accessories used are given below:

### 3.1.3.1.1 Gas sampling valve

An 8-port gas sampling valve with a sampling loop of known volume is used for sampling the Ar-H<sub>2</sub> mixture from the hydrogen collection chamber. The sampling valve operates in two modes as shown in Fig. 3.8. In mode 1, the gas from the collection chamber is sampled. This mode is shown in Fig. 3.8 (a). In this mode, the inlet of the sampling loop is connected to the collection chamber (sample gas) through port 7 and port 8 and the outlet is open to atmosphere through port 4 and port 3. This mode allows only the carrier gas which enters through port 5 to pass onto the detector/sensor through port 2 and port 1. In mode 2, the sampled gas is injected onto the detector. This mode is shown in Fig. 3.8 (b). In this mode, the inlet of the sampling loop is connected to the carrier gas line through ports 5 and port 4 and outlet to the detector/sensor through port 8 and port 1. This mode allows the sample gas collected in the loop while operating in mode 1 to be carried by the carrier gas into the sensor. While operating in this mode collection chamber is kept closed so that gas inside is conserved.



(a) Valve in Mode 1 for sampling the gas



(b) Valve in Mode 2 for injection of sampled gas onto the PEMHS

Fig. 3.8 Schematic diagram of sampling valve

For analysis of the gas, initially the valve is operated at mode 1. The gas from the specimen chamber, which is filled at a higher pressure than the ambient pressure, is used to flush and subsequently fill the sampling loop while the carrier gas is flowing into the PEMHS. After this, the valve is switched over to mode 2 operation in which the carrier gas flows through the sampling loop carrying the gas sampled in the loop into the PEMHS. The sensor gives a response corresponding to concentration of hydrogen in the gas mixture.

### 3.1.3.1.2. Proton exchange membrane hydrogen sensor (PEMHS)

A comparison of all the available solid and liquid electrolytes showed that Nafion is the best available polymer membrane to be chosen as electrolyte in PEM fuel cell applications because of its high longevity (>60,000 hours), high chemical stability and high ionic conductivity [8-10]. Nafion based electrochemical fuel cell, also known as Nafion based proton exchange membrane hydrogen sensor (PEMHS) has been used for measurement of hydrogen in argon [11-13]. Since this sensor is used for  $H_D$

measurement, a brief description of the principles of this sensor and its application for hydrogen detection is given below.

In PEMHS, the electrolyte, Nafion®117 polymer membrane acts as the proton conductor (Nafion®117 membrane employs the polymer with equivalent weight of 1100g and has a thickness of 7 mils (1 mil = 1/1000 of an inch = 25.4 μm). At 100% relative humidity, the proton conductivity of Nafion®117 is generally about 0.1 S cm<sup>-1</sup> at 60°C that drops by several orders of magnitude as humidity decreases. Depending upon its water content, its proton conductivity is governed by various proton transport mechanisms, namely, proton hopping along surface, Grotthuss diffusion, and ordinary mass diffusion of hydronium ions [14]. In the PEMHS, the Nafion®117 is cast as a film and coated with Pt on both sides. The coatings on either sides form the anode and cathode respectively of the electrochemical cell. The anode is the sensing electrode and the cathode is the counter electrode. The cell is represented as follows:



The sensing side of the coated Nafion®117 is exposed to the hydrogen- argon gas mixture while the counter side is exposed to air. Thus the PEMHS consists of hydrogen-exposed inner platinum film and air-exposed outer platinum film, with the conducting polymer, Nafion®117, sandwiched between them. A mechanical barrier called the diffusion barrier is kept above the sensing electrode (anode). This barrier limits the supply of hydrogen at the sensing electrode thus balances the rate of hydrogen arrival and the rate of hydrogen oxidation at the sensing electrode. This is essentially used to control the kinetics of this process. This results in a better response behavior of the PEMHS. A schematic of the PEMHS with conducting leads is shown in Fig. 3.9. During measurement, hydrogen in the Ar-H<sub>2</sub> mixture gets chemisorbed at the sensing electrode and loses its electron to form proton, H<sup>+</sup>. The proton permeates through the polymer,

reaches the counter electrode where it encounters oxygen from the ambient ( $O_2$  combines with the electrons lost by hydrogen to form  $O^{2-}$ ) to form  $H_2O$ .

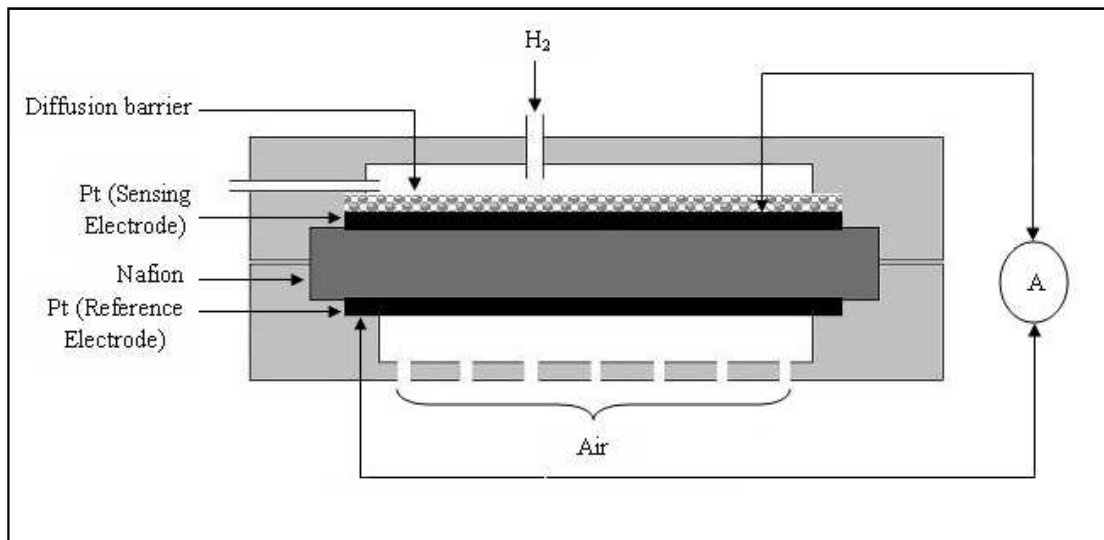
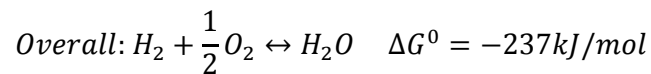
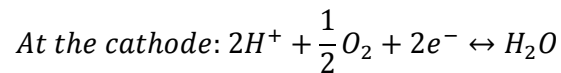
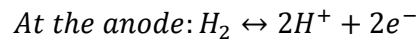


Fig. 3.9 Schematic of PEMHS

The electrochemical reactions taking place at the anode and cathode of the cell are as follows [15]



The Gibbs free energy change ( $\Delta G^0$ ) of the overall reaction is related to the cell voltage by

$$\Delta G^0 = -nFE^0 \dots \dots \dots (3.1)$$

Where,  $n$  = Number of electrons involved in the overall reaction

$F$  = Faraday Constant

$E^0$  = Open circuit potential at thermodynamic equilibrium = 1.23V

During conduction of the proton through Nafion®117, a limiting circuit current is produced. The expression for this limiting circuit current is given in equation (3.2) [13]:

$$i = \frac{2DACF}{t} \dots \dots \dots (3.2)$$

In the above relation,

$i$  = Limiting current,       $D$  = Diffusion coefficient,       $F$  = Faraday Constant,

$A$  = Area of the electrode,       $C$  = Concentration,       $T$  = Time of diffusion

A peak corresponding to this limiting current was observed in the data acquisition system. The peak height is proportional to concentration of hydrogen in the sampling chamber. The response of the PEMHS for hydrogen is acquired with the help of data acquisition unit which contains an amplifier, a display unit and a computer. The photographs of the Nafion membrane coated with platinum, the PEMHS, the preamplifier and hydrogen display unit are shown in Fig. 3.10.

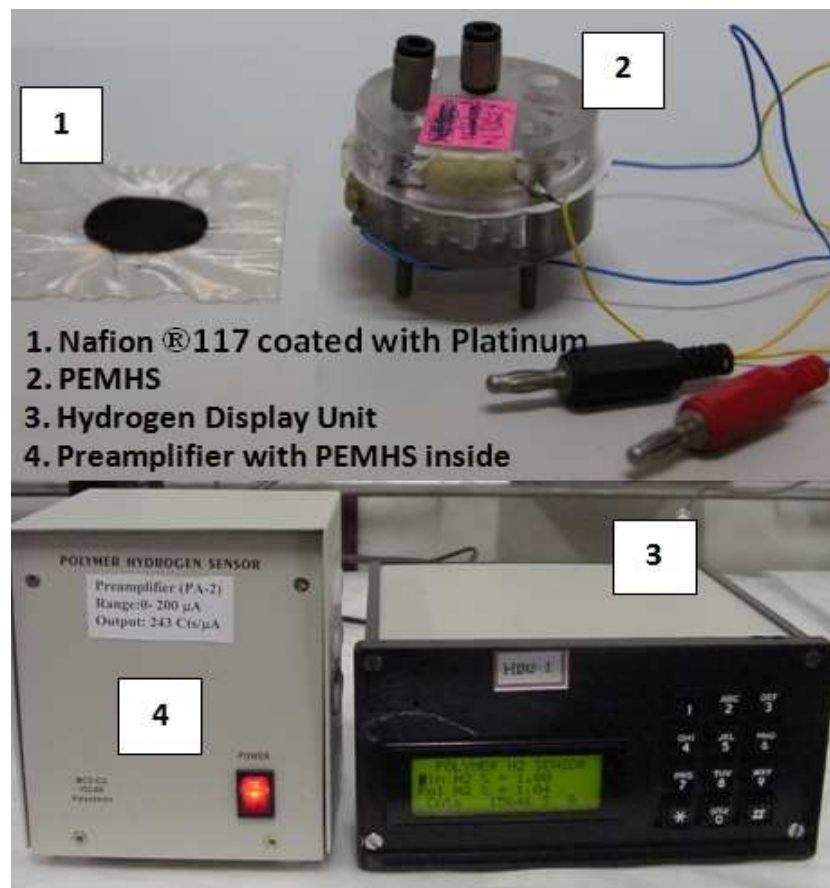


Fig. 3.10 Photograph of PEMHS and Data acquisition unit

### 3.1.3.1.3. Procedure for measurement of $H_D$ using PEMHS

Estimation of  $H_D$  using the PEMHS involves calibration of the PEMHS and subsequent measurement of concentration of hydrogen in the gas mixture sampled from the chamber. A schematic and a photograph for the measurement of  $H_D$  using the PEMHS are shown in Fig. 3.11 and 3.12 respectively. For the calibration of the PEMHS, initially, a baseline for the PEMHS is obtained by purging it with a continuous flow of argon gas. On attaining the baseline, Ar- $H_2$  gas mixtures of different known hydrogen concentrations are injected through the 8-port valve onto the PEMHS. The different Ar- $H_2$  mixtures are prepared by mixing argon and hydrogen gases in the desired proportions by mass flow controllers. Response of PEMHS is obtained as peaks of different heights corresponding to different concentrations of hydrogen in Ar- $H_2$  gas mixtures. Each concentration is injected three times. The average of peak height was plotted against the concentration of hydrogen to obtain the calibration plot of the PEMHS. To avoid any bias, the PEMHS was calibrated before each measurement.

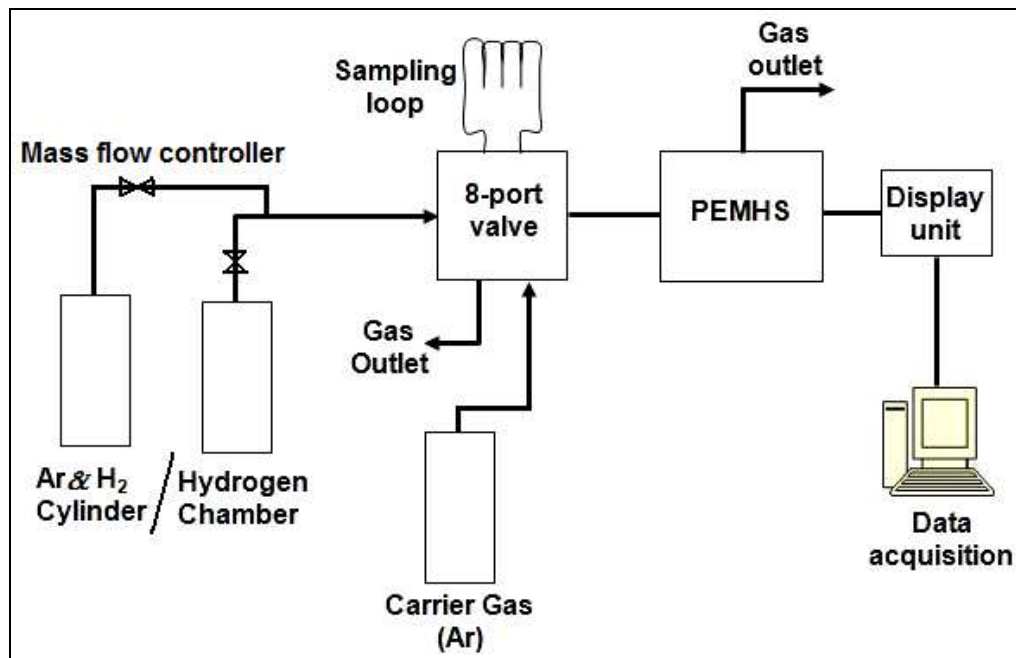


Fig. 3.11 Schematic of measurement of  $H_D$  using PEMHS

After the calibration, the sampling loop inlet of the 8-port valve is connected to the specimen chamber. The loop is first flushed with the gas mixture from the chamber, and then the mixture is injected onto the PEMHS by switching over to the injection mode of the eight-port valve. A response corresponding to the concentration of hydrogen in the chamber is recorded in the data acquisition system. As the specimen chamber is at a higher pressure than ambient, it is possible to repeat the measurement at least three times using the gas mixture available in the chamber. The average of peak height is compared with the calibration to estimate the unknown hydrogen concentration. For each set of weld specimen, several measurements are carried out and the average values are reported.

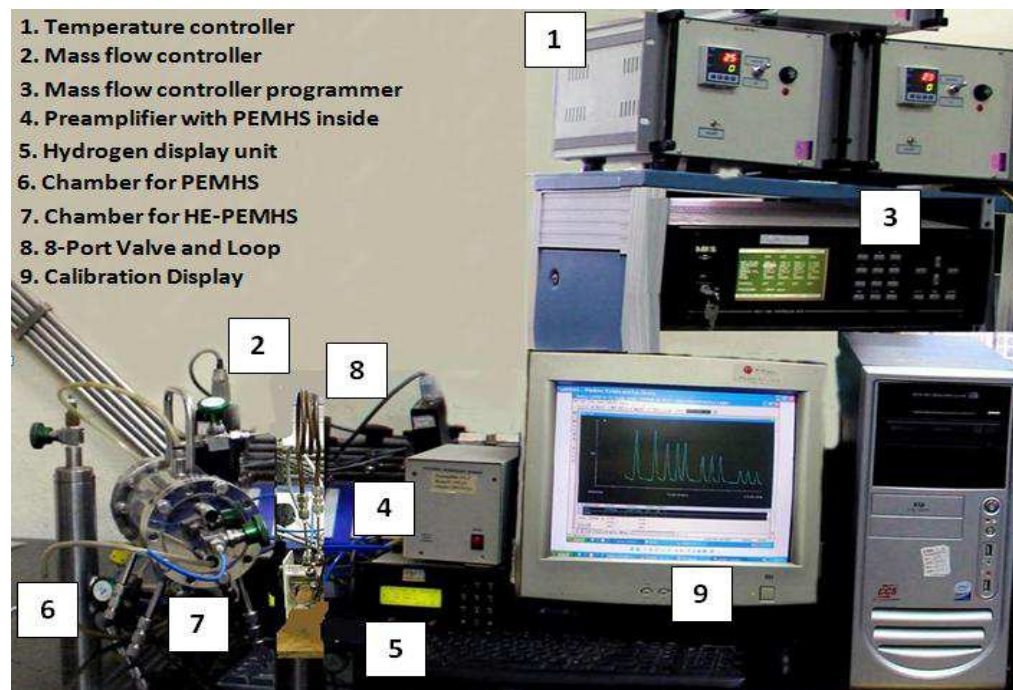


Fig. 3.12 Photograph of measurement of  $H_D$  using PEMHS

After measuring the diffusible hydrogen concentration, the weld specimen is taken out, cleaned, dried, and weighed to the nearest 0.01g. From the volume of the chamber, hydrogen concentration in the gas mixture, pressure of the gas inside the chamber, weight of deposited metal,  $H_D$  is estimated in the units of volume of hydrogen

in ml/100g of deposited metal at standard temperature and pressure is measured using the following relation:

$$H_{PEMHS} = \left(\frac{PVC}{10^6}\right) \left(\frac{100}{M_2 - M_1}\right) \frac{ml}{100g} \dots \dots \dots (3.3)$$

In the above relation,

$H_{PEMHS} = H_D$  obtained by PEMHS method in ml/100 g;

$P$  = Pressure of argon in the hot extraction chamber in atmosphere;

$V$  = Available volume of the chamber for gas accumulation (in ml);

$C$  = Concentration of  $H_D$  gas in the chamber after collection in ppm;

$M_1$  = Weight of the specimen before welding, in gram;

$M_2$  = Weight of the specimen after welding, in gram

### **3.1.3.2 Measurement of $H_D$ using GCTCD**

#### **3.1.3.2.1 $H_D$ Collection Unit**

This is the portion of the GCTCD which consists of heater, chamber for the extraction of  $H_D$  and two valves (provided at the inlet and outlet of the chamber) which control the carrier gas flow into the chamber.

#### **3.1.3.2.2 Gas Chromatography**

Principle of gas chromatography involves the separation of a mixture of gases in its column. It separates the mixture of gases depending upon their retention time in its stationary phase that is present in the column. Different constituents of the gas mixture have their characteristic retention time. This makes them elute out of the GC column at different times to reach the detector, TCD. In the present case, pure argon is used as the carrier gas which carries the hydrogen collected in the collection chamber of GCTCD to the analyzer, TCD.

### 3.1.3.2.3 Thermal Conductivity Detector (TCD)

The gas chromatography used for  $H_D$  measurement uses a thermal conductivity detector for analysis of the gas. The principle of analysis using TCD involves measuring the change in resistance of its filaments due to the lowering in temperature caused by the sample gas mixture/reference gas, argon that is in contact with the filament

The present TCD setup uses four Tungsten–Rhenium alloy filaments connected in two channels in a Wheatstone bridge configuration. These filaments are heated to a particular temperature. When the hot filament is in contact with a gas, depending on the thermal conductivity of the gas some heat is taken away from the hot filament reducing its temperature. This change in temperature induces some change in resistance of the filaments. A reference gas is passed over both the channels to set the base line. On setting the base line, the gas mixture for analysis/calibration is allowed to enter one of the channels and the reference gas on the other. The difference in thermal conductivity produces a change in resistance. This change in resistance gives rise to a net output voltage ( $V_{out}$ ) whose response is displayed as a peak. The area under the peak is proportional to the volume of the sample gas.

#### 3.1.3.1.4. Procedure for measurement of $H_D$ using GCTCD

Estimation of  $H_D$  using the GCTCD involves calibration of the GCTCD and subsequent measurement of volume of  $H_D$  in the collection chamber. A photograph of the GCTCD is shown in Fig. 3.13. GC is calibrated for volume for hydrogen, by injecting known volumes of hydrogen through the septum provided in the GC. Area under peak obtained for each injection is plotted against the corresponding volume injected to obtain the calibration graph.

After calibration, the weld specimen is admitted into the chamber. The chamber is flushed with the carrier/reference gas. On completion of flushing, the gas flow into the

chamber is blocked and the chamber is heated at 400°C for 0.5h. After the heating, carrier gas is allowed to pass through the chamber. The carrier gas carries the hydrogen evolved from the weld sample through the column to the TCD. A response corresponding to this volume is recorded and the volume of hydrogen is estimated from the calibration curve and displayed. Knowing the weight of the deposited metal in the weld sample, the volume of  $H_D$  evolved from the weld sample is expressed in volume of hydrogen in ml/100g of deposited metal.

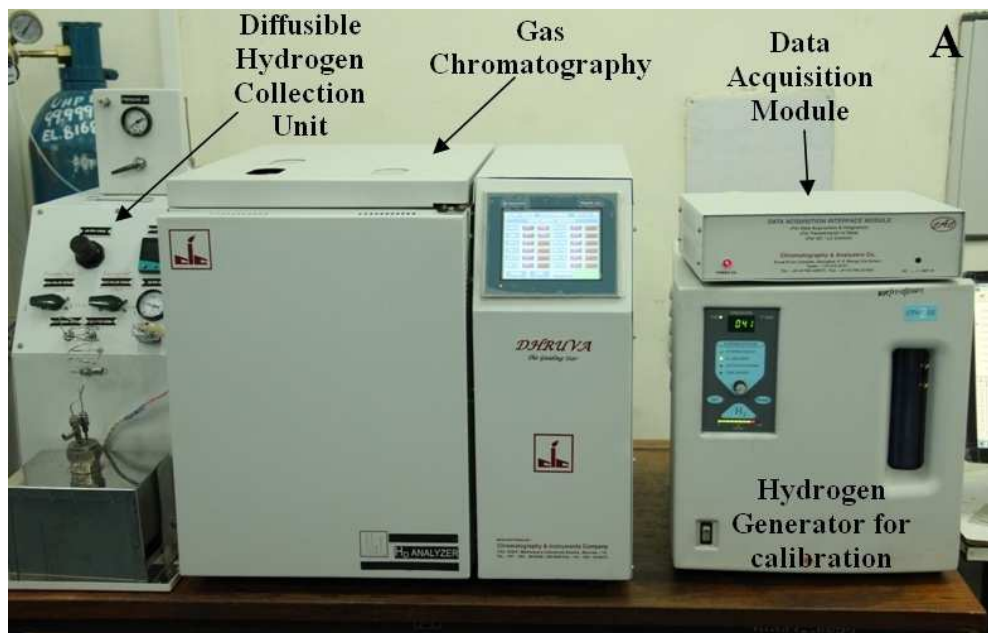


Fig. 3.13 Photograph of GCTCD setup for measurement of  $H_D$

### 3.1.4 Determination of $H_D$ using mercury method

Mercury method is the primary standard recommended by ISO 3690:2000 for  $H_D$  measurement. This standard also recommends a comparison of  $H_D$  obtained by any new technique with that obtained by the standard mercury method. Therefore,  $H_D$  measurement was carried out using mercury method for similar weld specimens used in the techniques described above. For the collection of  $H_D$  from the weld specimen,

temperature and time durations specified in ISO 3690:1977 were used. The mercury apparatus used for  $H_D$  collection and measurement is shown in Fig. 3.14.

For measurement, weld specimen, after quenching and cleaning, is admitted through the open limb into the Y-tube of the mercury apparatus and the limb is closed. The weld specimen is moved to the graduated close limb of the Y-tube with the help of a magnet. At this point, the Y-tube along with the weld specimen is evacuated by a suction/rotary pump. After evacuation, the vacuum is released and the initial reading in the graduated limb of the Y-tube is recorded. The Y-tube was evacuated again and the weld specimen inside is allowed to evolve hydrogen for 72h, and final reading is recorded. The difference in the initial and final readings is equal to the volume of  $H_D$ . From the weight of deposited metal, ambient temperature and pressure, collected hydrogen volume is converted into volume of hydrogen at standard temperature and pressure in ml/100g of deposited metal using equation 3.4.

$$H_{Mercury} = (V_f - V_i) \left( \frac{273}{273 + T} \right) \left( \frac{B - H}{760} \right) \left( \frac{100}{W_f - W_i} \right) \dots \dots \dots (3.4)$$

In the above relation,

$H_{Mercury}$  =  $H_D$  measured in mercury method at STP (ml/100g of deposited metal)

$V_f$  and  $V_i$  = Final and initial volume of gas in the burette of Y-tube respectively

$T$  = Ambient temperature (K)

$W_f$  and  $W_i$  = Weight specimen after and before welding respectively

$B$  = Ambient pressure in Barometer in mm Hg

$H$  = Mercury head, i.e., Final difference of height of mercury in the two limbs of Y-tube



Fig. 3.14 Mercury apparatus used for  $H_D$  measurement

Three such measurements were carried out simultaneously in three Y-tubes and the average values of  $H_D$  were reported.

### ***3.1.5. Measurement of $H_D$ with respect to time using RT-PEMHS***

Evolution of  $H_D$  from weld specimen was studied as a function of time using PEMHS. For this study, weld specimens were prepared by depositing E7018 electrode on mild steel. The conditions for degassing of base metal and baking of electrode and preparation of specimen in this case were similar to those discussed earlier.

In this study,  $H_D$  from the weld specimen is collected and measured for different time intervals (0–24, 24–48, 48–72, 72–120, 120–192, and 192–264 hours) using the PEMHS at room temperature. For durations up to 72 hours, hydrogen evolved for each 24-hour interval is measured. However, beyond 72 hours, the duration of hydrogen collection increased because the hydrogen evolved from the specimen decreased considerably. The procedure of  $H_D$  measurement is the same as that discussed in the

section 3.1.3.1.3. After measuring the concentration of hydrogen evolved within a certain time interval, the chamber containing the specimen is flushed, pressurized again with argon gas to a known pressure. Hydrogen collection and measurement is repeated for the next interval. Measurements are continued until hydrogen concentration in the gas inside the chamber decreased below the measurable limit of the PEMHS.

## **3.2 Effect of preheat and post-heating on H<sub>D</sub> content in welds**

The effect of preheating the specimen prior to welding and post-heating it after welding on the H<sub>D</sub> contents in welds was studied. In this study, all the H<sub>D</sub> measurements were carried out using HE-PEMHS. The measured H<sub>D</sub> contents were compared with the results obtained by mercury method from similar weld specimens. The base metals, electrodes, equipments used in this study, the procedure of preheat and post-heating etc. are discussed below.

### ***3.2.1. Specimen Preparation***

To study the effect of preheat and post-heating on H<sub>D</sub>, test assemblies were prepared from two different base metals: mild steel and modified 9Cr–1Mo steel. The chemical compositions of the base metals are given in Table 3.3. The dimension of test assembly and the procedure of weld specimen preparation were as per ISO 3690 and discussed earlier in this chapter. For weld specimen preparation, E7018 electrode is deposited on the preheated mild steel assembly and E9015-B3 electrode on preheated modified 9Cr–1Mo assembly. Prior to deposition, the electrodes were baked as per Table 3.2. For the study of the effect of preheat, preheat temperatures employed are 100, 150, 200 and 250°C. In case of preheating combined with post-heating, preheated weld specimen was subjected to post-heating. Preheating and post-heating was carried out on a copper jig. Weld specimens were also prepared as per ISO 3690 for the determination of

actual  $H_D$  content of the welds. The detailed procedures of specimen preparation with preheating and post-heating are discussed below.

### ***3.2.1.1 Preparation of specimens with preheating and preheating combined with post-heating***

Fig. 3.15 shows the heater unit and test assembly used for preheating and post-heating studies. This heater unit comprises of a heating element, a thermocouple and a temperature controller. During preheating and post-heating, the test assembly was placed on the copper jig with the heater placed on the test assembly. The temperature of the specimen was measured by a thermocouple inserted through a hole provided in the copper jig, in contact with the side face of the specimen

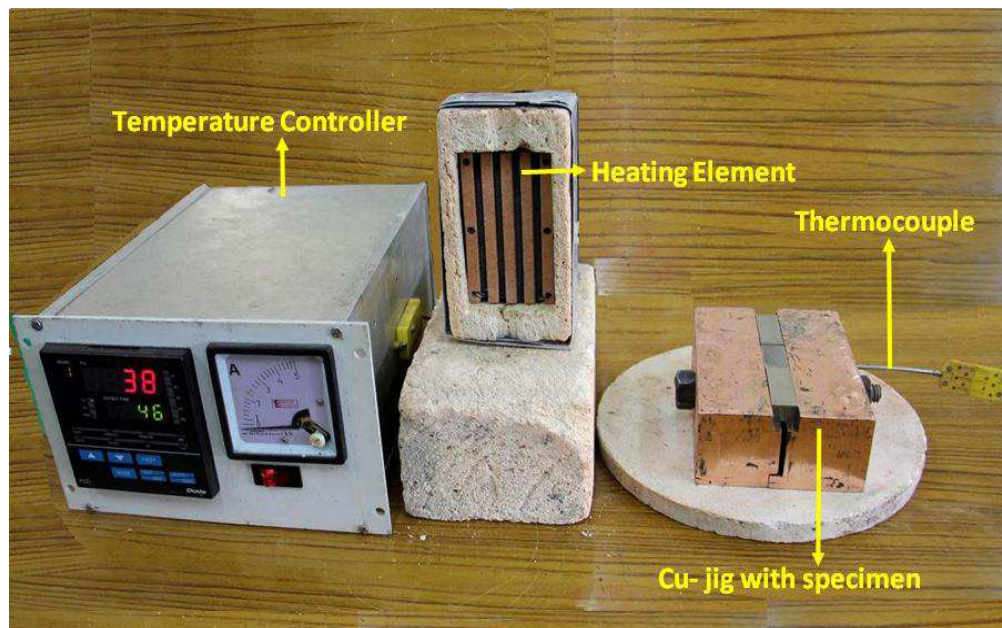


Fig. 3.15 Heater unit for preheating and post heating

Specimen was first preheated to the desired temperature. The temperature was controlled using the temperature controller, which receives input from the thermocouple. Welding was carried out on the preheated specimen. Soon after welding, the thermocouple was used to record the cooling profile of the specimen.

It is difficult to simulate the effects of preheating of an actual weld joint on the test assembly used for  $H_D$  measurement. Removing the test assembly soon after welding will be too fast and waiting for it to cool down to room temperature would be too slow to simulate the effect of preheating on weld joints. Hence, the test assembly was removed from the copper jig for three different conditions: when it is cooled down to the respective preheat temperatures, when it is cooled down to  $100^\circ\text{C}$  and when 10 min is completed after welding.

To measure the  $H_D$  remaining in the specimen after post-heating, studies were conducted with specimens which were prepared with preheating and subsequently post-heated at the preheating temperature for 30 minutes. For this, the preheated test assembly with weld bead was maintained at the post-heating temperature without removing it from the copper jig. The post-heating was carried out by reintroducing the heating element on the copper jig with temperature in the controller set at the post-heating temperature. The time temperature profile of this post-heating is shown in Fig. 3.16.

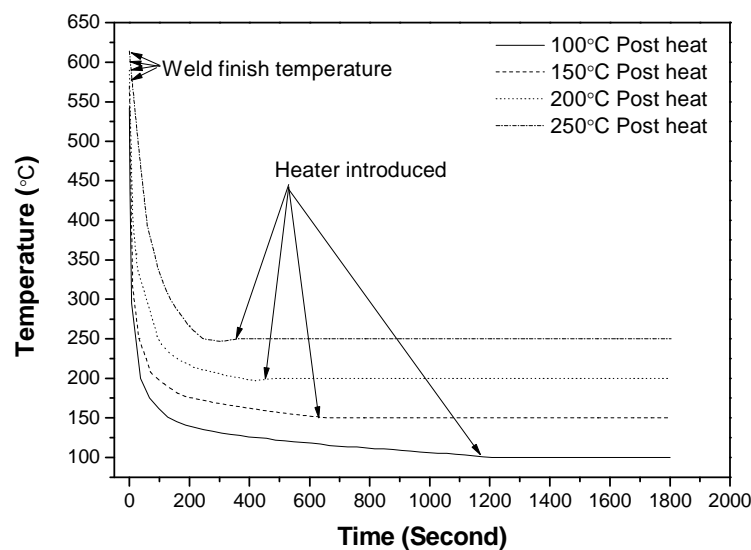


Fig. 3.16 Time-Temperature profile of post-heating

After carrying out the necessary preheating and post-heating treatments as above, the test assembly was removed from the jig, quenched in cold water then in liquid nitrogen. Specimen was detached from run-on and run-off pieces and was stored in liquid nitrogen until used for  $H_D$  measurement.

### ***3.2.1.2 Measurement of $H_D$***

Hydrogen evolved from the specimens was measured using HE-PEMHS technique. The results obtained in this method were compared with the  $H_D$  contents obtained using the standard mercury method from similar specimens. The procedures for  $H_D$  measurement using HE-PEMHS technique and mercury method has been discussed earlier in this chapter. Three separate measurements were carried out for each condition using both HE-PEMHS technique and mercury method.

### ***3.2.2 Measurement of hydrogen evolved from weld specimen during its post-heating***

After measuring the  $H_D$  remaining in the weld specimen with preheating and post-heating, measurement of hydrogen evolved during post-heating of the specimen was carried out. For this study, mild steel-E7018 and modified 9Cr-1Mo-E9015-B3 combinations were used. Weld specimen was prepared by depositing electrode on preheated specimen and it was soon transferred to hot extraction chamber which is already heated to the post-heating temperature. The chamber was flushed and filled with argon to a known pressure. Specimen was held at the post-heating temperature for 30 minutes, the duration of post-heating employed to study  $H_D$  remaining in the weld after post-heating. The heating, cooling and holding operations were programmed with the help of the programmable temperature controller in such a way that post-heating of the

specimen within the hot extraction chamber simulates post-heating of the specimen in the copper jig as closely as possible. Hydrogen collected in the chamber was subsequently measured using the PEMHS.

### 3.3 Study on apparent diffusivity of hydrogen in steel

Apparent diffusivity of hydrogen in steel was determined from the hydrogen evolved from the electrochemically charged specimens. For estimating diffusivity at ambient temperature, evolved hydrogen was measured using mercury methods. For hydrogen diffusivity in the temperature range of 100-400°C, hot extraction techniques were used for measurement of hydrogen. Details of materials used, specimen preparation and procedure for measurement are given below.

#### 3.3.1 Materials used and specimen

For this study, specimens were prepared from modified 9Cr-1Mo steel, 2.25 Cr-1Mo steel and mild steel. The chemical compositions of these steels are given in Table 3.3. Before preparation of specimen, these steels were given heat treatment as given in Table 3.4.

Table 3.3: Chemical composition of steels used in this study in Wt%

Elements	Modified 9Cr-1Mo	2.25Cr-1Mo	Mild steel
Carbon	0.114	0.162	0.205
Chromium	8.838	2.319	-
Molybdenum	0.860	0.895	-
Manganese	0.403	0.516	0.553
Nickel	-	0.346	-
Silicon	0.309	0.071	0.062
Phosphorous	0.014	0.006	0.039
Sulphur	-	0.009	0.047
Niobium	0.080	-	-
Vanadium	0.027	0.004	-
Copper	-	0.107	0.324

Table 3.4: Heat treatment conditions of of steels used in this study

Steels	Heat treatment conditions
Modified 9Cr-1Mo	1050°C/10Min/Air cooling
2.25Cr-1Mo	970°C/10Min/Air cooling
Mild steel	970°C/10Min/Air cooling

The objective was to get the specimen with a microstructure that would be present in the heat affected zone of the weld joints of these steels in the as-welded condition. For modified 9Cr-1Mo steel, the microstructure is fully martensite. For 2.25Cr-1Mo steel, it would be predominantly bainite and for mild steel, it would be a mixture of ferrite + pearlite. The specimens used in this study were solid cylinders of 25mm length and 10 mm diameter. A photograph of specimens used is shown in Fig. 3.17. Each of these specimens has a 3M threading of 5mm depth from the top. An electrically conducting rod is threaded with the specimen to hold it dipped in a medium for charging it with hydrogen.



Fig. 3.17 Photograph of specimen for hydrogen charging

### ***3.3.2 Hydrogen charging of the specimen***

Prior to hydrogen charging, the cylindrical specimen was cleaned in ultrasonic bath followed by cleaning in acetone. Excess of acetone was removed with warm air. Charging of hydrogen in the specimen was carried out in an electrochemical cell

specified in standard ASTM G5-94 [16]. The schematic of this cell is shown in Fig. 3.18. The electrochemical cell has a saturated calomel electrode, platinum and the specimen as its reference, auxiliary and working electrodes respectively. The reference electrode was connected to the rest of the cell through a luggin probe-salt bridge containing an aqueous solution of 20% agar agar and 10% KCl. The electrolyte of the cell, a solution of 0.5M  $\text{H}_2\text{SO}_4$  + 0.2 g/l  $\text{As}_2\text{O}_3$ , was used as the hydrogen charging medium.  $\text{As}_2\text{O}_3$  in the charging medium acts as poison for hydrogen recombination.  $\text{As}_2\text{O}_3$  combines with hydrogen to form  $\text{AsH}_3$ , thereby inhibits the hydrogen recombination reaction in the charging medium and promotes the entry of hydrogen atoms into the bulk metal [17, 18]. A photograph of hydrogen charging of the specimen in the cell is shown in Fig. 3.19.

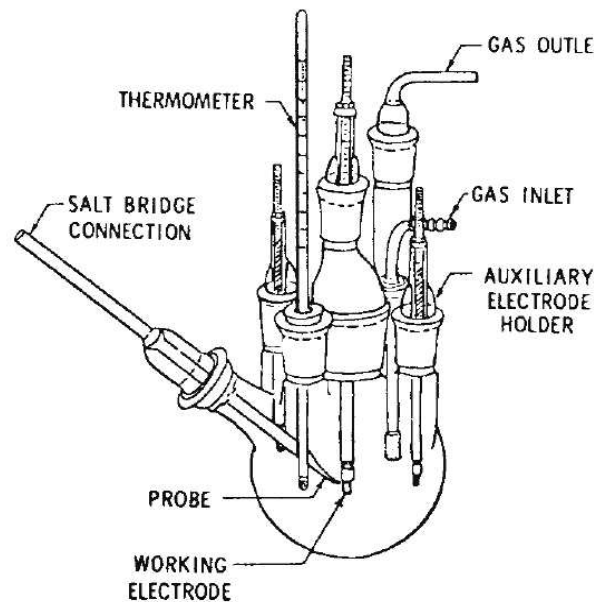


Fig. 3.18 Schematic of electrochemical cell for hydrogen charging [16]

Before admitting the specimen, the cell was purged with high purity argon to generate an inert atmosphere. The specimen was dipped 90-95% along its length into the charging medium with the help of a 316L stainless steel rod. The rest of the specimen was covered with Teflon. Hydrogen charging of the specimen was carried out at a

constant potential of  $-1.5\text{ V}$  applied to the working electrode (cathode) against the reference electrode. As a first step, hydrogen charging of the specimen was carried out

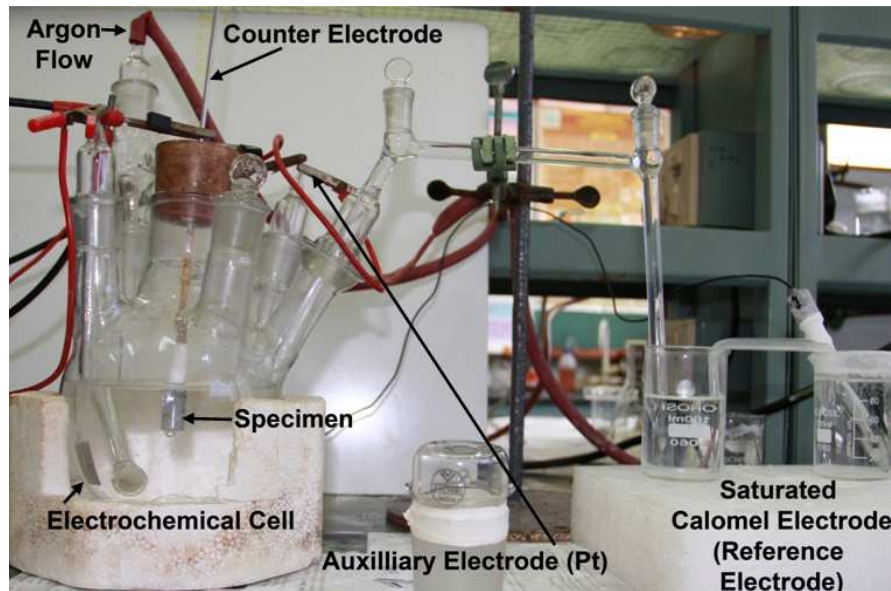


Fig. 3.19 Photograph of hydrogen charging

for different time durations of 1-5 hour to optimise the time duration of charging. On completion of charging, specimen was transferred into liquid nitrogen within 4-5 seconds. Hydrogen evolved out of the charged specimens was measured using the mercury method, the standard method recommended for  $H_D$  measurement in welds. The results of this study are presented in Table 3.5. From this table, it is evident that the hydrogen content of the specimen remained nearly constant over the variation in the charging time from 1 to 5 hour. In other words, the specimen is saturated with hydrogen during the first hour of its charging. Based on these results, the specimens were charged for 1 hour for the rest of the study. After the completion of charging, the specimen was quickly stored in liquid nitrogen until its further use for measurement of hydrogen.

Table 3.5 Optimization of time duration for hydrogen charging

Time (Hour)	Hydrogen content obtained (ml/100g)		
	Modified 9Cr-1Mo	2.25Cr-1Mo	Mild Steel
1	27.22	27.67	28.93
2	26.96	-	-
3	27.01	27.25	28.42
4	27.64	-	-
5	27.53	27.91	28.81

### ***3.3.3 Measurement of hydrogen evolved at different temperatures***

Hydrogen extraction was carried out from the hydrogen charged specimens at test temperatures 100, 200, 300 and 400°C. For measurement of hydrogen evolved from modified 9Cr-1Mo specimen, HE-PEMHS technique was used. Hydrogen evolved from 2.25Cr-1Mo and mild steel specimens was measured using the HE-GCTCD technique. These techniques were originally developed for rapid measurement of  $H_D$  in welding consumables. The calibration and the procedures of hydrogen measurement using these techniques were detailed earlier in this chapter.

Hydrogen evolved from the charged specimens was measured for different time durations at different temperatures. It is known that the maximum hydrogen content obtained for different time durations at different test temperatures depends upon the apparent diffusivity of hydrogen at those temperatures. To determine the total hydrogen evolved at a given temperature, hydrogen collection was continued for sufficiently long time durations until it is confirmed that hydrogen evolved beyond this duration is practically negligible and beyond the detectable limit of the sensors. However, it should be noted that hydrogen measurement was not carried out at time durations with equal intervals. This is because hydrogen content evolved from the specimen decreases with increase in time. Hence time interval between two successive measurements increased as the hydrogen remaining in the specimen reduces with time at a given test temperature.

Total hydrogen evolved at 25, 100, 200, 300 and 400°C for different time durations were plotted against the corresponding time duration of measurement to obtain hydrogen evolution profiles at these temperatures. These profiles were used to calculate the apparent diffusivity of hydrogen in the above steels.

## Reference

1. *ISO 3690:1977/ Add 1:1983*, , Welding - Determination of hydrogen in deposited weld metal arising from the use of covered electrodes for welding and low alloy steels; Addendum 1
2. *ISO 3690:2000*, Welding and allied processes – Determination of hydrogen in ferritic steel arc weld metal.
3. D. J. Kotecki, Hydrogen measurement and standardisation, Proceedings of the Joint Seminar on Hydrogen Management in steel Weldments, Melbourne, October, 1996, 87-102.
4. C. Ramesh, G. Velayutham, N. Murugesan, V. Ganesan, K.S. Dhathathreyan, G. Periaswami, An improved polymer electrolyte-based amperometric hydrogen sensor, *Journal of Solid State Electrochemistry*, 2003, Vol. 7, No. 8, 511–516
5. Albert S.K.: Some aspects of weldability of Cr Mo steels, Ph.D Thesis, 1996, Indian Institute of Technology, Bombay.
6. CF Components, [http://www.vacom.es/files/katalog/01\\_cf\\_vacuumcomponents.pdf](http://www.vacom.es/files/katalog/01_cf_vacuumcomponents.pdf)
7. ISO/TS 3669-2:2007 [Vacuum Technology - Bakable Flanges - Part 2: Dimensions Of Knife-edge Flanges](#)

8. B. Smitha,, S. Sridhar and A.A. Khan, **Solid polymer electrolyte membranes for fuel cell applications - A review**, Journal of Membrane Science, 2005, Vol. 259, No. 1-2, 10–26.
9. V. Neburchilov, J. Martin, H. Wang and J. Zhang, A review of polymer electrolyte membranes for direct methanol fuel cells, 2007, Journal of Power Sources, Volume. 169, No. 2, 221–238
10. B. Viswanathan and M. Helen, Is Nafion®, the only choice?, Bulletin of the Catalysis Society of India, 2007, Vol. 6, No. 2, 50-66
11. M. Sakthivel, and W. Weppner, Development of a hydrogen sensor based on solid polymer electrolyte membranes, Sensors and Actuators B, 2006, Vol. 113, No. 2, 998–1004
12. G. Velayutham, C. Ramesh, N. Murugesan, V. Manivannan, K.S. Dhathathreyan and G. Periaswami, Nafion based amperometric hydrogen sensor, Ionics, 2004, Vol. 10, No.1/2, 63–67
13. C. Ramesh, N.Murugesan, M.V. Krishnaiah, V. Ganesan and G. Periaswami, Journal of Solid State Electrochemistry, 2008, Vol. 12, No.9, 1109-1116
14. P. Choi, N. H. Jalani, and R. Datta, Thermodynamics and proton transport in Nafion II. Proton diffusion mechanisms and conductivity, Journal of the Electrochemical Society, 2005, Vol. 152, No.3, E123-E130
15. J. R. Stetter, J. Li, Amperometric gas sensors - A review, Chemical Reviews, 2008, Vol. 108, No. 2, 352-366
16. ASTM G 5-94(2004): Standard reference test method for making potentiostatic and potentiodynamic anodic polarization measurements.
17. T. Zakroczymski, A. Oriani, M. Smialowski (Eds.), Hydrogen Degradation of Ferrous Alloys, Noyes, Park Ridge, NJ, 1985.

18. T. Zakroczymski, Z. S. Sniatowska and M .Smialowski, Effect of arsenic on permeation of hydrogen through steel membranes polarized cathodically in aqueous solution, *Werkstoffe und Korrosion*, 1975, Vol.8, 617-624

**CHAPTER 4**

**MEASUREMENT OF  $H_D$  CONTENTS  
USING INDIGENOUSLY DEVELOPED  
TECHNIQUES**

# Measurement of $H_D$ contents using indigenously developed techniques

---

---

Materials used in weld specimen preparation and procedure of measurement of their diffusible hydrogen ( $H_D$ ) content using indigenous techniques are given in Chapter 3. The techniques include collection of  $H_D$  at room temperature and its measurement using proton-exchange-membrane hydrogen sensor (RT-PEMHS), hot extraction of diffusible hydrogen at 400°C and its measurement using PEMHS (HE-PEMHS) and a gas chromatography using a thermal conductivity detector (HE-GCTCD). In this chapter, results of  $H_D$  measurement using these techniques and their comparison with the standard ISO 3690 are presented.

## 4.1. Results of $H_D$ measurement using PEMHS

### 4.1.1 Calibration of the PEMHS

As diffusible hydrogen evolved from the weld specimen is collected in a chamber filled with Argon (Ar), the measurement using sensor is actually carried out for concentration of  $H_2$  in this Ar- $H_2$  mixture. Hence, the sensor calibration is done using known concentrations of  $H_2$  in the Ar- $H_2$  mixtures. A typical in-situ response of the sensor during one such calibration is shown in Fig. 4.1. The baseline in the figure is the response of the PEMHS when argon alone is flowing through it. The peaks are the response for different concentrations of hydrogen in the Ar- $H_2$  mixture. In the figure, sets of three peaks of nearly equal heights are for identical concentrations that were injected thrice in the PEMHS. The calibration curve of PEMHS is obtained by plotting the average peak height against the hydrogen concentration in the gas mixture as shown in

Fig. 4.2. From the figure, it is evident that the peak height varies linearly with concentration of hydrogen in the gas mixture.

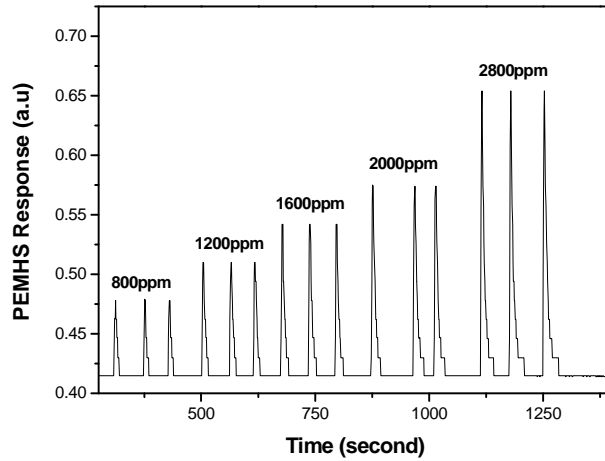


Fig. 4.1 Response of the PEMHS during calibration

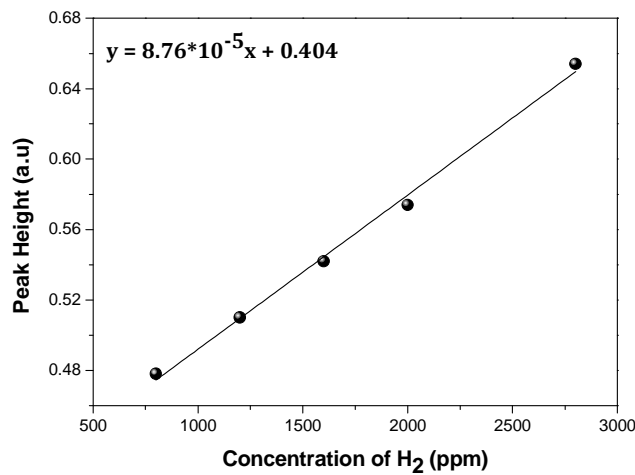


Fig. 4.2 Calibration plot of PEMHS

PEMHS was calibrated prior to each set of measurements. Unknown concentration of hydrogen in the Ar-H<sub>2</sub> mixture collected from weld specimen was estimated using the calibration curve. From the concentration, volume of hydrogen can be calculated using equation 3.3.

#### 4.1.2 Results of $H_D$ measurement using RT-PEMHS and their comparison with mercury method

For this study, different welding electrodes having  $H_D$  content in the range of 2-18ml/100g were used. The accuracy of RT-PEMHS technique was examined by comparing the  $H_D$  contents obtained in this method with that obtained from similar weld specimens using the standard mercury method.

The results of measurements carried out using both these techniques are given in Table 4.1. From this table, it is evident that the results obtained using both these methods are in good agreement. In fact, the standard deviations of measurements using the RT-PEMHS are lower than that using mercury method. This indicates better precision of the RT-PEMHS technique. Further agreement between both the techniques is shown in Fig. 4.3. This figure is a plot of  $H_D$  contents obtained using RT-PEMHS technique against that obtained using the mercury method. This figure shows a linear relation between the  $H_D$  contents obtained in these methods. An empirical formula for the hydrogen contents obtained by these two methods is also shown in the figure. This formula shows one to one correspondence between the methods. Therefore, the PEMHS can be used for  $H_D$  measurements in the weld joints as an alternative to mercury method.

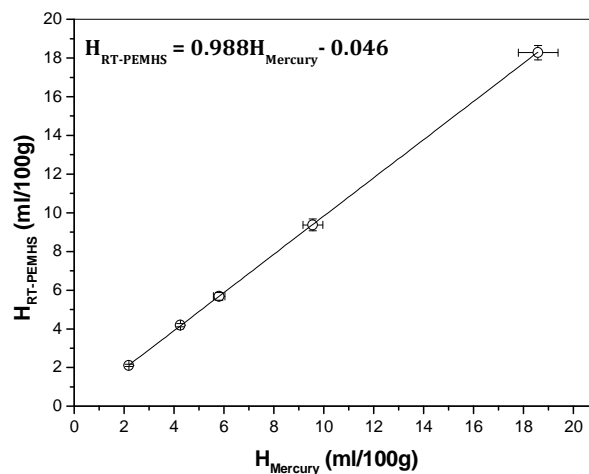


Fig. 4.3 Correlation between RT-PEMHS and Mercury method

Table 4.1 H<sub>D</sub> contents obtained using RT-PEMHS and ISO/Mercury method

S. No	Mild Steel +Electrodes	H <sub>RT-PEMHS</sub> (ml/100g)	H <sub>Mercury</sub> (ml/100g)
1	E6010	18.26	18.31
		18.46	19.76
		18.00	17.28
		18.87	19.24
		17.81	18.73
2	E6013	9.54	9.5
		9.46	10.02
		9.11	9.56
		9.78	8.91
		8.94	9.31
3	E7018-1	5.55	6.14
		5.62	5.66
		5.97	5.85
		5.81	5.46
		5.43	6.02
4	E7016	4.28	4.12
		4.15	4.19
		4.31	4.48
		4.17	4.30
		4.06	4.25
6	9Cr-1Mo + E9015-B3	2.16	2.15
		2.12	2.25
		2.16	2.43
		2.30	2.29
		2.26	2.11
		2.15	2.32

#### ***4.1.3 Application of RT-PEMHS to study hydrogen evolution with time***

RT- PEMHS was successfully employed to study evolution of hydrogen as a function of time. In this study, hydrogen concentration in the chamber was measured for different time intervals from weldment of modified 9Cr-1Mo electrode (modified E9015-B3) on mild steel base metal up to 264 h after welding. This electrode was chosen because it is an alloy steel electrode and in the as welded condition, the microstructure of the weld metal is fully martensitic and diffusion coefficient for hydrogen in this class of

steel at ambient temperature is lower than that in mild steel. It was observed that evolution of hydrogen did not stop even after 264 h. The  $H_D$  contents measured at various intervals for modified E9015-B9 deposited on mild steel is given in Table 4.2.

Rate of hydrogen evolution per hour was estimated by dividing the hydrogen evolved by duration of evolution, and variation in rate of hydrogen evolution with time is shown in Fig. 4.4. This plot reveals that hydrogen evolution is the maximum within the first 24 h and evolution rate decreases with time. The cumulative  $H_D$  collected after different time durations of measurement is plotted against time in Fig. 4.5. Both these figures clearly show that the hydrogen evolution continues much beyond 72 h, the maximum recommended duration for standard methods  $H_D$  measurements in the earlier standards for  $H_D$  measurements [1]. However, it should be noted that the total  $H_D$  measured after 72 h (1.85 ml/100 g) in the measurement carried out for different durations is lower than the  $H_D$  obtained for the single measurement carried out for 72 h (2.1 ml/100 g). This is because single specimen was used in the measurements carried out for different durations of hydrogen evolution. The first 72 h is divided into three intervals of duration 24 h each and during the measurements carried out for each of these intervals some time is lost in between two successive measurements. Hydrogen evolved during this lost time is not collected.

Table 4.2 Diffusible hydrogen evolution with time

Time Intervals of hydrogen collection (Hour)	Time Duration of hydrogen collection (Hour)	$H_D$ collected within time interval (ml/100g)	Total $H_D$ collected (ml/100g)	Hydrogen evolution rate (ml/100g*h)
0	0	0	0	0
0-24	24	0.84	0.84	0.035
24-48	24	0.60	1.44	0.025
48-72	24	0.41	1.85	0.017
72-120	48	0.37	2.22	0.008
120-192	72	0.34	2.56	0.005
192-264	72	0.16	2.72	0.002

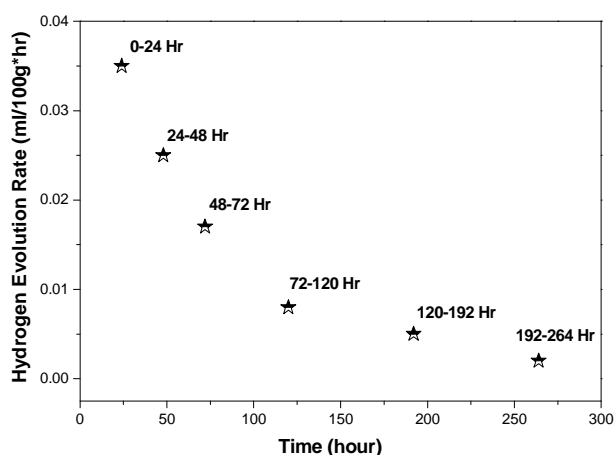


Fig. 4.4 Variation in rate of hydrogen evolution with time

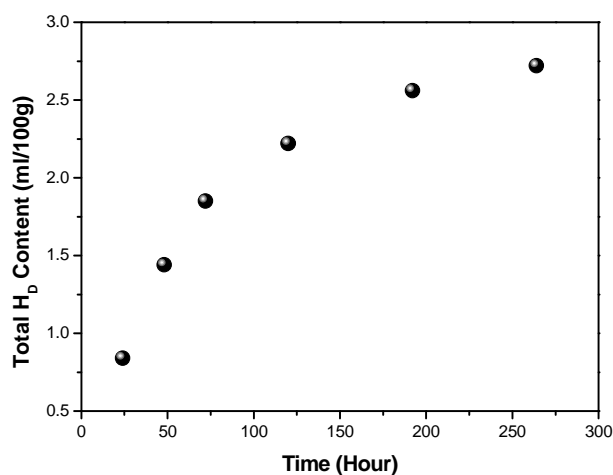


Fig. 4.5 Cumulative H<sub>D</sub> content obtained with time

#### 4.1.4 Results of H<sub>D</sub> measurement using HE-PEMHS and their comparison with mercury method

This study is similar to the one reported above for collection of hydrogen at ambient temperature; the differences are a different set of electrodes were employed and hot extraction chamber is used. H<sub>D</sub> contents obtained using both mercury and HE-PEMHS are given in Table 4.3. It is obvious that the results are comparable. Linear relationship between the H<sub>D</sub> content measured using HE-PEMHS and mercury method is

shown in Fig. 4.6. The empirical relation given in the figure confirms one to correspondence between these two methods.

Table 4.3 H<sub>D</sub> contents obtained using HE-PEMHS and mercury method

S. No.	Mild Steel +Electrodes	H <sub>HE-PEMHS</sub> (ml/100g)	H <sub>Mercury</sub> (ml/100g)
1	modified E9015-B3	3.81	3.89
		3.70	3.24
		3.94	3.71
2	E8016-C2	4.09	4.04
		4.18	4.27
		4.13	4.17
3	E7018	5.08	5.11
		5.19	5.27
		5.02	5.21
4	E7018	5.21	5.43
		5.37	5.42
		5.33	5.31
5	E7016	6.46	6.39
		6.37	6.62
		6.24	6.47
6	E7018+ Redried at 375°C	10.42	10.61
		10.05	10.87
		10.78	10.18
7	E6013	18.66	17.20
		18.31	18.21
		18.61	17.94
8	E6010	23.44	23.77
		21.64	23.22
		23.05	21.63
9	E6013	31.35	31.47
		30.89	29.98
		29.61	31.12

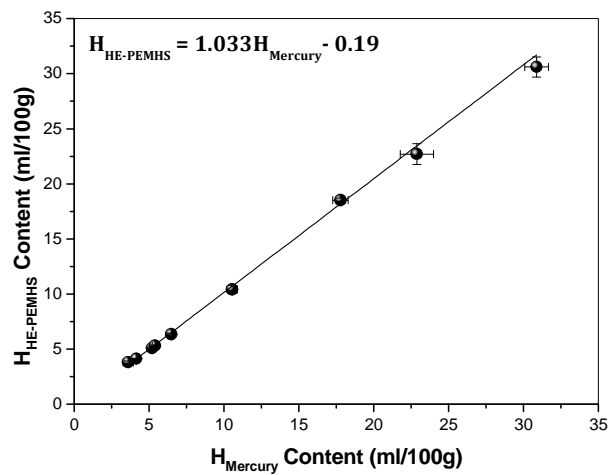


Fig. 4.6 Correlation between HE-PEMHS and Mercury method

## 4.2 Results of $H_2$ measurement using HE-GCTCD

### 4.2.1 Calibration of GCTCD

As detailed in chapter 3, GCTCD facility was calibrated before collection and measurement of diffusible hydrogen with known volumes of hydrogen; not for known concentration as in the PEMHS. A typical TCD response is shown in Fig. 4.7. In this response, the large peak represents the response of TCD for hydrogen. The area covered by this peak is representative of the volume of hydrogen. The smaller peak is due to disturbance in the TCD response during injection of gas. It is to be noted that the facility directly displays the volume of hydrogen detected by TCD for an injected volume of hydrogen. For calibration, different known volume of hydrogen was injected three times each on to the GCTCD facility. The average volume of hydrogen detected was plotted against the volume of hydrogen injected. This plot is shown in Fig. 4.8. From this plot, it is clear that the volume of hydrogen detected by TCD is linearly related to the volume of hydrogen injected.

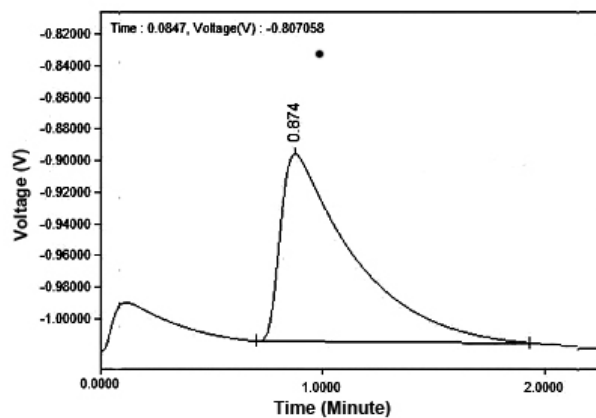


Fig. 4.7 Response of GCTCD on injection of hydrogen

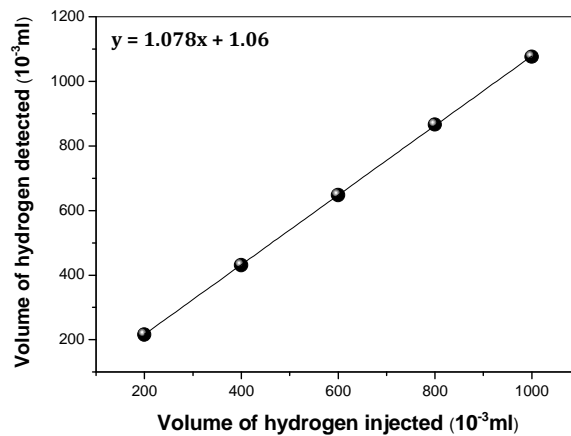


Fig. 4.8 Calibration plot of GCTCD

#### 4.2.2 Results obtained using HE-GCTCD and their Comparison with mercury method

For this study, different welding electrodes having  $H_D$  content in the range of 4-29ml/100g were used. In this study, diffusible hydrogen from weld specimen was collected for the same temperature and time duration as in HE-PEMHS method. However, a different chamber was used for this collection. The accuracy of this technique was examined by comparing the  $H_D$  contents obtained in this method with that obtained from similar weld specimens using the standard mercury method. The results of measurements carried out using both these techniques are given in Table 4.4. It is obvious from the table that the results are in good agreement.

The variation of  $H_D$  contents obtained using HE-GCTCD technique varied linearly with those obtained using the mercury method as shown in Fig. 4.9. This figure also contains the empirical relation between the  $H_D$  contents obtained from these methods. The relation confirms one to correspondence between these two methods.

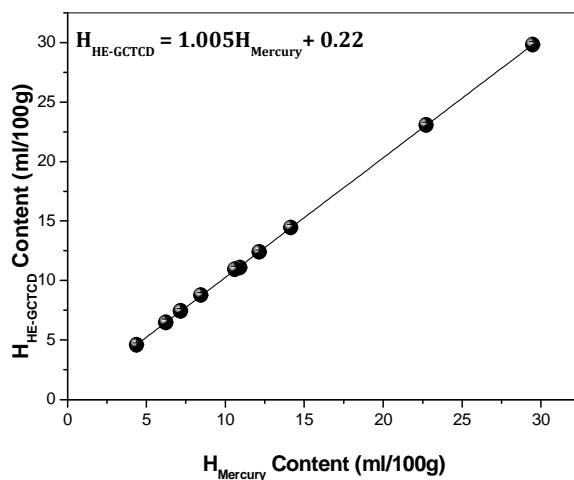


Figure 4.9 Correlation between HE- GCTCD and mercury method

Table 4.4 H<sub>D</sub> contents obtained using HE-GCTCD and mercury method

Electrode	H <sub>HE-GCTCD</sub> (ml/100g)	H <sub>Mercury</sub> (ml/100g)
E7016	12.25	12.01
	12.54	12.12
	12.49	12.36
E7018	6.79	6.12
	6.43	6.29
	6.24	6.17
E7018-A1	4.45	4.37
	4.79	4.59
	4.67	4.18
E8018-B2	7.57	7.36
	7.42	7.11
	7.36	7.05
E8018-W2	11.22	10.85
	10.89	10.55
	10.76	10.43
E9018-B3	14.74	14.35
	14.43	14.12
	14.22	13.99
E9018-G	11.30	11.12
	10.95	10.92
	11.09	10.85
E11018-M	8.57	8.32
	9.02	8.65
	8.76	8.41
E6013	23.15	22.54
	22.82	22.93
	23.24	22.69
E6010	29.58	29.50
	29.87	29.29
	30.05	29.64

### 4.3 Statistical analysis of results

As per the recommendation of ISO 3690, to validate the accuracy of a new method (alternate method) for diffusible hydrogen measurement, results obtained in this method has to be statistically compared with those obtained with standard mercury method (primary method) using Student's t-Test. Accordingly, t-Test was carried out for comparing the results obtained from each of the new techniques, RT-PEMHS, HE-PEMHS and HE-GCTCD, with corresponding results obtained from mercury method. A two-sided t-Test was chosen for this analysis because the objective of this test was to prove that the one to one correlation obtained between the mercury method and the new techniques are genuine and not by chance. The t-value for the results obtained for each set of electrode ( $t_{estimated}$ ) was estimated using equation 4.4.  $t_{estimated}$  for each electrode was compared with a  $t_{statistical}$  chosen from the t-table of statistics [2].  $t_{statistical}$  was chosen using the degree of freedom ( $\nu$ ) involved in the t-Test and the desired confidence level. The degree of freedom is calculated from the sample size i.e., number of measurements carried out in each method, using equation 4.5 and  $t_{statistical}$  was chosen at 95% confidence level. The sample size, degree of freedom and choice of  $t_{statistical}$  for each new method are given in Table 4.5. A confidence level of 95% corresponds to a probability of finding significant difference between the means of the alternate and primary methods,  $\alpha$ , is less than 0.025 on either side of the t-distribution for two-sided t-Test (Fig.4.10). In other words, if  $t_{estimated}$  falls within the range of  $t_{statistical}$ , the correlation obtained is genuine and not by chance. Accordingly, the new method is said to be reliable and the results are accurate.

$$t_{estimated} = \frac{X_A - X_P}{\sqrt{\frac{S_A^2}{N_A} + \frac{S_P^2}{N_P}}} \dots \dots \dots (4.4)$$

$$v = N_p + N_A - 2 \dots \dots \dots (4.5).$$

In the above relations,

$X_p$  and  $X_A$  = Means of the primary and alternate methods

$S_p$  and  $S_A$  = Standard deviations of the primary and alternate methods

$N_p$  and  $N_A$  = Number of measurements carried out using the primary and alternate methods or sample size of measurement

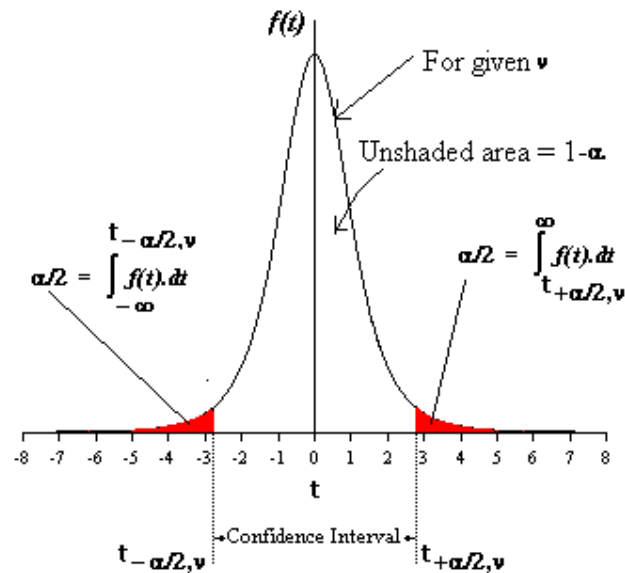


Figure 4.10 Representation of t-Distribution

The details of this t-Test carried out for RT-PEMHS, HE-PEMHS and HE-GCTCD are given in Tables 4.6, 4.7 and 4.8 respectively. For RT-PEMHS, it is obvious from Table 4.6 that  $t_{estimated}$  for all the electrodes fall within the interval of tabulated value of  $t_{statistical} = \pm 2.262$  at a confidence level of 95%. This proves that 'good correlation between the  $H_D$  contents measured by RT-PEMHS and mercury methods is 'by chance' is less than 5%. In other words, with more than 95% confidence level, it can be said that  $H_D$  measurement using RT-PEMHS is as accurate and reliable as the standard mercury method. The differences in the means of results obtained using these methods are only due to random errors and not due to any systematic errors. Similarly

for HE-PEMHS and HE-GCTCD techniques, also  $t_{estimated}$  falls within the  $t_{statistical} = \pm 2.776$  confirming 95% confidence on the correlation obtained with mercury method.

Table 4.5 Sample size, degree of freedom and choice of  $t_{statistical}$  at 95% confidence

	RT-PEMHS	HE-PEMHS	HE-GCTCD
$N_A$	5	3	3
$N_P$	6	3	3
$\nu$	9	4	4
$t_{statistical}$	$t_{\pm 0.025, 9}$	$t_{\pm 0.025, 4}$	$t_{\pm 0.025, 4}$

Table 4.6 t-Test of means of  $H_D$  obtained from RT-PEMHS and mercury methods

Electrodes	Average $H_D$ content (ml/100g)		Standard Deviation of $H_D$ content (ml/100g)		t-Value	
	RT-PEMHS	Mercury	RT-PEMHS	Mercury	$t_{estimated}$	$t_{statistical}$
E6010	18.28	18.58	0.412	0.871	-0.7444	$\pm 2.262$
E6013	9.37	9.56	0.338	0.438	-0.8352	
E7018-1	5.68	5.81	0.214	0.248	-0.9488	
E7016	4.19	4.26	0.102	0.124	-0.9449	
9Cr-1Mo + E9015-B3	2.19	2.26	0.0711	0.117	-1.1950	

Table 4.7 t-Test of means of  $H_D$  obtained from HE-PEMHS and mercury methods

Sl.No.	Mild Steel + Electrodes	Average $H_D$ content (ml/100 g)		Standard Deviation of $H_D$ content (ml/100 g)		t-value	
		HE-PEMHS	Mercury	HE-PEMHS	Mercury	$t_{estimated}$	$t_{staistical}$
1	E9015-B3	3.82	3.61	0.120	0.336	1.019	±2.776
2	E8016-C2	4.13	4.16	0.045	0.115	-0.421	
3	E7018	5.1	5.2	0.086	0.081	-1.464	
4	E7018	5.30	5.39	0.083	0.067	-1.460	
5	E7016	6.36	6.49	0.111	0.118	-1.391	
6	E6013	18.53	17.78	0.189	0.523	2.336	
7	E6010	22.71	22.87	0.947	1.111	-0.190	
8	E6013	30.62	30.87	0.902	0.779	-0.363	
9	E7018 Redried at 375°C	10.42	10.55	0.365	0.348	-0.446	

Table 4.8 t-Test for  $H_D$  obtained from HE-GCTCD and mercury methods

Sl.No.	Mild Steel + Electrodes	Average $H_D$ content (ml/100 g)		Standard Deviation of $H_D$ content (ml/100 g)		t-value	
		HE-GCTCD	Mercury	HE-GCTCD	Mercury	$t_{estimated}$	$t_{staistical}$
1	E7016	12.49	12.36	0.155	0.179	1.902	±2.776
2	E7018	6.49	6.23	0.279	0.227	1.252	
3	E7018-A1	4.61	4.38	0.172	0.205	1.489	
4	E8018-B2	7.45	7.17	0.206	0.164	1.842	
5	E8018-W2	10.96	10.61	0.237	0.216	1.89	
6	E9018-B3	14.46	14.15	0.262	0.182	1.683	
7	E9018-G	11.11	10.93	0.176	0.185	1.221	
8	E11018-M	8.78	8.46	0.226	0.170	2.054	
9	E6013	29.83	29.48	0.237	0.176	2.048	
10	E6010	23.07	22.72	0.221	0.197	2.054	

### 4.3 Discussion

From the results presented above, it is clear that methods using Nafion based PEMHS for  $H_D$  measurements are reliable and accurate. Therefore, it can be used for routine measurement of diffusible hydrogen in industry. However, it should be demonstrated that sensor used is robust and its calibration does not alter with time or by repeated use.

Ramesh *et al* reported that Nafion based PEMHS has good sensitivity ( $0.56\mu\text{A/ppm}$ ) [3]. This sensitivity is much higher than the previously reported PVA based PEMHS [4]. This study [3] also reported that the response of Nafion based PEMHS varied only marginally ( $\pm 10\%$ ) over a period of prolonged use (1 month). Therefore, it was reported to have good long term stability. In addition, this study reported that the sensor has excellent short term stability in its response which is essential for the  $H_D$  measurement in steel. Hence, the PEMHS can be adopted for commercial use in an industry like welding consumable manufacturing where  $H_D$  measurement for different consumables is carried out routinely.

Since the PEMHS could measure concentration of hydrogen in Ar- $H_2$  mixtures down to ppm levels, it was used to estimate  $H_D$  evolved from weld specimen as a function of time where concentrations of hydrogen evolved after certain period of measurement becomes as low as 50 ppm. This leaves open wide scope for the measurement of hydrogen evolved from a specimen as a function of time and other studies in which, hydrogen evolved is expected to be too low. Further, it is known that apparent diffusivity of hydrogen varies widely with alloy content and microstructure [5]. Hence, hydrogen evolution rate can vary accordingly and measurement method presented here can be used to study the effect of composition and microstructure of the weld metal and HAZ on hydrogen evolution.

In the present study,  $H_D$  contents obtained using RT-PEMHS, HE-PEMHS and HE-GCTCD were compared with those obtained using mercury method. It is mentioned earlier in this thesis that, for this comparison, diffusible hydrogen was collected in the mercury apparatus for 72 h following the earlier versions of ISO 3690 whereas a recent version of this standard recommends complete evolution of hydrogen from the weld specimen. However, complete evolution of hydrogen in mercury method (at room temperature) from the weld specimen takes very long time and some studies in literature reported that 92-97% of the total diffusible hydrogen (hydrogen evolved after complete evolution) evolves from the weld specimen within the first 72 h [6, 7] while some other studies reported it as 85-90% after 72 h [8]. Therefore, the time of  $H_D$  collection is quite unclear for the measurement using mercury method. Since PEMHS and GCTCD have options to collect  $H_D$  both at room temperature and high temperature, the optimization of time for  $H_D$  collection can be studied in more details using these methods.

HE-PEMHS and HE-GCTCD techniques are designed for hot extraction of hydrogen from the weldment up to 400°C. Nevertheless, the hot extraction units in these techniques, being isolated from the measuring units, can be easily modified so that they can be used for measuring not only diffusible hydrogen, but also residual hydrogen.

Using the PEMHS, only the concentration of hydrogen in a small sample volume of Ar- $H_2$  mixture is measured and not the total volume of hydrogen collected in the chamber. However, in the GCTCD, the total volume of hydrogen collected in the chamber is measured. PEMHS can be modified for measurement of total volume of hydrogen collected as in the case of GCTCD. This may require proper optimization of the sensitivity of the sensor by optimizing the orifice size in the diffusion barrier. By using the diffusion barriers with relatively smaller orifice, the kinetics of the hydrogen reaching the electrodes can be slowed down. This would reduce the sensitivity of the

sensor but would enable the sensor for measurement of total volume of hydrogen collected. However, this would make the technique much more adaptable to the industry, which measures total hydrogen collected in other methods of  $H_D$  measurement.

At present, methods recommended by standards for  $H_D$  measurement include the inaccurate and erroneous glycerin method, time consuming and hazardous mercury method and commercially expensive hot extraction method. In the present study, laboratory results have shown that HE-PEMHS and HE-GCTCD techniques are as accurate as mercury method. Results obtained with these techniques are also reproducible. The long term stability of the PEMHS has been proven; it can be easily assembled and is inexpensive. In HE-GCTCD, hot extraction unit developed for the collection of  $H_D$  is very simple and integrated to a commercially available GC. Both these methods are safe to use and can be developed further that would bring down the cost and making them cheaper than the commercially available hot extraction equipments available in market for  $H_D$  measurement.

## Reference

1. *ISO 3690:1977/ Add 1:1983*, , Welding - Determination of hydrogen in deposited weld metal arising from the use of covered electrodes for welding and low alloy steels; Addendum 1
2. T. G. Beckwith,, R. D. Maragoni, and J.H. Lienhard, *Mechanical Measurements*, Fifth Edition, Pearson Education, 2006
3. C. Ramesh, N. Murugesan, M. V. Krishnaiah, V. Ganesan and G. Periaswami, Improved Nafion-based amperometric sensor for hydrogen in argon, *Journal of Solid State Electrochemistry*, 2008, Vol. 12, No. 9, pp 1109-1116

4. C. Ramesh, G. Velayutham, N. Murugesan, V. Ganesan, K. S. Dhathathreyan and G. Periaswami, An improved polymer electrolyte-based amperometric hydrogen sensor, *Journal of Solid State Electrochemistry*, 2003, Vol. 7, No.8, 511-516
5. S. K. Albert, V. Ramasubbu,, N. Parvathavarthini, and T. P. S. Gill, *Sadhana*, Influence of alloying on hydrogen-assisted cracking and diffusible hydrogen content in Cr–Mo steel welds, 2003, Vol. 28, No. 3/4, 383-393
6. R. Veeraragavan, V.P. Raghupathy, K.S. Raman and R.S. Babu, Correlation between diffusible hydrogen values determined by IIW mercury and gas chromatographic methods, *Proceedings National Welding Seminar*, 24-26<sup>th</sup> November, 1994, Jamshedpur, India.
7. R. Ravi, D. S. Honnover, Hydrogen in steel weldments – A review, *Proceedings of National welding seminar*, 26-28<sup>th</sup> November, 1987, Bangalore, India, E23-E43
8. FT Fabling and B Chew, Diffusible hydrogen analysis, *Metal Construction and British Welding Journal*, 1972, Vol. 4, No. 2, 64-67.

**EFFECTS OF PREHEAT AND  
POST-HEATING ON  $H_D$  IN WELDS**

# Effects of preheat and post-heating on $H_D$ in welds

---

---

Systematic study was conducted to examine the effectiveness of preheating and post-heating to bring down the diffusible hydrogen ( $H_D$ ) content in the welds. In this study,  $H_D$  measurement was carried out using specimens of mild steel and modified 9Cr-1Mo steel prepared with preheating and preheating combined with post-heating. The preheat and post-heat temperatures employed were 100, 150, 200, and 250°C. After welding,  $H_D$  measurement from these specimens was carried out using the hot extraction method based on proton exchange membrane hydrogen sensor (HE-PEMHS). The detailed procedures of the above processes were discussed in chapter 3. This chapter presents the results obtained in the study.

## 5.1 Results

### 5.1.1 Cooling behavior

In this study, the surface temperature of preheated weld specimen was monitored as a function of time starting from the completion of welding to its cooling down to 100°C. Temperature of the weld specimen was plotted against time to obtain the cooling curves for different preheat temperatures. These curves are shown in Fig. 5.1. It is clear from the figure that the temperature of the specimen surface in contact with the thermocouple has gone up to ~ 600°C during the deposition of the weld bead. The figure also makes clear that the cooling rate decreases with the increase in preheat temperatures. As already described in Chapter 3, three separate sets of  $H_D$  measurements were carried out for each of the preheating temperatures; a) after the specimen is cooled

down to the preheating temperature, b) after the specimen is cooled down to 100°C and c) after the completion of 10 minutes of welding. These are indicated in the cooling curves with arrows. It may be noted that the time required for the specimen to cool down to preheat temperature is less at high preheat temperatures than at low preheat temperatures. However, the time duration for the weld specimen to cool down to 100°C increases significantly with the increase in preheat temperature.

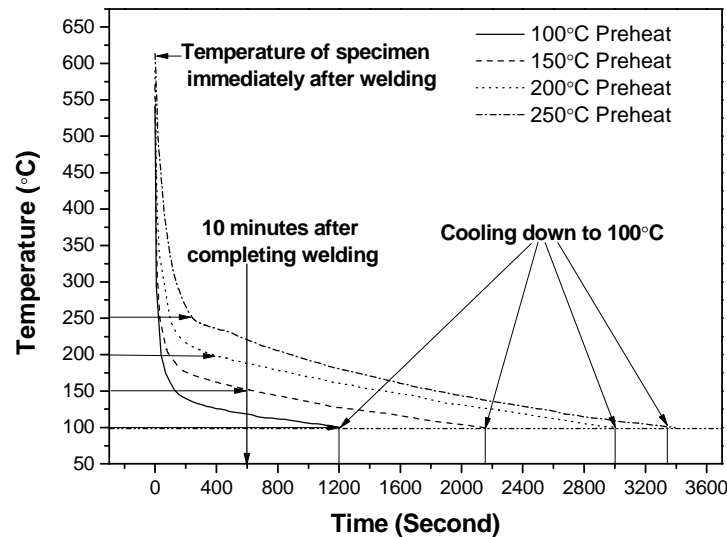


Fig. 5.1 Cooling behavior of preheated weld specimen

### 5.1.2 Comparison of $H_D$ obtained using mercury and HE-PEMHS

It is discussed in Chapter 3 that the measurement of  $H_D$  from weld specimens prepared with different preheating and post-heating conditions was carried out using HE-PEMHS method. Since the method is relatively new, each result obtained from this method was compared with that obtained with standard mercury method. For the comparison, the  $H_D$  content obtained in HE-PEMHS ( $H_{HE-PEMHS}$ ) was plotted against  $H_D$  content obtained in mercury method ( $H_{Mercury}$ ) for weld specimens prepared under similar conditions. The plot is shown in Fig. 5.2. It is to be noted that there exists one to one correspondence between both methods with a very good correlation even for very small

amounts of diffusible hydrogen ( $< 2\text{ml}/100\text{g}$ ). This confirms the accuracy and reliability of the results using HE-PEMHS. In the remaining sections of this chapter, only the results obtained using HE-PEMHS are presented.

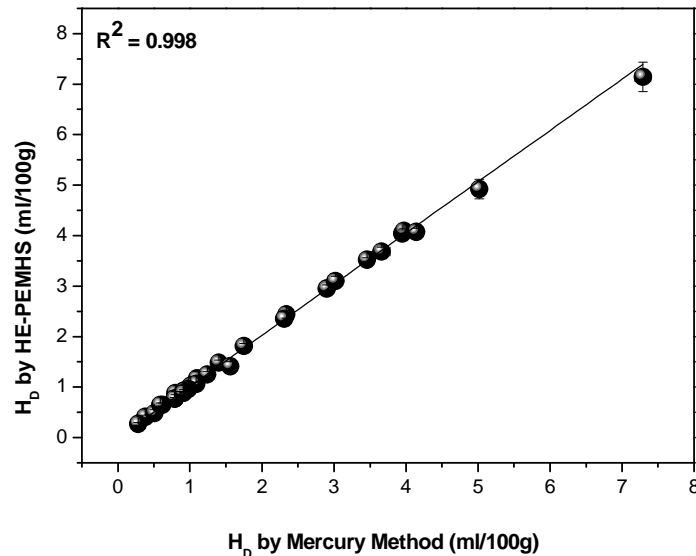


Fig. 5.2 Comparison of  $H_D$  contents obtained from preheated and post-heated specimens in HE-PEMHS and mercury method

### 5.1.3 Effect of preheat on $H_D$ content

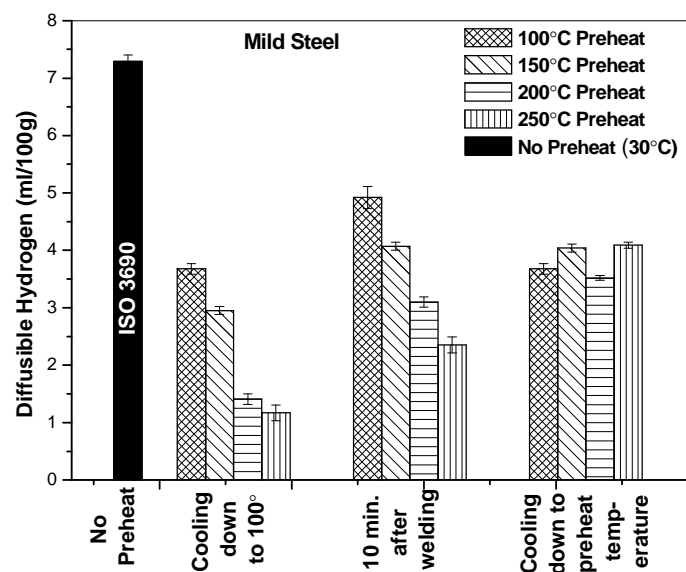
Increase in the preheat temperature causes reduction in cooling rate of the weld specimen. This results with the specimen experiencing higher temperature for longer periods of time thereby giving more time for hydrogen to diffuse out. The  $H_D$  contents obtained from preheated weld specimens of mild steel and modified 9Cr–1Mo steel prepared for the three conditions are given in Table 5.1. The average values of the  $H_D$  contents are shown in Fig. 5.3a and 5.3b for mild steel and modified 9Cr–1Mo steel respectively. The actual  $H_D$  obtained as per ISO 3690 (without any preheating) is also shown in the same figures. The results obtained can be summarized as given below:

- (i) The  $H_D$  content measured for E7018 deposited on mild steel is much higher than that measured for E9015-B3 deposited on modified 9Cr–1Mo steel.

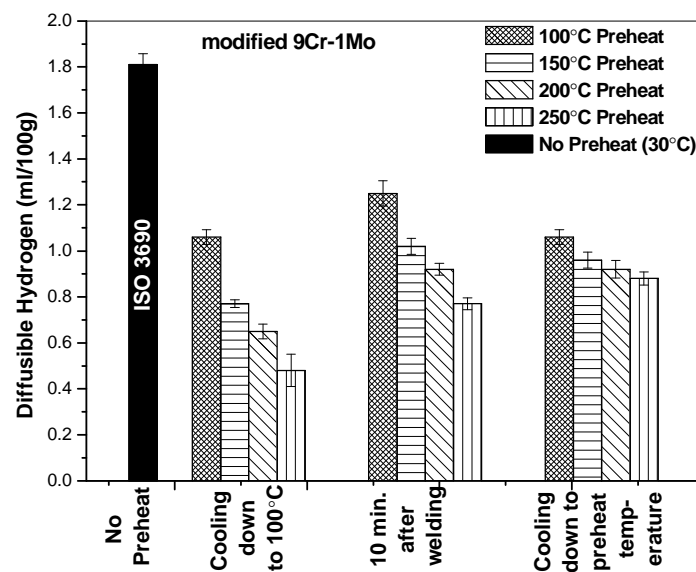
- (ii) Preheating has substantially reduced  $H_D$  content in the welds.
- (iii) The  $H_D$  remaining in the welds after cooling down the weld to preheat temperature in the copper jig does not vary significantly with preheat temperature. Approximately 50% reduction in  $H_D$  content from that of the  $H_D$  content without preheat is observed in this condition irrespective of the preheat temperature for both steel welds.
- (iv) The  $H_D$  content showed maximum reduction for a given preheat temperature for the condition in which measurements were carried out after the weld was cooled to 100°C. Further, the  $H_D$  content remaining in the weld decreased with the increase in preheat temperature for this measurement condition. The  $H_D$  content remaining in mild steel weld was only 16% of the actual  $H_D$  content for welds made with a preheat of 250°C, and the corresponding value for modified 9Cr–1Mo steel was 27%.
- (v) The  $H_D$  content remaining in the weld showed a decrease with an increase in preheat temperature for the measurements carried out after the weld was cooled for 10 min. The trend observed is similar to those obtained for cooling down to 100°C before measurement. However, the  $H_D$  content remaining in the weld is higher for the former condition.
- (vi) In general, it was observed that the relative amount of  $H_D$  remaining in the weld made with preheating is more for welds made with modified 9Cr–1Mo steel and E9015-B3 electrode than that made with mild steel and E7018 electrode.

Table 5.1 H<sub>D</sub> collected from preheated weld specimens using HE-PEMHS

Preheat (°C)	H <sub>D</sub> (ml/100g)				
	After Cooling to Preheat Temp.	After cooling to 100°C	After 10 min. of welding	After post- heating for 30 m	During post- heating for 30 min
100	3.76	3.76	4.98	2.53	4.28
	3.58	3.58	5.14	2.41	4.16
	3.71	3.71	4.77	2.39	4.33
150	4.03	3.01	4.14	1.49	5.28
	4.11	2.86	4.07	1.42	5.20
	3.97	2.99	4.00	1.52	5.25
200	3.57	1.42	3.03	0.89	5.98
	3.51	1.35	3.20	0.84	6.06
	3.49	1.45	3.06	0.90	6.00
250	4.10	1.21	2.35	0.43	6.52
	4.03	1.15	2.48	0.37	6.45
	4.14	1.14	2.21	0.42	6.63
100	1.05	1.05	1.31	0.62	1.03
	1.03	1.03	1.21	0.56	1.07
	1.09	1.09	1.22	0.59	1.08
150	1.00	0.76	0.99	0.27	1.36
	0.93	0.76	1.06	0.25	1.31
	0.96	0.79	1.02	0.32	1.28
200	0.89	0.63	0.91	0	1.67
	0.96	0.69	0.90	0	1.64
	0.90	0.64	0.95	0	1.73
250	0.91	0.56	0.75	0	1.63
	0.86	0.43	0.77	0	1.62
	0.86	0.45	0.80	0	1.67



(a)



(b)

Fig. 5.3 Effect of preheat on the  $H_D$  content a) Mild steel and b) Modified 9Cr-1Mo steel

### 5.1.4 Effect of preheat and post-heating on $H_D$ content

Results of the measurement of the  $H_D$  content remaining in the weld after preheating and post-heating at the temperature for 30 min for mild steel and modified 9Cr–1Mo welds are given in Fig. 5.4. There is a significant reduction in the  $H_D$  content remaining in the weld from those obtained with preheating alone. In fact, for welds made with E9015-B3 electrode on modified 9Cr–1Mo steel, for which the  $H_D$  content measured as per ISO 3690 itself is very less, the  $H_D$  remaining in the weld after preheating and post-heating at 200 and 250°C is below the measurable limits for the techniques used. As expected, a systematic decrease in  $H_D$  remaining in the weld with increase in preheating and post-heating temperature was also observed. It was seen that for the mild steel, the  $H_D$  content remaining in the weld after preheating + post-heating at 250°C reduced to ~6% of the actual  $H_D$  content measured for welds made without preheating or post-heating (as per the ISO standard).

### 5.1.5 Hydrogen evolution from specimen during post-heating

Results of the measurements in which hydrogen diffused out of the weld specimen during post-heating for 30 minutes at different post-heating temperatures in the HE-PEMHS chamber are given in Table 5.1. The average values of hydrogen contents diffused out during post-heating is shown for various post-heating temperature in Fig. 5.5. There is a clear increase in hydrogen diffused out of the weld specimen with the increase in post-heat temperature for both sets of specimens. For the modified 9Cr–1Mo weld, the hydrogen diffused out at post-heating of 200 and 250°C is close to the  $H_D$  content measured as per ISO 3690. This means that almost all the  $H_D$  is evolved from the weld during post-heating. Ideally, the sum of hydrogen diffused out during post-heating and  $H_D$  content remaining in the specimen after post-heating shall add up to the  $H_D$  content in the weld measured as per ISO 3690 (i.e. weld made without preheat and post-heating), and this comparison is given in

Table 5.2 and shown in Fig. 5.6. It may be noted that the sum of two measurements is slightly lower than the  $H_D$  content in the weld prepared without preheating and post-heating in all cases. This difference is expected and can be explained as follows. Each measurement involves transferring the specimen to the extraction chamber, closing the chamber leak tight and then flushing and filling it with argon. Though the time for these operations is kept as minimum as possible, hydrogen diffusing out during these operations is not collected for the measurement. In Fig. 5.6, the sum of two separate measurements is compared with the value obtained in a single measurement. Hence, it is expected that this sum would be lower than that of the single measurement. Further, for standard  $H_D$  measurement, the specimen is not preheated, while for the other two measurements, the weld bead is deposited on the preheated specimen assembly. This would result in loss of some hydrogen before collection of  $H_D$  in the chamber. Thus, lower values for the sum than the  $H_D$  content in the weld are expected. The closeness of the sum with the actual  $H_D$  content in the weld with only an expected and explainable deviation shows that the measurements carried out in the present study on preheated and preheated + post-heated specimens are fairly accurate and reliable.

Table 5.2 Total H<sub>D</sub> measured during and after post-heating in HE-PEMHS chamber

Temperature (°C)	H <sub>D</sub> (ml/100g)			
	During post-heating	Remaining in weld after post-heating	Total	Actually measured as per ISO 3690
<b>Mild Steel + E7018</b>				
100	4.26 ± 0.087	2.44 ± 0.076	6.70 ± 0.116	7.29 ± 0.111
150	5.24 ± 0.04	1.48 ± 0.051	6.72 ± 0.065	
200	6.01 ± 0.042	0.88 ± 0.032	6.89 ± 0.052	
250	6.53 ± 0.091	0.41 ± 0.032	6.94 ± 0.096	
<b>9Cr 1Mo + E9015-B3</b>				
100	1.06 ± 0.026	0.59 ± 0.03	1.65 ± 0.04	1.81 ± 0.049
150	1.32 ± 0.04	0.28 ± 0.036	1.60 ± 0.054	
200	1.68 ± 0.046	0 ± 0	1.68 ± 0.046	
250	1.64 ± 0.026	0 ± 0	1.64 ± 0.026	

Note: Error in the total H<sub>D</sub> was calculated by considering the propagation of errors in the measurement of H<sub>D</sub> during post-heating and H<sub>D</sub> after post-heating by the following equation:

$$\partial z = \sqrt{(\partial x)^2 + (\partial y)^2}$$

Where,  $\partial z$  = Propagated error in the measurement of total H<sub>D</sub> in ml/100g

$\partial x$  = Error in the measurement of hydrogen evolved during post-heating in the chamber in ml/100g

$\partial y$  = Error in the measurement of hydrogen remaining in the weld after post-heating in the chamber in ml/100g

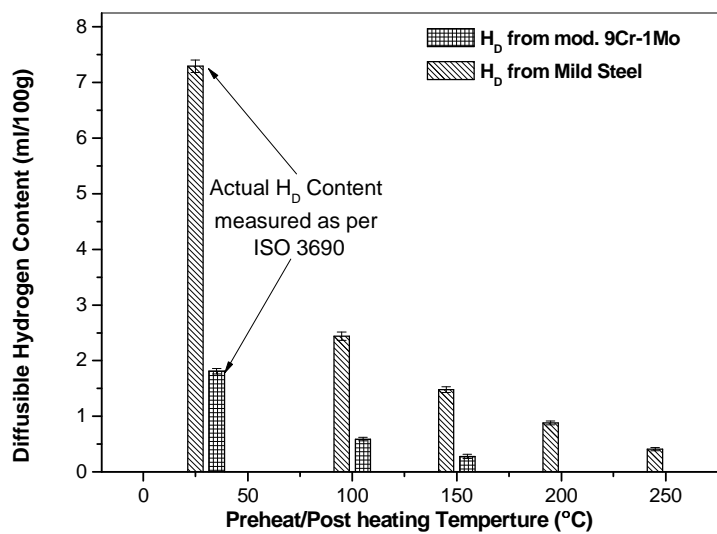


Fig. 5.4  $H_D$  obtained after post-heating

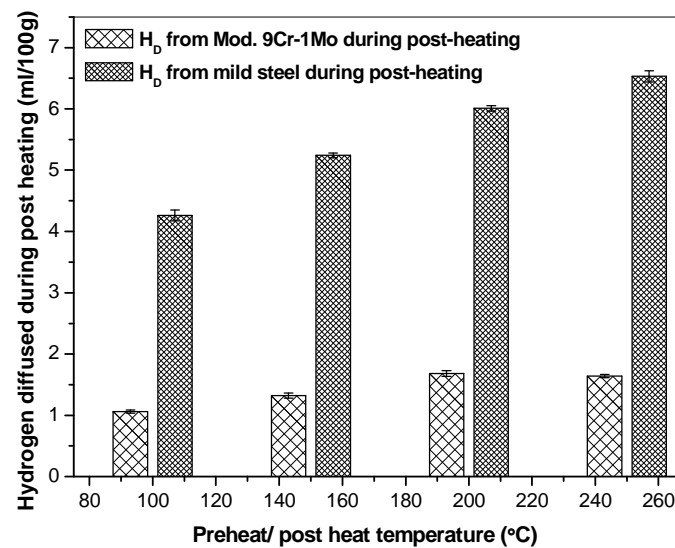


Fig. 5.5 Hydrogen diffused during post-heating

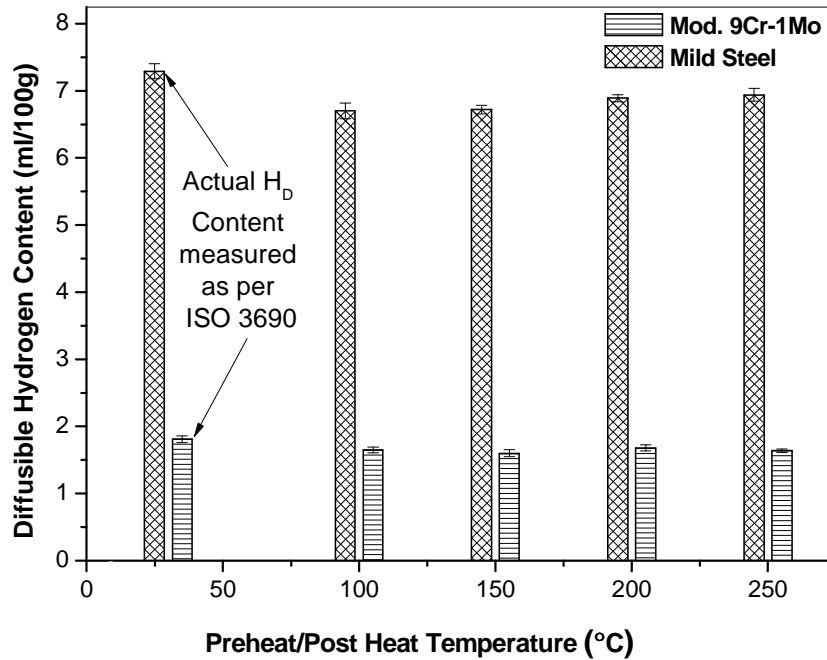


Fig. 5.6 Hydrogen diffused out of weld during post-heating +  $H_D$  after post-heating

## 5.2 Discussion

A major purpose of welding with preheating is to reduce the cooling rate of the welds soon after welding. This will provide more time for hydrogen to diffuse out of the specimen. Welding with preheating, as presented in this study, involves, in addition to preheating and welding, cooling of the weld, during which hydrogen diffuses out from the weld. However, the time taken by the weld specimen clamped to the preheated copper fixture to cool down to room temperature would be enormous, and this time would not simulate the cooling of the actual weld in practice. Hence, three different times to remove the specimen from the copper fixture and start measurement were proposed based on the criteria described above. The objective is to choose the best procedure that would reflect the effect of preheat on  $H_D$  measurement and hence could be used to compare the  $H_D$  levels after heating the steel specimen to different preheat

temperatures. The results indicate that the  $H_D$  measurement soon after the specimen has cooled down to its respective preheat temperature after welding may not be a good procedure to study the effect of preheating on  $H_D$  content, as there is no clear trend from the results. This is because with the increase in preheat temperature, the time taken by the specimen to cool down to preheat temperature decreases, as seen in figure 5.1. The benefit of higher diffusivities of hydrogen at higher temperatures is nullified by the shorter times spent by the specimen at these temperatures. The other option of waiting for a duration of 10 min after welding for the start of the measurement gives reasonably good results, which can be used to examine the effect of preheat on  $H_D$  content. One of the limitations of this procedure is that, after 10 min of welding, the specimens prepared at different preheat temperatures would be at different temperatures. However, measurement of specimen temperature is not required to choose the measurement start time. The third alternative is to wait until the specimen cools down to 100°C. As it is clear from the results, this criterion can also be used to compare the effect of preheat temperature on  $H_D$  remaining in the weld. It is generally reported that hydrogen diffusivity reduces considerably below 100°C, and the time taken by the weld to cool down to 100°C ( $t_{100}$ ) is often chosen as a parameter that represents the cooling rate in various empirical relations used to predict preheat temperatures [1]. Hence, this procedure of cooling the specimen on the copper fixture down to 100°C before the start of  $H_D$  measurement is recommended to study the effect of preheat temperature on  $H_D$  content remaining in the weld. Comparison of the results under this condition clearly brings out the effect of preheat temperatures in bringing down the  $H_D$  content in the weld. It is known that hydrogen diffusivity increases with temperatures [2-4], and preheating effectively increases the time spent by the weld at high temperature, allowing more hydrogen to diffuse out. It also reveals that for a given preheat temperature; the

fraction of the total  $H_D$  remaining in the weld is always higher in modified 9Cr–1Mo steel welds than in mild steel welds. This is expected because the diffusivity of hydrogen in alloyed steel is much lower than that in mild steel or carbon steel [5-9]. Combining post-heating with preheating further brings down the  $H_D$  content remaining in the weld. For a given temperature, there is ~50% reduction in the  $H_D$  content by combining post-heating with preheating from that can be achieved only with preheating. It is interesting to note that the effect of post-heating is significant in welds of modified 9Cr–1Mo steel than in welds of mild steel. The  $H_D$  content in the weld of this steel after preheating and post-heating at 200 and 250°C is too low to be measured. The low initial  $H_D$  content in the welding consumable is certainly one of the reasons for this. Increase in hydrogen diffusivity with temperature [7, 8] could also be contributing to these extremely low values of  $H_D$  remaining in these welds prepared with both preheating and post-heating. Results also indicate that preheating and post-heating at lower temperatures are more effective in reducing the  $H_D$  content remaining in the welds than in preheating alone of the weld at a higher temperature. For example, in mild steel, the  $H_D$  content remaining in the weld after preheating alone at 150°C is ~3 ml/100 g of weld metal and after preheating and post-heating at 100°C is ~2 ml/100 g of weld metal. In case of modified 9Cr–1Mo steel, this difference is more significant; for the welds with 100°C preheating and post-heating, the  $H_D$  content is only ~0.5 ml compared with ~0.7 ml/100 for welds with a preheat of 150°C alone. These observations are important in the context of the recently published results on the effect of preheating and post-heating on residual stresses present in high strength steel welds. It is reported [10, 11] that the tensile residual stresses in the welds are higher in welds made only with preheating than in welds made without preheating or those made with both preheating and post-heating. Higher residual stresses resulting from preheating would at least partially nullify the

benefit of preheating in avoiding HAC. One of the practical applications of the results from this study is that if the  $H_D$  content in the consumable and critical  $H_D$  content below which cracking is not likely to take place is known, then it is possible to recommend preheating and post-heating temperatures that will bring down the  $H_D$  content below the critical values and thus prevent HAC. This would in turn help to optimize the preheating and post-heating requirement and thus reduce the energy spent on these.

## Reference

1. P. Nevasmaa, Predictive model for the prevention of weld metal hydrogen cracking in high-strength multipass welds, University of Oulu, 2003,  
Web Source: <http://herkules.oulu.fi/isbn9514271815/>
2. N. Bailey, F. R. Coe, T. G. Gooch, P. H. M. Hart, H. Jenkins and R. J. Pargeter, Welding steels without hydrogen cracking; 1992, Materials Park, OH, ASM International.
3. M. R. Louthan, Jr, Hydrogen embrittlement of metals: A primer for the failure analyst, *Journal of Failure Analysis Prevention*, 2008, Vol. 8, No. 3, 289–307.
4. B. S. Chaudhuri and T. P. Radhakrishnan A reexamination of the trapping of hydrogen in iron and steel, *Materials Transactions JIM*, 1993, Vol. 3, No. 5, 443–449.
5. S. K. Albert, V. Ramasubbu, N. Parvathavarthini and T. P. S. Gill, Influence of alloying on hydrogen-assisted cracking and diffusible hydrogen content in Cr–Mo steel welds, *Sadhana*, 2003, 28, (3/4), 383–393.
6. H. J. Grabke and E. Riecke, Absorption and diffusion of hydrogen in steels, *Materials Technology*, 2000, Vol. 34, No. 6, 331–342.
7. D. L. Dull and K. Nobe, Hydrogen trapping in Ferrovac E-iron, mild steel and 4340 steel, *Materials and Corrosion*, 1982, Vol. 33, No. 8, 439–448.
8. R. C. Brouwer, Hydrogen diffusion and solubility in vanadium modified pressure vessel steels, *Scripta Metallurgical et Materialia*, 1992, Vol. 27, No. 3, 353–358.

9. T. Bollinghaus, H. Hoffmeister and C. Middel, Scatterbands for hydrogen diffusion coefficients in steels having a ferritic or martensitic microstructure and steels having an austenitic microstructure at room temperature, *Welding in the World*, 1996, Vol. 37, No. 1/2, 16–23
10. P. Wongpanya, T. Boellinghaus and G. Lothongkum, Effects of hydrogen removal heat treatment on residual stresses in high strength structural steel welds, *Welding in the World*, 2006, Vol. 50, (Special Issue), 96–103.
11. P. Wongpanya, T. Boellinghaus and G. Lothongkum, Heat treatment procedures for hydrogen assisted cracking avoidance in S 1100 QL steel root welds, *Welding in the World*, 2008, Vol. 52, 671–678.

**CHAPTER 6**

**DETERMINATION OF APPARENT  
DIFFUSIVITY OF HYDROGEN IN STEEL**

# Determination of apparent diffusivity of hydrogen in steel

---

Hydrogen diffusivity for three different steels, mild steel, 2.25Cr-1Mo and modified 9Cr-1M steels at different temperatures were estimated from the hydrogen evolved from specimens charged to saturation, with hydrogen. Hydrogen evolved from these steels at 25°C was measured using the mercury method and at temperatures 100, 200, 300 and 400°C using HE-PEMHS and HE-GCTCD. The hydrogen evolution profiles were used in an equation that describes diffusion through a cylinder and apparent diffusivity of hydrogen in steel was calculated. The diffusion equation through cylinder, its existing solutions and application of this solution for estimating apparent diffusivity of hydrogen in three different steels are presented in this chapter.

## 6.1 Diffusion through a cylinder

### 6.1.1 Equation for the diffusion through finite cylinder

In general, non-steady state diffusion of any substance through a point P ( $x, y, z$ ) in Cartesian co-ordinate system follows Fick's second law [1] which is expressed as

$$\frac{\partial C}{\partial t} = D(\nabla^2 C) \dots \dots \dots (6.1) \text{ or}$$

$$\frac{\partial C}{\partial t} = D \left( \frac{\partial^2 C}{\partial x^2} + \frac{\partial^2 C}{\partial y^2} + \frac{\partial^2 C}{\partial z^2} \right) \dots \dots \dots (6.2)$$

Where,

C = Concentration of the diffusing species,

D = Apparent diffusivity or diffusion coefficient of the diffusing species in a medium

In general, a cylinder is characterized by cylindrical polar co-ordinate system ( $\rho, \varphi, z$ ) as shown in Fig. 6.1. It is related to the Cartesian co-ordinate system ( $x, y, z$ ) as follows

$$x = \rho \cos \varphi \dots \dots \dots (6.3a)$$

$$y = \rho \sin \varphi \dots \dots \dots (6.3b) \text{ and}$$

$$z = z \dots \dots \dots (6.3c)$$

In the above relations,

$\rho$  = Perpendicular distance from Z -axis and

$\varphi$  = The angle generated by the plane through Z-axis.

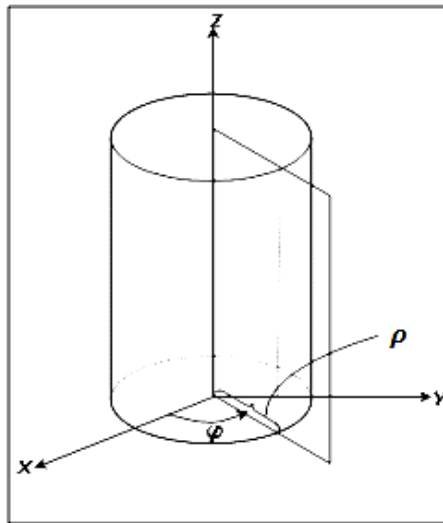


Fig. 6.1 Cylinder co-ordinate system

Using equations 6.3(a), (b) and (c) in equation 6.2, the chain rule and simple rearrangements, the concentration (C) of diffusing species over the Laplace Operator can be expressed as:

$$\frac{\partial^2 C}{\partial x^2} + \frac{\partial^2 C}{\partial y^2} + \frac{\partial^2 C}{\partial z^2} = \left( \frac{\partial^2 C}{\partial \rho^2} + \frac{1}{\rho} \frac{\partial C}{\partial \rho} \right) + \frac{1}{\rho^2} \frac{\partial^2 C}{\partial \varphi^2} + \frac{\partial^2 C}{\partial z^2} \dots \dots \dots (6.4)$$

Equation (6.4) can be further rearranged as

$$\frac{\partial^2 C}{\partial x^2} + \frac{\partial^2 C}{\partial y^2} + \frac{\partial^2 C}{\partial z^2} = \frac{1}{\rho} \frac{\partial}{\partial \rho} \left( \rho \frac{\partial C}{\partial \rho} \right) + \frac{1}{\rho^2} \frac{\partial^2 C}{\partial \varphi^2} + \frac{\partial^2 C}{\partial z^2} \dots \dots \dots (6.5)$$

Substituting equation 6.5 in equation 6.2, one arrives at

$$\frac{\partial C}{\partial t} = D \left( \frac{1}{\rho} \frac{\partial}{\partial \rho} \left( \rho \frac{\partial C}{\partial \rho} \right) + \frac{1}{\rho^2} \frac{\partial^2 C}{\partial \varphi^2} + \frac{\partial^2 C}{\partial z^2} \right) \dots \dots \dots (6.6)$$

Equation 6.6 is the non-steady state diffusion equation for the diffusion of species of concentration,  $C$  in a cylinder. Assuming a homogeneous flow of diffusing species through the cylindrical body,

$$\frac{\partial C}{\partial \varphi} \rightarrow 0 \dots \dots \dots (6.6a)$$

Equation 6.6a causes the  $\varphi$  term to diminish from equation 6.6. Therefore, equation 6.6 reduces to

$$\frac{\partial C}{\partial t} = \frac{D}{\rho} \frac{\partial}{\partial \rho} \left( \rho \frac{\partial C}{\partial \rho} \right) + D \frac{\partial^2 C}{\partial z^2} \dots \dots \dots (6.7)$$

The two terms on the right side of equation 6.7 are independent of each other. Each of these terms contains  $C$  and only one of its derivatives. Therefore equation 6.7 is homogeneous and each term can be isolated by separation of variables [2, 3]. Each of these is independently solved by substituting appropriate initial and boundary conditions.

### **6.1.2 Solutions of the diffusion equation available in literature**

If the specimen used in the present study is considered as a finite solid cylinder of radius  $r$  and length  $l$ , and hydrogen as the diffusing species with its initial concentration,  $C_0$ , the initial and boundary conditions for the solution of the  $\rho$ -term of in equation 6.7 are as follows

$$C(\rho, \varphi, z, t) = C_0 \text{ at } t = 0 \text{ when } 0 < \rho < r \text{ for } 0 < z < l \text{ (for all } z) \dots \dots \dots (6.8)$$

$$C(\rho, \varphi, z, t) = 0 \text{ at } t > 0 \text{ when } \rho = r \text{ for } 0 < z < l \text{ (for all } z) \dots \dots \dots (6.9)$$

Similarly, initial and boundary conditions for solution of the  $z$ -term are

$$C(\rho, \varphi, z, t) = C_0 \text{ at } t = 0 \text{ when } 0 < z < l \text{ for all } \rho \dots \dots \dots (6.10)$$

$$C(\rho, \varphi, z, t) = 0 \text{ at } t > 0 \text{ when } z = l \text{ for all } \rho \dots \dots \dots (6.11)$$

The general solution of equation 6.7 satisfying the initial and boundary conditions in equations 6.8-6.11 are available in the literature in terms of hydrogen diffused out [3,4]

and in terms of hydrogen remaining [5-9] in a specimen. The latter solutions are normalized and are given in Table 6.1.

Table 6.1 Normalized solutions for the diffusion equation of finite cylinder

	Author	Solutions of diffusion equation for finite cylinder
1	Damerez [5] (1954)	$\frac{M(t)}{M(0)} = \frac{32}{\pi^2} \left[ \sum_{n=0}^{\infty} \frac{\exp\left\{- (2n+1)^2 \pi^2 \frac{Dt}{l^2}\right\}}{(2n+1)^2} \right] \left[ \sum_{n=1}^{\infty} \frac{\exp\left\{-4 \frac{Dt}{l^2} \alpha_n^2\right\}}{\alpha_n^2} \right]$
2	Whitaker [6] (1972)	$\frac{M(t)}{M(0)} = \frac{32}{\pi^2} \sum_{n=1}^{\infty} \frac{1}{\alpha_n^2 r^2} \exp(-\alpha_n^2 Dt) \sum_{m=0}^{\infty} \frac{1}{(2m+1)^2} \exp\left\{- \frac{(2m+1)^2 \pi^2 Dt}{l^2}\right\}$
3	Katlinsk [7] (1981)	$\frac{M(t)}{M(0)} = \frac{32}{\pi^2} \sum_{m=0}^{\infty} \sum_{n=1}^{\infty} \frac{1}{(2m+1)^2 \alpha_n^2} \exp\left[- \left\{ \frac{\alpha_n^2}{r^2} + \frac{(2m+1)^2 \pi^2}{l^2} \right\} Dt\right]$
4	Brouwer [8] (1992)	$\frac{M(t)}{M(0)} = \frac{32}{\pi^2} \sum_{n=1}^{\infty} \frac{1}{\alpha_n^2} \exp\left(- \frac{\alpha_n^2 Dt}{r^2}\right) \sum_{m=0}^{\infty} \frac{1}{(2m+1)^2} \exp\left[- \frac{(2m+1)^2 \pi^2 Dt}{l^2}\right]$
5	Dilthey [9] (1993)	$\frac{M(t)}{M(0)} = \frac{32}{\pi^2} \sum_{m=0}^{\infty} \sum_{n=1}^{\infty} \frac{1}{(2m+1)^2 \alpha_n^2} \exp\left[- \left\{ \frac{\alpha_n^2}{r^2} + \frac{(2m+1)^2 \pi^2}{l^2} \right\} Dt\right]$

In context of the present study,

$M(0)$  = Total hydrogen evolved from the specimen at temperature, T

$M(t)$  = Hydrogen remaining after heating for time, t at temperature, T

$D$  = Apparent diffusivity of hydrogen

$\alpha_n$  = Roots of Bessel's function,  $J_0(r\alpha_n) = 0$   $m, n$  are integers

$\frac{M(t)}{M(0)}$  = Fraction of remaining hydrogen

### 6.1.3 Relationship between $D$ and $t_{0.5}$

Amongst the solutions given in the Table 1, the solution provided by Dilthey *at al* [9] was originally used to study hydrogen diffusion in steel welds. Therefore this solution is chosen for all the further calculations in this study. The solution is given below

$$\frac{M(t)}{M(0)} = \frac{32}{\pi^2} \sum_{m=0}^{\infty} \sum_{n=1}^{\infty} \frac{1}{(2m+1)^2 \alpha_n^2} \exp\left[- \left\{ \frac{\alpha_n^2}{r^2} + \frac{(2m+1)^2 \pi^2}{l^2} \right\} Dt\right] \dots \dots \dots (6.12)$$

Since the solution is a zero order Bessel's equation,  $m = 0$ . Therefore equation 6.12 reduces to

$$\frac{M(t)}{M(0)} = \frac{32}{\pi^2} \sum_{n=1}^{\infty} \frac{1}{\alpha_n^2} \exp \left[ - \left\{ \frac{\alpha_n^2}{r^2} + \frac{\pi^2}{l^2} \right\} Dt \right] \dots \dots \dots (6.13)$$

Suppose at  $t = t_{0.5}$ , the initial amount hydrogen in charged specimen is reduced to half, i.e.

$$\frac{M(t)}{M(0)} = 0.5 \dots \dots \dots (6.14)$$

In the condition in equation 6.14, incorporating Bessel's root,  $\alpha_n$  from the table of roots of Bessel's function, ( $\alpha_n$  for  $n = 1, 2, 3, 4, 5$  given in Table 6.2) and the cylinder dimensions ( $r = 5 \text{ mm}$ ,  $l = 25 \text{ mm}$ ) in equation 6.13, the following relation is obtained

$$D = \frac{8.223}{t_{0.5}} \times 10^{-7} \text{ m}^2 \dots \dots \dots (6.15)$$

In the equation 6.15, the apparent diffusivity,  $D$  is expressed in terms of  $t_{0.5}$ . Therefore, from experimentally determined values of  $t_{0.5}$ ,  $D$  can be calculated from this equation.  $t_{0.5}$  is determined from the hydrogen evolution data.

Table 6.2 Bessel's roots for  $m = 0$  [2]

	$n = 1$	$n = 2$	$n = 3$	$n = 4$	$n = 5$
$\alpha_n$	2.4048255577	5.5200781103	8.6537279129	11.791534439	14.930917708

## 6.2 Results

### 6.2.1 Hydrogen evolution profiles at different temperatures

Experimental details of hydrogen charging, collection of hydrogen evolved from the charged specimen at various temperatures and time durations and its measurement using the hot extraction methods are discussed in Chapter 3. At 1 h duration of hydrogen charging specimens of all the three steels were saturated with hydrogen (Table 3.3).

Hydrogen evolved from a charged specimen at a given temperature for maximum duration of measurement with no increase in the hydrogen evolved for longer duration is taken as the total hydrogen evolved,  $M(0)$  for that temperature. Units for hydrogen concentration in the specimens is taken as ml/100g as used for  $H_D$  content in the previous chapters. Hydrogen contents obtained for different time durations were plotted against the total time of measurement to generate the hydrogen evolution profiles at different temperatures. The evolution profiles for modified 9Cr-1Mo, 2.25Cr-1Mo and mild steels are shown in Fig. 6.2 (a), (b) and (c) respectively. From these profiles it is clear that complete evolution of hydrogen at 25°C occurred at a relatively long time period of 9-14 days and with increase in temperature, time period for complete evolution of hydrogen came down. The hydrogen evolution data were further processed for calculation of hydrogen remaining in the specimen.

### **6.2.2 Calculation of $t_{0.5}$ and apparent diffusivity, $D$**

The plots in Fig. 6.2 (a), (b) and (c) gives variation of hydrogen evolved at a given time,  $M'(t)$ , with time for different temperatures for the three steels. From these data, hydrogen remaining in the specimen,  $M(t)$  was calculated for all the time durations as follows

$$M(t) = M(0) - M'(t) \dots \dots \dots (6.16)$$

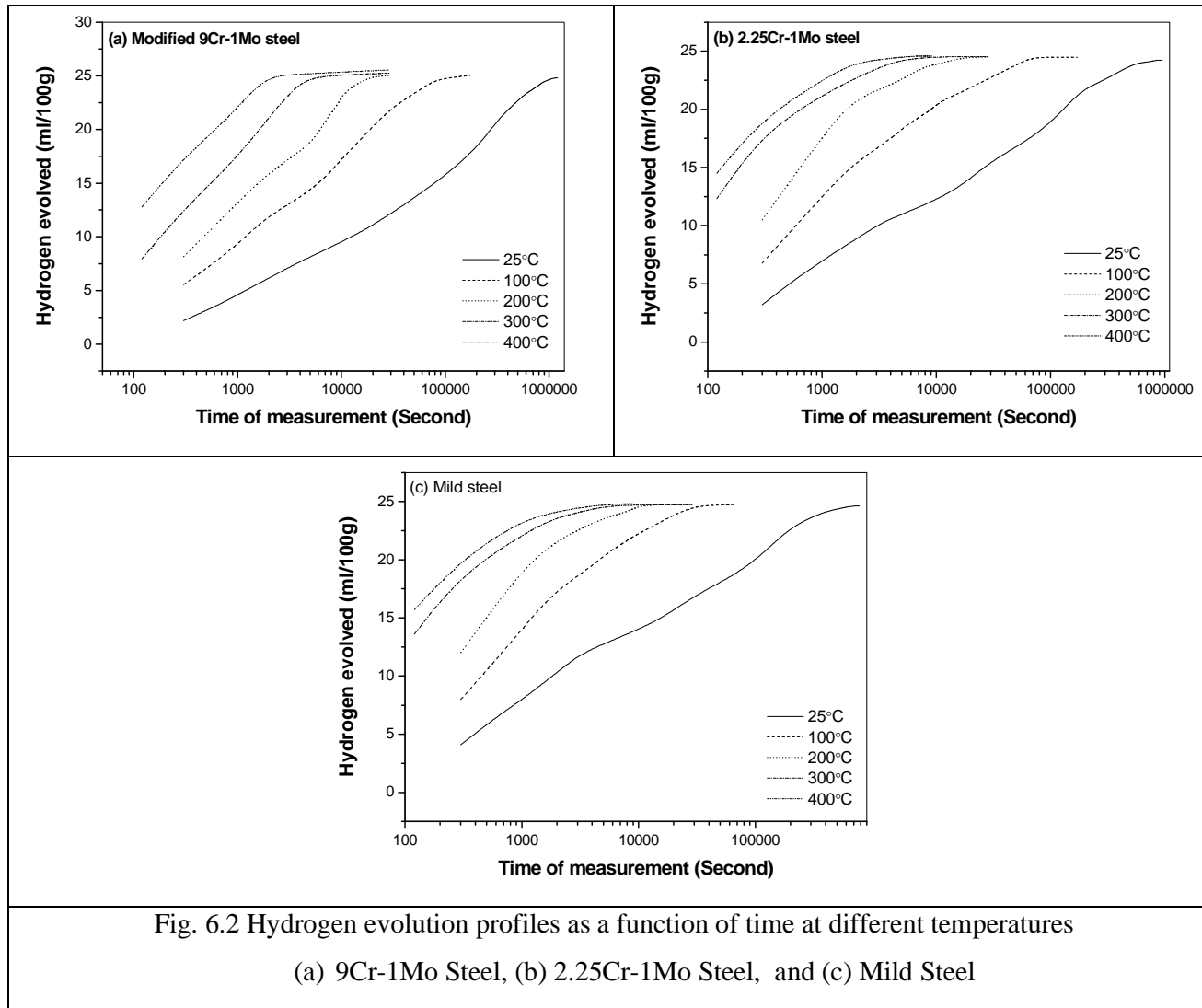
From these, the fraction of hydrogen remaining in the charged specimen,  $\frac{M(t)}{M(0)}$  was estimated and plotted as a function of time of measurement. The plots are shown in Fig. 6.3 (a), (b) and (c) for all the steels. From these remaining hydrogen profiles, the time taken for the total hydrogen content in the specimen (hydrogen present in the specimen at the completion of charging) to be reduced to half,  $t_{0.5}$ , was calculated for each test temperature. Substituting  $t_{0.5}$  in equation 6.15, the apparent diffusivity,  $D$  was calculated for each temperature. The calculated values  $t_{0.5}$  and  $D$  are given in Table 6.3.

In this estimation of apparent diffusivity, it is assumed that all the hydrogen evolved from the specimens are collected in the chamber and measured. However, in

practice, not all hydrogen could be collected as some hydrogen will invariably be lost during cleaning and transferring of the specimen, and during flushing and filling of the chamber. Correspondingly there will be an error in the estimation. An attempt was made to calculate this loss and revise the previous estimation by using the new values for hydrogen evolved. Procedure adopted for estimation of lost hydrogen is detailed below.

Table 6.3  $t_{0.5}$  and apparent diffusivity of hydrogen, D at different temperatures

Temperature (°C)	$t_{0.5}$ (Second)			Apparent Diffusivity $\times 10^{11}$ (m <sup>2</sup> /s)		
	Modified 9Cr-1Mo	2.25Cr- 1Mo	Mild steel	Modified 9Cr-1Mo	2.25Cr- 1Mo	Mild steel
25	31686	9892	4667.5	2.6	8.31	17.6
100	2783.5	901	736	29.5	91.3	111
200	788	396	321	104	208	256
300	314.5	119	100	261	691	822
400	117.5	87	64	700	945	1280



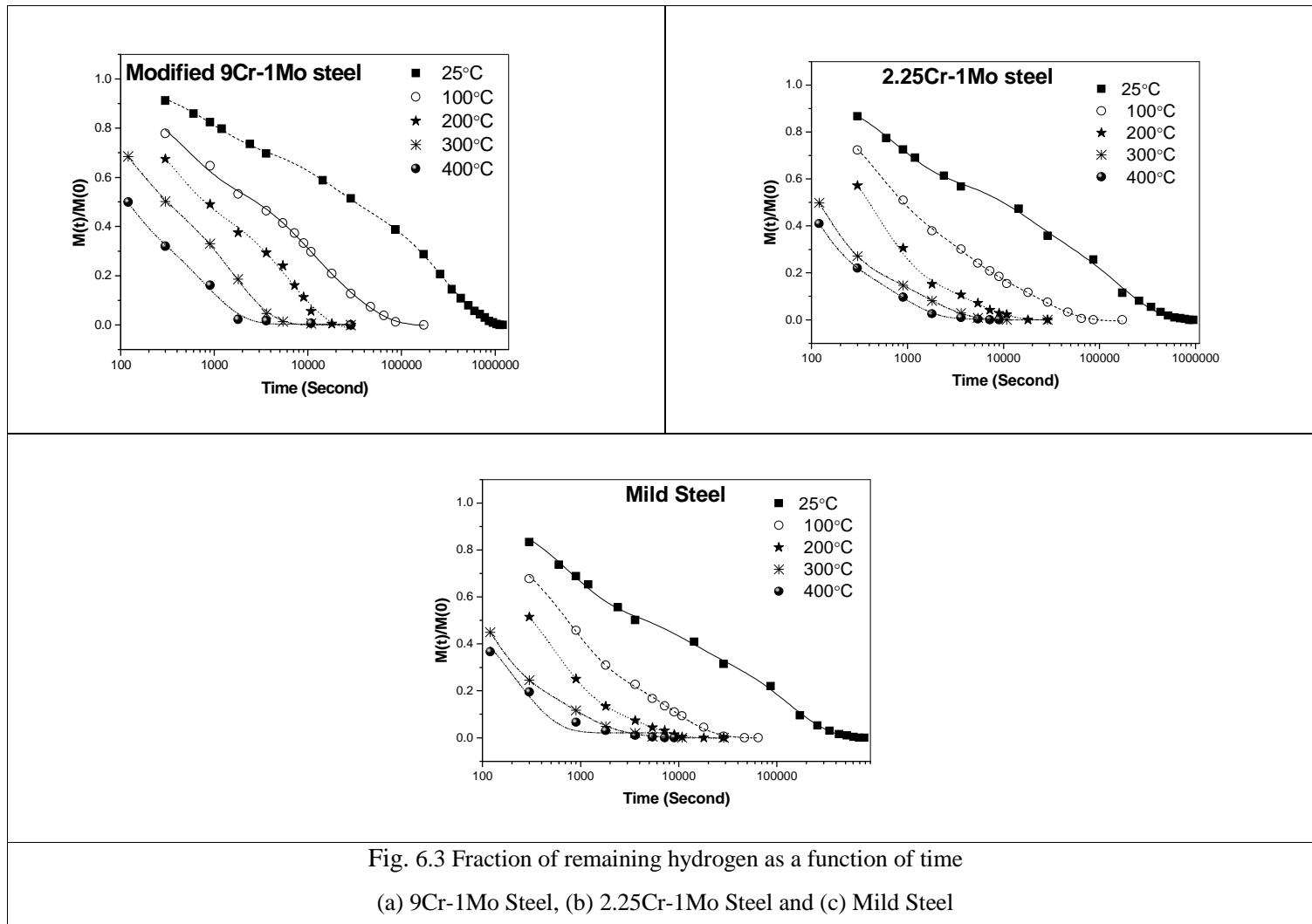


Fig. 6.3 Fraction of remaining hydrogen as a function of time  
 (a) 9Cr-1Mo Steel, (b) 2.25Cr-1Mo Steel and (c) Mild Steel

### 6.2.3 Calculation of the lost hydrogen content

Most of the operations that results in loss of hydrogen, like cleaning of specimen and flushing of chamber etc, are taking place at room temperature. From experience, it was found that time taken for completion of all these activities is around 150 s. This means hydrogen is lost for the first 150 s of taking the specimens from liquid nitrogen where they were stored soon after charging and collection of evolving only after this time lag ( $t^{lag}$ ). Hence, this delay in time is referred to as the initial time lag in this chapter and it is assumed that specimen is at ambient temperature (25°C). For the calculation of the lost hydrogen, the following procedure was used.

First, 150 s was added to the initial part of the total hydrogen evolution profile obtained at 25°C (ambient temperature). Subsequently rate of hydrogen evolution,  $S_t$  (ml/100g.s) was calculated for each time interval of measurement by assuming it to be constant over the interval (For example, the first hydrogen evolution was measured after 300 s, which is actually after 450 s of hydrogen charging and rate of evolution for the time period of 150 - 450s was estimated by dividing the amount of hydrogen evolved by 300 s, the duration of measurement) and  $S_t$  was plotted against the corrected time of measurement,  $t$ . The plots are shown in Fig. 6.4 (a), (b) and (c). It was found that  $S_t$  is exponentially related to time. The best fit empirical models between  $S_t$  and  $t$  for 9Cr-1Mo steel, 2.25Cr-1Mo steel and mild steel are given in equations 6.17, 6.18 and 6.19 respectively. These models have a  $R^2 = 0.99$ .

$$S_t = 0.01695 \exp\left(-\frac{t}{344.45}\right) + 0.00036 \exp\left(-\frac{t}{26298.7}\right) + 0.00289 \exp\left(-\frac{t}{2113.1}\right) + 0.00002 \dots \quad (6.17)$$

$$S_t = 0.00357 \exp\left(-\frac{t}{536.22}\right) + 0.00139 \exp\left(-\frac{t}{9303.4}\right) + 0.01866 \exp\left(-\frac{t}{537.16}\right) + 0.00002 \dots \quad (6.18)$$

$$S_t = 0.03648 \exp\left(-\frac{t}{391.78}\right) + 0.00231 \exp\left(-\frac{t}{6291.1}\right) + 0.00002 \dots \quad (6.19)$$

Knowing  $S_t$  from the above equations, hydrogen evolved from the charged specimen ( $H_E$ ) during initial time lag of 150 s can be calculated using the following equation.

$$H_E = S_t \times 150 \dots \dots \dots (6.20)$$

However,  $S_t$  is not constant and it varies with time. Hence,  $H_E$  was estimated separately for  $t = 1s$  and  $t = 150s$  and the average is taken as the value for hydrogen lost before the start of measurement. These results are given in Table 6.5.

### **6.2.3.1 Experimental verification of lost hydrogen content calculated**

Using mercury method, it is possible estimate the hydrogen lost during the initial time lag by making two separate measurements of hydrogen evolved; one from transferring the specimen immediately to the measuring apparatus after charging and another transferring the specimen after a predetermined delay of 150 s. Difference in the hydrogen content between these two measurements is the hydrogen lost during initial 150 s after charging. Results of these measurements are given in Table 6.4. A comparison of hydrogen loss estimated from the experiment with that calculated by extrapolation (Table 6.5) agree well indicating the estimation of hydrogen lost before the start of high temperature measurement using hot extraction techniques is reasonably accurate.

### **6.2.4 Calculation of time lags at 100, 200, 300 and 400°C**

It is obvious that, time taken would be less at high temperature for the same amount of hydrogen diffused out from the specimen at room temperature than the time taken at room temperature. This means hydrogen lost at ambient temperature during 150 s would be lost at a shorter duration at high temperatures. Hence, for diffusivity calculation this time shall be estimated for each of the temperatures. This was done using regression analysis of the variation of  $\frac{M(t)}{M(0)}$  with time and predicting the time for evolution at the measurement temperature corresponding to initial evolution of same

amount hydrogen that evolved at 25°C for first 150 s. For this purpose, the hydrogen evolution data corresponding to these temperatures (Fig. 6.2) were modified by adding the calculated lost hydrogen content to each of the measured hydrogen contents and the known time lag (150 seconds) to the corresponding time durations of measurement. Using this modified data,  $\frac{M(t)}{M(0)}$  was plotted against time. The modified data in the plot were fit with an empirical equation having a correlation coefficient of  $R^2=0.999$ . Using this equation, a new initial time lag (time taken for  $\frac{M(t)}{M(0)}$  to reduce to the value corresponding to lost hydrogen), which is less than the initial 150s, was calculated. Using this new time lag and keeping the lost hydrogen unchanged, regression was repeated and another time lag was calculated. These steps were iterated several times with a new time lag in each step until the following condition is satisfied.

$$t_{i+1}^{lag} - t_i^{lag} < 3s \dots \dots \dots (6.21)$$

Where,

$t_{i+1}^{lag}$  = Time lag obtained after the  $(i + 1)^{th}$  iteration

$t_i^{lag}$  = Time lag obtained after the  $i^{th}$  iteration

$i = 1, 2, 3 \dots$

The time lags obtained in the final iteration for all steels and temperatures under consideration are given in Table 6.6. This time lag and the lost hydrogen were used for the correction of the as-measured hydrogen evolution profile at each temperature for all the steels.

Table 6.4 Volume of lost hydrogen 25°C estimated from experiment

Material	H <sub>D</sub> obtained with immediate transfer (ml/100g)	H <sub>D</sub> obtained with predetermined delay of 150 s in transfer (ml/100g)	Hydrogen lost within 150 s (ml/100g)
Modified 9Cr-1Mo	27.22	24.79	2.43
2.25Cr-1Mo	27.67	24.23	3.44
Mild Steel	28.93	24.62	4.31

Table 6.5 Calculated amount of hydrogen lost at 25°C

Material	Rate of Evolution (ml/100g*sec)		Hydrogen lost (ml/100g)		
	$S_t = S_1$	$S_t = S_{150}$	$H_E$ at $t = 1$	$H_E$ at $t = 150$	Average
Modified 9Cr-1Mo	0.0202	0.0140	3.02	2.10	2.56
2.25Cr-1Mo	0.0235	0.0182	3.53	2.73	3.13
Mild Steel	0.0387	0.0272	5.81	4.07	4.94

Table 6.6 Time lags calculated for different steels

Temperature (°C)	Modified 9Cr-1Mo	2.25Cr-1Mo	Mild Steel
100	94	94	101
200	59.5	51.5	68
300	25.5	18	21
400	13	1	3

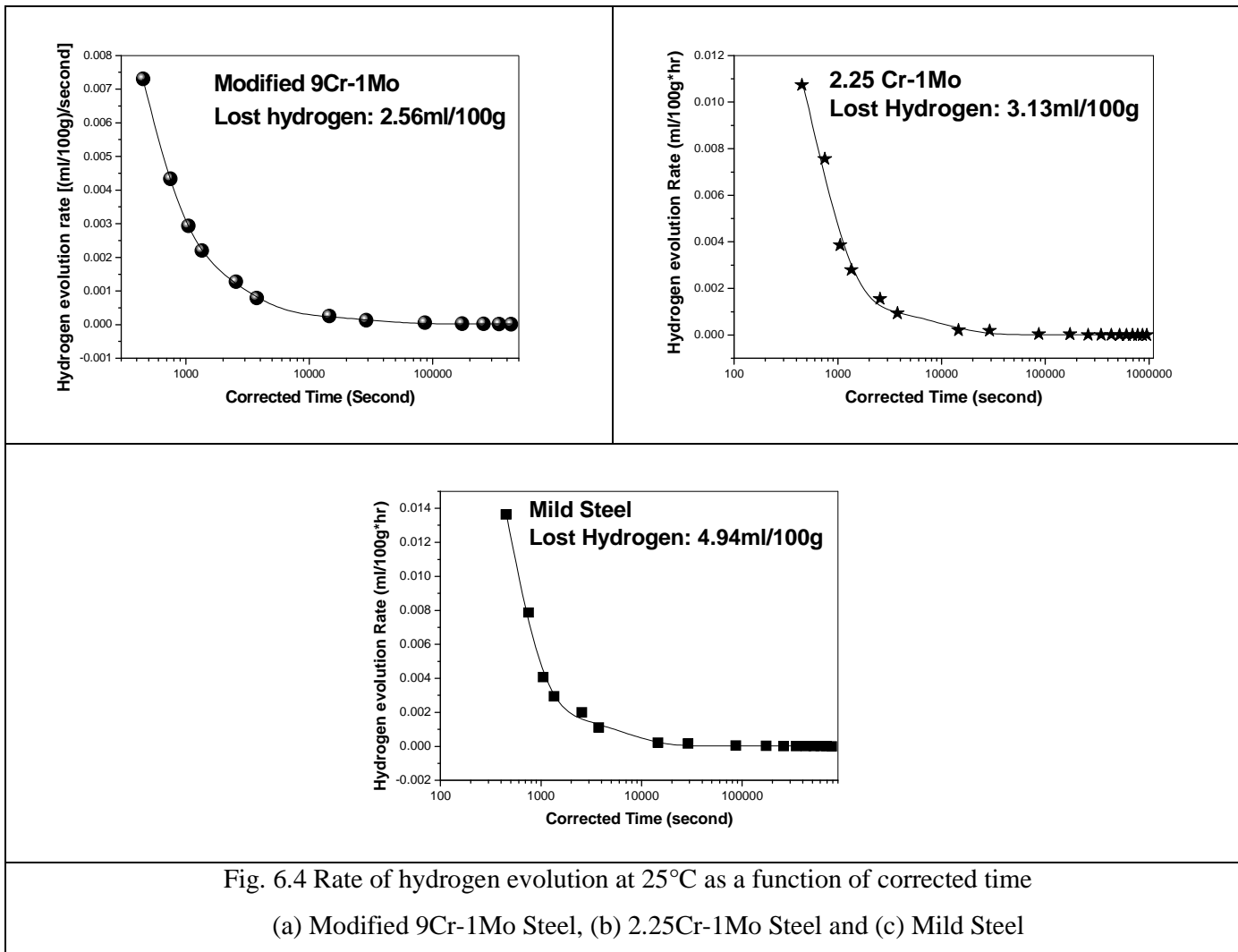


Fig. 6.4 Rate of hydrogen evolution at 25°C as a function of corrected time  
 (a) Modified 9Cr-1Mo Steel, (b) 2.25Cr-1Mo Steel and (c) Mild Steel

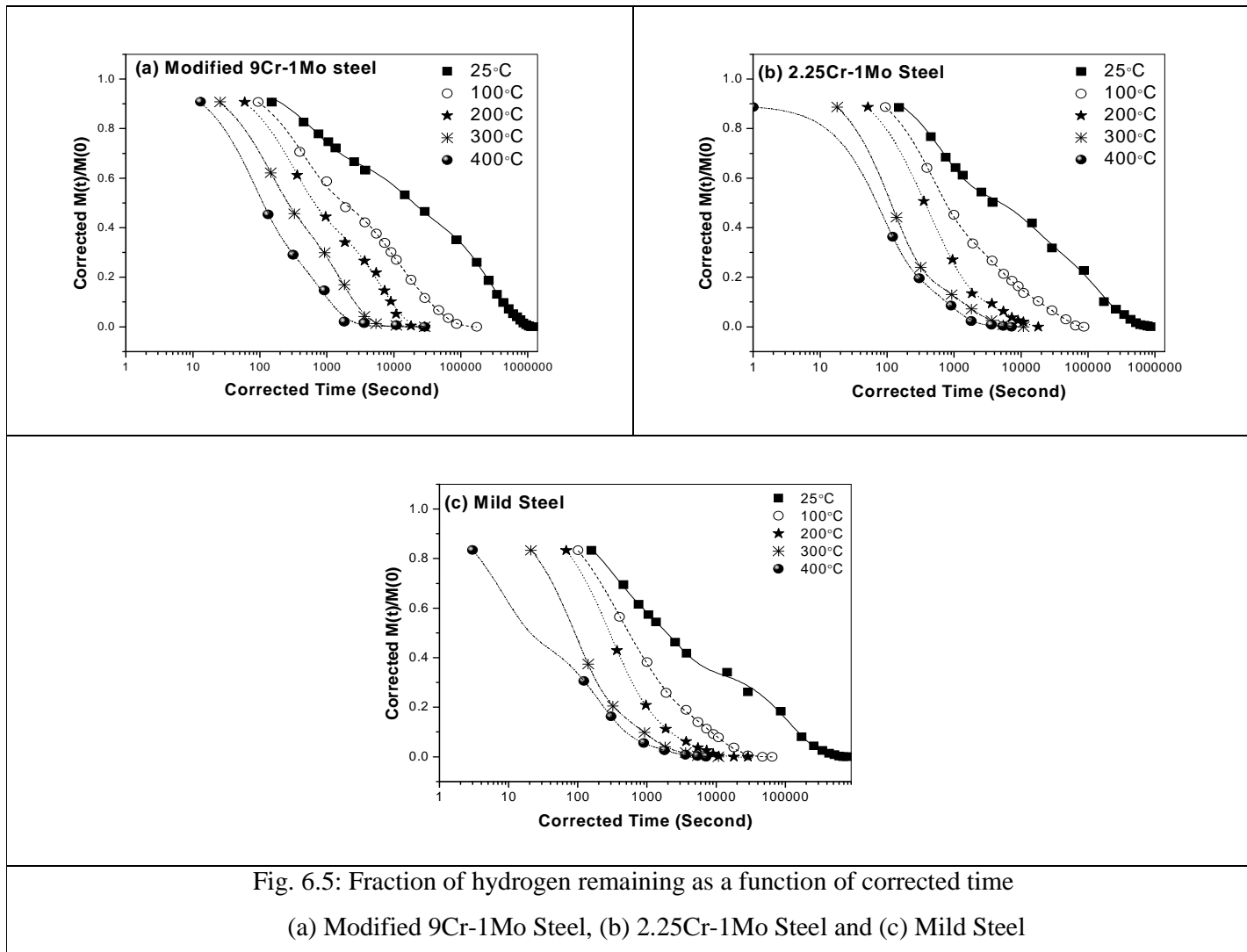
### 6.2.5 Calculation of $t_{0.5}$ and $D$ using corrected data

Calculation of  $t_{0.5}$  from the corrected data was similar to that described in section 6.3.3. Using the corrected hydrogen evolution profile, fraction of remaining hydrogen,  $\frac{M(t)}{M(0)}$  was plotted as a function of corrected time,  $t_{0.5}$  and apparent diffusivity of hydrogen in steels. The profiles thus obtained for modified 9Cr-1Mo, 2.25Cr-1Mo and mild steel are shown in Fig. 6.5 (a), (b) and (c) respectively. From an exponential relation between  $\frac{M(t)}{M(0)}$  and corrected time obtained from these profiles,  $t_{0.5}$  for each of the temperatures were revised. The apparent diffusivities of hydrogen,  $D$ , at 100, 200, 300 and 400°C were calculated by substituting these revised values of  $t_{0.5}$  in equation 6.15.

The revised  $t_{0.5}$  and corrected apparent diffusivity ( $D$ ) of hydrogen in steels under consideration for each test temperature are given in Table 6.7.

Table 6.7 Revised  $t_{0.5}$  and apparent diffusivity of hydrogen from corrected data

Temperature (°C)	$t_{0.5}$ (Second)			$D \times 10^{11}$ (m <sup>2</sup> /s)		
	Modified 9Cr-1Mo	2.25Cr- 1Mo	Mild steel	Modified 9Cr-1Mo	2.25Cr- 1Mo	Mild steel
25	19647	4576	1928	4.18	18	42.6
100	2260	749.5	547	36.4	110	150
200	647	367.5	290	127	224	283
300	263	113	91	313	727	904
400	110.5	63	48	744	1310	1710



## 6.3 Discussion

### 6.3.1 Variation in apparent diffusivity by incorporating lost hydrogen

Table 6.3 presents the apparent diffusivities hydrogen calculated from the measured hydrogen evolution data (without lost hydrogen) where as Table 6.7 presents the apparent diffusivities hydrogen calculated from the corrected hydrogen evolution data (with lost hydrogen) From these tables, it is clear that, the apparent diffusivity obtained from corrected data is only marginally higher than that obtained from the measured evolution data. The variations in apparent diffusivity obtained from both the cases are shown in Fig. 6.6. This difference is highest at 25°C, decreases with increase in temperature and is least at 400°C. Therefore, it can be said that correction for lost hydrogen has only marginal effect on the apparent diffusivity data estimated for hydrogen in steel.

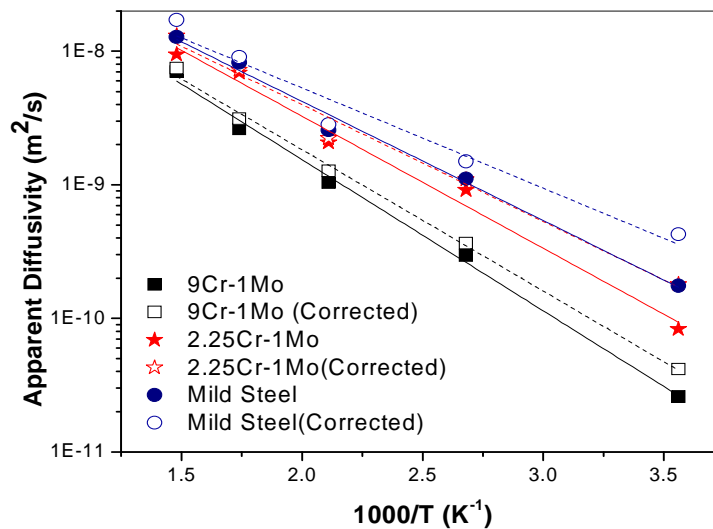


Fig. 6.6 Variation of apparent diffusivity of hydrogen in different steels with temperature

### 6.3.2 Comparison of apparent diffusivities obtained in the present study with the data in literature

The hydrogen apparent diffusivities determined in the present study are compared with the data available in literature for various temperatures [8, 10-13]. Fig. 6.7 shows the scatter bands of hydrogen apparent diffusivity proposed by Bollinghaus et al [13] for low and high alloyed steels having ferritic or martensitic microstructure. It is seen from the figure that all the apparent diffusivity values obtained in the present study are either lying within or close to the scatter bands.

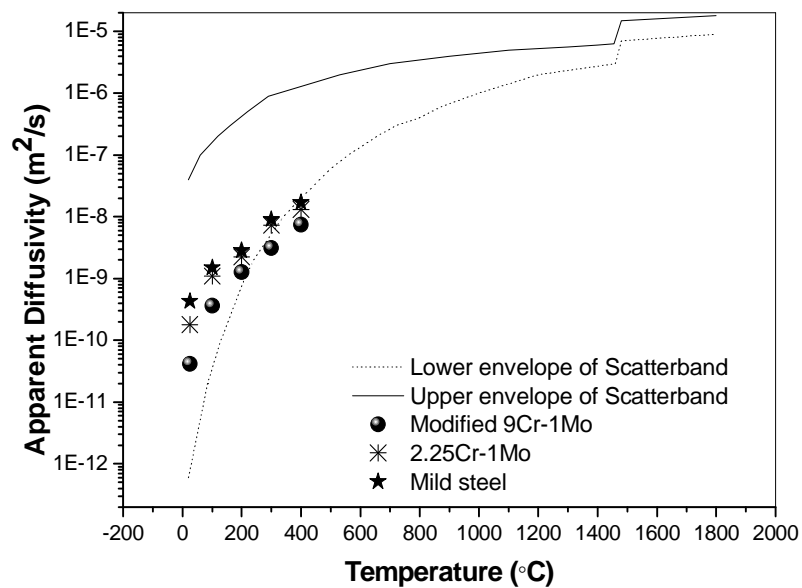


Fig. 6.7 Comparison of apparent diffusivity of hydrogen obtained from present study with Bollinghaus scatterbands

Comparison of the diffusivity data generated for modified 9Cr-1Mo and 2.25Cr-1Mo steels in this study with those reported in literature are shown in Fig. 6.8. Difference between the various reported diffusivity values decreases at high temperatures. Among the diffusivity data available in literature, those reported by Brouwer has been claimed to be most accurate by the author since the results reported in that study are corrected for

lost hydrogen. It is interesting to note that the diffusivity data in this study matches closely with that of Brouwer for the entire temperature range [8].

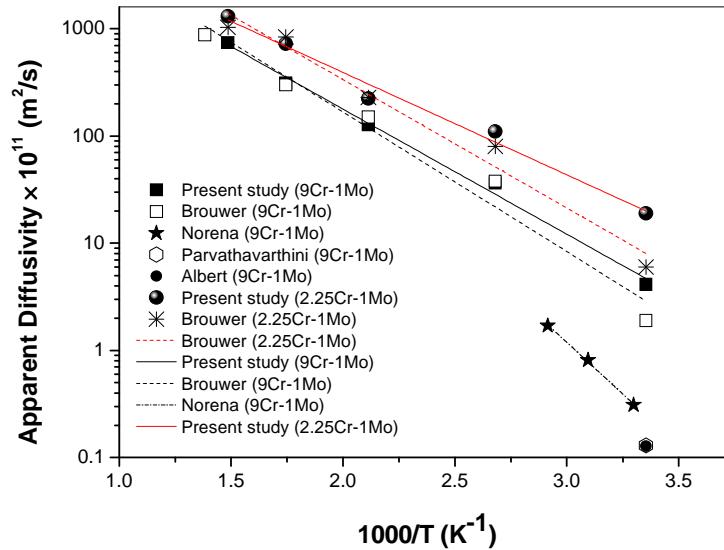
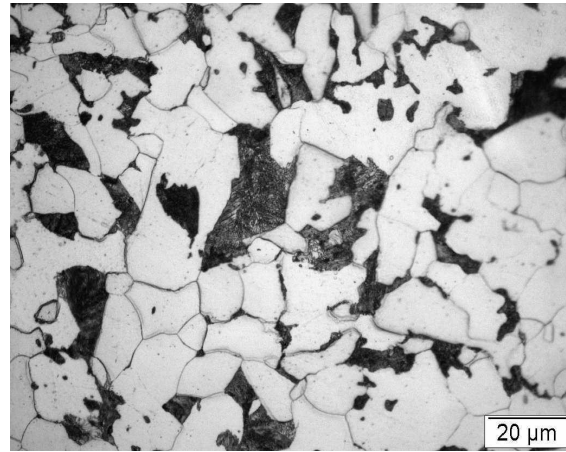


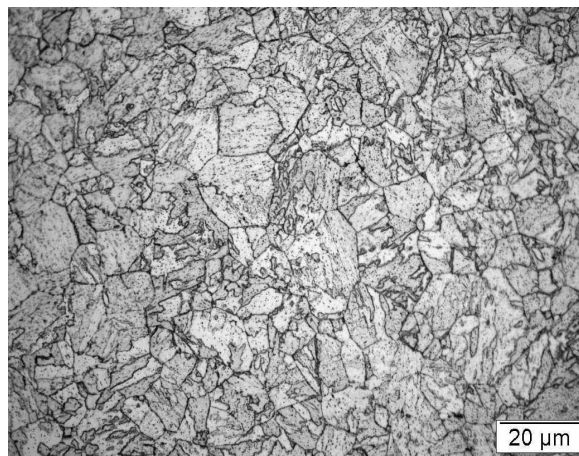
Fig. 6.8 Comparison of apparent diffusivity of hydrogen obtained from present study with that in literature

### 6.3.3 Variation in apparent diffusivity with temperature and alloying

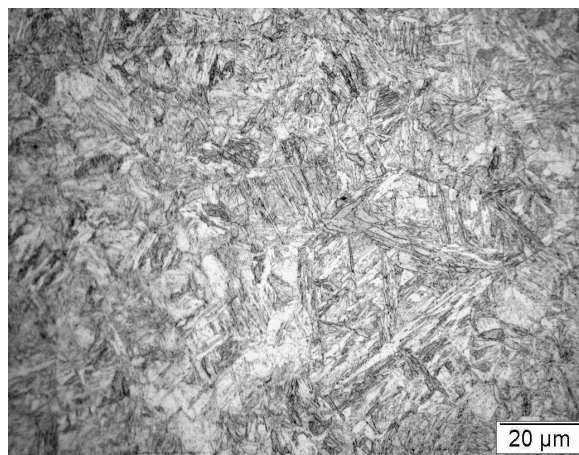
The variation in apparent diffusivities of hydrogen in steel as a function of temperature is already shown in Fig. 6.6. From this figure, it is clear that there is a two order of magnitude increase in the diffusivity of hydrogen in steel with increase in temperature from 25°C to 400°C. The variation in apparent diffusivity of hydrogen in steels as a function of alloying can also be explained from Fig. 6.6. It is clear from the figure that among the three steels used in the study, the apparent diffusivity of hydrogen is maximum in mild steel and minimum in modified 9Cr-1Mo steel at all temperatures. These facts reveal that for a given temperature, apparent diffusivity of hydrogen in steel decreases with increase in alloy content. The difference in diffusivity of hydrogen from mild steel and modified 9Cr-1Mo steel is an order of magnitude (a factor of 10) at 25°C. This difference reduces significantly with increase in temperature.



(a)Mild Steel



(b) 2.25Cr-1Mo Steel



(c) Modified 9Cr-1Mo Steel

Fig. 6.9 Microstructure of different steel used after heat treatment

Alloying elements affect the diffusivity of hydrogen in steel in two ways. First, various alloying elements and their concentration in steel affect the solubility and diffusivity of hydrogen in steel to different degrees. For example, in modified 9Cr-1Mo steel, vanadium atoms act as traps for hydrogen at lower temperatures [8]. This would reduce the diffusivity of hydrogen in this steel from that of mild steel. Second, the alloying elements also vary the microstructure of the steel which affects the diffusivity. Measurements were carried out in all the three steels in normalized condition; they are heat treated above the temperature in which complete transformation of ferrite to austenite takes place and then cooled in air. In mild steel, austenite transforms to a mixture of ferrite and pearlite, in 2.25Cr-1Mo, it transforms predominantly to bainite and in modified 9Cr-1Mo, it transforms to martensite. Fig. 6.9 shows the microstructure of the three steels after the normalizing heat treatment. Dislocations and other defects which can act as traps for hydrogen would be more in martensitic structure and less in a ferrite+pearlite structure. In a bainitic structure defect density would be between these two. Accordingly, apparent diffusivity should be least for modified 9Cr-1Mo steel and maximum for mild steel. Further, with increase in temperature, effectiveness of these defects as hydrogen traps decreases and accordingly the difference in the diffusivity of hydrogen in the steels also comes down. Our results are in agreement with these arguments.

#### ***6.3.4 Hydrogen diffusivity and $H_D$ in the welds***

In the context of  $H_D$  measurement, it is interesting to examine the percentage of total hydrogen diffused out from mild steel and modified 9Cr-1Mo steel after 72 h at 25°C and 30 minutes at 400°C which, as indicated in the previous chapters, are the temperatures and time durations recommended for  $H_D$  measurement using mercury method and hot extraction method respectively. From Table 6.4, the total hydrogen

evolved from both these steels are roughly same.  $H_D$  contents obtained from mild steel, 2.25Cr-1Mo steel and modified 9Cr-1Mo steel after (1) 72 h at 25°C, (2) 30 minutes at 400°C and (3) the completion of hydrogen evolution are given in Table 6.8. After 72 h at 25°C, almost 96% of the total hydrogen has been evolved for mild steel, while for modified 9Cr-1Mo steel, this is only 81%. Hydrogen continued to evolve for 9 days in mild steel while it continued for 14 days for modified 9Cr-1Mo steel. This implies that, for same amount of  $H_D$  in a mild steel or carbon steel weld and modified 9Cr-1Mo steel weld,  $H_D$  measurement using mercury method, if it is carried out only for 72 h, would always result in lower  $H_D$  content for modified 9Cr-1Mo steel welds than for mild steel welds. This could be the reason why the time duration for hydrogen collection in standard mercury method was changed from 72 h in the early versions of the ISO standard to till the total evolution is completed in the latest version [14].

Table 6.8  $H_D$  contents measured at standard temperature + time durations

Temperature (C°)	25 [15]		400 [14]	
	72 h	Complete evolution	30min	Complete evolution
Modified 9Cr-1Mo steel	22.23	27.35	27.52	28.1
2.25 Cr-1Mo steel	25.01	27.36	27.59	27.92
Mild steel	28.27	29.56	29.35	29.75

It is interesting to note that this difference in the percentage of total hydrogen evolved from the charged specimens of mild steel and 9Cr-1Mo steel decreases considerably at 400°C for 30 minutes, the temperature and duration specified for hot extraction methods for  $H_D$  measurements. At this temperature and duration, almost 99% of the total hydrogen has been evolved from mild steel, while for modified 9Cr-1Mo steel, this is 98%. This shows that hot extraction methods not only reduce the total time

of  $H_D$  measurements, but also provide more accurate values than the mercury method for alloy steel welds.

It was observed from the hydrogen evolution studies that total hydrogen evolved from specimens of all the three steels are same, indicating they are all charged with hydrogen to the same extent. However, for a given time duration, hydrogen evolved is lowest for modified 9Cr-1Mo specimen and highest for mild steel at all the temperatures considered in this study. This shows that the hydrogen evolved for a given time duration increases with decrease in alloy content of the steel. This is also in agreement with hydrogen diffusivities estimated for all the three steels. This means that at a given time after introducing hydrogen in the steel (as in welding or charging) the fraction of hydrogen remaining in steel would increase with increase in alloy content of the steel. In other words apparent solubility of hydrogen would increase with increase in alloy content. This, in addition to a susceptible microstructure, would increase the susceptibility of alloyed steels to hydrogen assisted cracking.

The above facts support and explain the results of an earlier study of Albert et al [12]. In this study, HAC susceptibility tests were conducted for three different steels in which hydrogen was introduced to the weld zone through shielding gas of GTAW process used for making the welds. For same amount of hydrogen introduced, the  $H_D$  contents measured were lower for 9Cr-1Mo welds than that measured for the other two low alloyed steels (2.25Cr-1Mo and 0.5 Mo steel); though susceptibility for cracking was highest for 9Cr-1Mo steel. The reason can be explained as follows. Due to the higher alloy content, apparent diffusivity of hydrogen in 9Cr-1Mo steel was lower than that in the other low alloyed Cr-Mo steels. This resulted lower amounts of  $H_D$  in 9Cr-1Mo steel. However, since all the Cr-Mo steels had their total  $H_D$  content equal, at a given time

amount of hydrogen retained in 9Cr-1Mo steel was higher than the other two Cr-Mo steels making it more susceptible to cracking.

## Reference

1. A. Fick, Uber Diffusion, Ann. der. Physik, 1855, Vol. 170, No.1, 59-86
2. G. B. Arfkens and H. J. Weber, Mathematical methods for physicists, Ed. 6, Elsevier, Academic Press, 2005
3. J. Crank, Mathematics of Diffusion, Clarendon Press, Oxford, 1975, 71-73.
4. R. M. Barrer, Diffusion in and through solids, Richard M, Cambridge University Press, 1951, 31-34.
5. A. L. Demarez, A. G. Hocks, and F. A. Meuniers, Diffusion of hydrogen in mild steel, *Acta Metallurgica*, 1954, Vol. 2, No. 3, 214-223
6. T. B. Whitaker, and J. H. Young, Simulation of moisture movement in peanut kernels: Evaluation of the diffusion equation, Transactions of the ASAE, 1972, Vol. 15, No. 1, 163-166
7. V. M. Katlinskii, L. L. Kotlik,, V. M. Egorova, and A. M. Viktorova, Diffusion of hydrogen in Hafnium and Titanium, Journal of Engineering Physics and Thermophysics, Vol. 39, No. 4, 1079-1083
8. R.C. Brouwer, Hydrogen diffusion and solubility in vanadium modified pressure vessel steels, *Scripta Metallurgica et Materialia*, 1992, Vol. 27, No. 3, 353-358.
9. U. Dilthey,, S. Trube,, I. K. Pokhodnya, and V. A. Pavlik, Determination of diffusion coefficient of hydrogen in steel subjected to deformation and in weld deposits of basic and rutile coated electrodes, *Welding Research Abroad*, 1993, Vol. 4, 2-5.

10. C. H. Norena, and P. Bruzzoni, Effect of microstructure on hydrogen diffusion and trapping in a modified 9%Cr–1%Mo steel, *Materials Science and Engineering A*, 2010, 527, 410–416
11. N. Parvathavarthini, S. Saroja, and R.K. Dayal, Influence of microstructure on the hydrogen permeability of 9%Cr-1%Mo ferritic steel, *Journal of Nuclear Materials*, 1999, 264, 35-47
12. S. K. Albert, V. Ramasubbu, N. Parvathavarthini, and T. P. S. Gill, Influence of alloying on hydrogen-assisted cracking and diffusible hydrogen content in Cr-Mo steel welds, *Sadhana*, 2003, 28 (3/4), 383–393
13. Th. Bollinghaus, H. Hoffmeister and C. Middel, Scatterbands for hydrogen diffusion coefficients in steels having a ferritic or martensitic microstructure and steels having an austenitic microstructure at room temperature, *Welding in the World*, 1996, 37(1/2), 16-23.
14. *ISO 3690:2012 (E), ISO 3690:2000 (E)*, Welding and allied processes – Determination of hydrogen in ferritic steel arc weld metal.
15. *ISO 3690:1977/ Add 1:1983*, , Welding - Determination of hydrogen in deposited weld metal arising from the use of covered electrodes for welding and low alloy steels; Addendum 1

**CHAPTER 7**

**CONCLUDING REMARKS  
AND  
SCOPE FOR FUTURE RESEARCH**

# Concluding remarks and Scope for future research

---

---

## 7.1 Conclusions

Diffusible hydrogen measurement was carried out using indigenously developed techniques which use specially designed chambers for collection of  $H_D$  and its measurement using PEMHS and GCTCD. These techniques were used in studying the effects of preheating and post-heating on  $H_D$  content of welds. Further, these techniques were used for the determination of apparent diffusivity of hydrogen in steel. Following conclusions were drawn out of the studies mentioned in this thesis:

### *7.1.1 Measurement of $H_D$ using indigenously developed techniques*

The studies carried out for the development of RT-PEMHS, HE-PEMHS and HE-GCTDC techniques for diffusible hydrogen ( $H_D$ ) measurement were concluded as follows:

1. Measurement of diffusible hydrogen content in steel welds was successfully demonstrated using a Nafion based hydrogen proton exchange membrane hydrogen sensor (PEMHS) by collecting hydrogen at room temperature (RT-PEMHS). This method takes the same time for collection of diffusible hydrogen as mercury method.
2. PEMHS combined with a specially designed hot extraction chamber (HE-PEMHS) and a gas chromatograph facility which uses a separately designed hydrogen extraction unit (HE-GCTCD), which allowed hot extraction of  $H_D$  from the weld specimen up to 400 °C are demonstrated for  $H_D$  measurement in steel welds.

3. Results obtained using all these methods show one to one correspondence with those obtained by the standard mercury method for a wide range of  $H_D$  contents which covers all the benchmarks set by IIW and AWS.
4. Statistical analysis of the results obtained in all these methods, as recommended by ISO 3690, confirms that confidence level on the accuracy of the measurement of  $H_D$  using these methods as compared to mercury method is better than 95%.
5. It is demonstrated that these new techniques can be used to study the hydrogen evolution from the weld or any material as a function of time. One such study carried out using RT-PEMHS showed that hydrogen evolution from a weldment of modified 9Cr-1Mo steel continues much beyond 72 h, the time for hydrogen collection proposed in the early version of standards of  $H_D$  measurement at ambient temperatures.

### ***7.1.2 Study on the effects of preheat and post- heating on $H_D$ content in welds***

Using the HE-PEMHS technique, effects of preheating and post-heating on  $H_D$  content of welds were studied. Following are the conclusions of the study:

1. A procedure has been developed for studying the effect of preheating and post-heating on the diffusible hydrogen content of welds. This procedure employs the same specimen and welding fixture (copper jig) as specified for standard measurements of  $H_D$  in the welding consumables along with an arrangement for preheating and post-heating. In order to compare the  $H_D$  content remaining in the weld after different preheat temperatures, it is recommended that  $H_D$  measurement should commence after the specimen cooled down to 100°C on the fixture.
2. Preheating substantially brings down the  $H_D$  content remaining in the weld from that present in welds prepared without preheat. Combining post-heating with preheating

results in further reduction in the  $H_D$  remaining in the weld. In fact, preheating and post-heating at lower temperature is better than using preheating alone at higher temperature to reduce the  $H_D$  content remaining in the weld.

3. Preheating combined with post-heating is more effective than mere preheating in lowering the  $H_D$  content in welds of modified 9Cr–1Mo steel,
4. It is demonstrated that HE-PEMHS technique can be used to measure diffusible hydrogen content as low as 0.2ml/100g.

### ***7.1.3 Determination of apparent diffusivity of hydrogen in steel***

Apparent diffusivity of hydrogen in steel was determined using the HE-PEMHS and HE-GCTCD techniques. The studies are summarized below:

1. Hydrogen evolution profiles were determined for modified 9Cr-1Mo, 2.25Cr-1Mo and mild steels at temperature in the range 25-400°C using mercury, HE-PEMHS and HE-GCTCD techniques and using a solution to Fick's second law, the apparent diffusivity of hydrogen is calculated.
2. Apparent diffusivities of all the three steels are re-estimated by incorporating the lost hydrogen were found to be only marginally higher than that calculated without lost hydrogen. These values are found to be in agreement with hydrogen diffusivity data reported in literature for different steels.

## **7.2 Scope for future research**

### ***7.2.1 Development of HE-PEMHS and HE-GCTCD for commercial application***

In the present study two techniques have been developed for hot extraction of diffusible hydrogen and its subsequent measurement using a PEMHS or GCTCD. The present configurations of these systems are suitable for use in research laboratories.

Some modification of these configurations is required to develop these devices into commercial products, which can be used for routine measurement of diffusible hydrogen by electrode manufacturers. These include packaging the measurement system and HE chamber in to single unit; simplifying the calibration procedure, provisions to measure  $H_D$  content from 3 or 4 specimens in one campaign etc. In the case of HE-PEMHS, configuration can be modified for estimation of volume of hydrogen collected instead of hydrogen concentration in the chamber.

In both HE-PEMHS and HE-GCTCD, hot extraction part is separate from the detector. Hence, we can just replace heater and chamber in the present systems suitably so that they can be adapted not only for diffusible hydrogen but also for total hydrogen measurement.

Demonstrated capability of these techniques to measure hydrogen levels as low as 0.2 ml/100g of weld metal makes them ideal choice for  $H_D$  measurement in materials like duplex stainless steels, in which  $H_D$  content is expected to be very low.

### ***7.2.2 Correlating diffusible hydrogen remaining in welds with cracking susceptibility***

A procedure to estimate  $H_D$  content remaining in the weld after preheating and post heating has been developed in this study. Information generated using this procedure can be used in conjunction with data on effect of preheating and post heating on hydrogen assisted cracking so that critical level of hydrogen in various steel welds below which cracking does not occur can be determined.

### ***7.2.3 Study on hydrogen trapping in steels***

Procedure presented here for determination of apparent diffusivity could be suitably modified to generate information on hydrogen trapping behaviour in steels. Hydrogen evolution studies can be carried out for a fixed duration for increasing temperatures (for example initially for 30 minutes at ambient temperature, then at 100, 200°C ...) and from the volume of hydrogen evolved at various temperatures, type of hydrogen traps and trap density can be estimated using the data available on binding energy of various traps.

**PUBLICATIONS OUT OF THIS WORK  
AND  
AWARDS**



## Publications out of this work and awards

---

---

### I. Publications in Refereed Journals

1. **G. K. Padhy**, V. Ramasubbu, N. Murugesan, C. Ramesh and S.K. Albert: Developing a sensor for diffusible hydrogen measurement, *Welding Journal*, 2011, Vol. 90, No. 3, 47-53.
2. **G. K. Padhy**, V. Ramasubbu, N. Murugesan, C. Ramesh and S.K. Albert: Hot extraction of diffusible hydrogen and its measurement using a hydrogen sensor, *Welding In the World*, 2012, Vol. 56, No. 7/8, 18-25
3. **G. K. Padhy**, V. Ramasubbu, N. Murugesan, C. Ramesh and S.K. Albert: Effect of preheat and post heating on the diffusible hydrogen content of welds, *Science and Technology of Welding and Joining*, 2012, Vol. 17, No 5, 408-413
4. **G. K. Padhy**, V. Ramasubbu, N. Murugesan, C. Ramesh and S.K. Albert : Diffusible hydrogen measurement in steel welds using an electrochemical hydrogen sensor, *Indian Welding Journal*, 2012, Vol.45, No.1, 35-46
5. **G. K. Padhy**, V. Ramasubbu, N. Murugesan, N. Parvathabarthini, C. Ramesh and S.K. Albert: Determination of apparent diffusivity of hydrogen in 9Cr-1MoVNbN steel using a hot extraction technique, *International Journal of Hydrogen Energy*, 2013, Vol. 38, 10683-10693

### II. Publications under progress

1. **G. K. Padhy**, V. Ramasubbu, N. Parvathabarthini, and S.K. Albert: Effect of composition/alloying elements on the apparent diffusivity of hydrogen in steel (*Manuscript submitted to Metallurgical and Materials Transactions A*)

2. **G. K. Padhy**, V. Ramasubbu, and S.K. Albert: Rapid determination of diffusible hydrogen in steel welds using a modified gas chromatography facility (*Manuscript submitted to Journal of Testing and Evaluation*)

### III. **Papers presented in Conferences and Assemblies**

1. **G. K. Padhy**, V. Ramasubbu, N. Murugesan, C. Ramesh and S.K. Albert: Diffusible hydrogen measurement in welding consumables using a new proton-exchange-membrane based hydrogen sensor, *National Welding Seminar*, 4<sup>th</sup>-6<sup>th</sup> February, 2009, Mumbai, India.
2. **G. K. Padhy**, V. Ramasubbu, N. Murugesan, C. Ramesh and S.K. Albert: : Diffusible hydrogen measurement in steel welds using an electrochemical hydrogen sensor, *National Welding Seminar*, 21<sup>st</sup>-23<sup>rd</sup> December, 2010, Visakhapatnam, India.
3. **G. K. Padhy**, V. Ramasubbu, N. Murugesan, C. Ramesh and S.K. Albert: Hot extraction of diffusible hydrogen and its measurement using a hydrogen sensor, *64<sup>th</sup> Annual Assembly and International Conference of International Institute of Welding*, 17<sup>th</sup>-22<sup>nd</sup> July, 2011, Chennai, India.
4. **G. K. Padhy**, V. Ramasubbu, K. R. Rangarajan, M. K. Singari, S. K. Albert: A new gas chromatography facility for rapid determination of diffusible hydrogen in steel welds. Paper ID: 263, *National Welding Seminar*, 7-9<sup>th</sup> February, 2013, Bangalore, India
5. S. K. Albert, **G. K. Padhy**: Measurement of diffusible hydrogen and hydrogen diffusivity using a newly developed hydrogen sensor. Paper ID: 512, *National Welding Seminar*, 7-9<sup>th</sup> February, 2013, Bangalore, India

#### IV. **Award**

1. **ESAB India Award for Best Paper among All Categories:** Diffusible hydrogen measurement in steel welds using an electrochemical hydrogen sensor, **G. K. Padhy**, V. Ramasubbu, N. Murugesan, C. Ramesh and S.K. Albert, *National Welding Seminar*, 21<sup>st</sup>-23<sup>rd</sup> December, 2010, Visakhapatnam, India.